Dissertation
submitted to the
Combined Faculty of Natural Sciences and Mathematics
of the Ruperto Carola University Heidelberg, Germany
for the degree of
Doctor of Natural Sciences

Presented by
M. Sc. Svenja Adrian
born in: Darmstadt, Germany.
Oral examination: 19th July 2019

FOXM1 and CKS1 –
novel cellular targets of the HPV oncogenes

Referees: Prof. Dr. Britta Brügger

Prof. Dr. Felix Hoppe-Seyler

Table of Contents

Summary

Persistent infections with oncogenic types of human papillomaviruses (HPVs) cause cervical and other anogenital carcinomas as well as cancers of the head and neck regions and thereby contribute significantly to the global cancer burden. Despite the existence of efficient prophylactic vaccines, the worldwide number of HPV-related cancer cases is estimated to rise. It therefore remains an important task to further investigate and delineate the molecular mechanisms that underlie HPV-driven tumorigenesis, in specific the actions of the two viral oncogenes *E6* and *E7* which promote and sustain the malignant phenotype of HPV-positive cancers. This is also hoped to offer new opportunities for HPV-targeted therapeutic intervention.

In the present study, the two host cell genes *FOXM1* and *CKS1B* were identified as novel target genes of HPV E6 and E7. Interestingly, both FOXM1 and CKS1 have been described to possess oncogenic properties in different types of cancers. By stimulating their transcriptional promoters, E6 and E7 increased FOXM1 and CKS1 mRNA and protein levels in HPV-positive cells. The inhibition of the tumor suppressor p53 and the pocket protein family by E6 and E7, respectively, was determined to mediate the activation of *FOXM1* and *CKS1B.* Hence, the disruption of the repressive DREAM complex by E6/E7 emerged as a likely mechanism involved in conveying HPV oncogene-induced promoter activation of *FOXM1* and *CKS1B.*

On the phenotypic level, the elevated level of CKS1 exerts pro-proliferative and senescence-suppressing effects in HPV-positive cancer cells. Furthermore, while not affecting proliferation *per se*, FOXM1 was shown to protect cervical cancer cells from the proliferation-suppressing effects of chemotherapy. In growth-arrested HPV-positive cells, neither FOXM1 nor CKS1 levels were found to decline, which would be in line with their activation by E6/E7 via DREAM disruption.

Collectively, the results presented in this thesis contribute to a deeper understanding of HPV-driven carcinogenesis and decipher how the viral oncogenes *E6* and *E7* promote tumorigenesis through extensive modulation of the host cell's molecular networks. They also provide evidence that interfering with FOXM1 or CKS1 expression or function could be an attractive future strategy for the therapy of HPV-induced cancers.

Zusammenfassung

Persistierende Infektionen mit onkogenen Typen humaner Papillomviren (HPVs) sind Auslöser von Gebärmutterhalskrebs, anderen Krebsarten im Anogenitalbereich, sowie von bestimmten Kopf-Hals-Tumoren. Sie tragen damit wesentlich zur weltweiten Krebsinzidenz bei. Obwohl wirksame prophylaktische Impfstoffe verfügbar sind, wird erwartet, dass die Anzahl HPV-assoziierter Krebsfälle weltweit weiter steigen wird. Die Aufklärung der molekularen Mechanismen der HPV-induzierten Krebsentstehung bleibt daher weiterhin eine wichtige Aufgabe, insbesondere der Funktionen der viralen Onkogene *E6* und *E7*, die für die Entstehung und Aufrechterhaltung des malignen Phänotyps HPV-positiver Tumorzellen entscheidend sind. Ein besseres Verständnis ihrer Wirkweise könnte auch zur Entwicklung innovativer, zielgerichteter Therapieoptionen gegen HPV-positive Tumore beitragen.

In der vorliegenden Arbeit wurden die zwei Wirtszellgene *FOXM1* und *CKS1B* als neue Zielgene von E6 und E7 identifiziert. Interessanterweise wird beiden Genprodukten onkogenes Potenzial in verschiedenen Krebsarten zugeschrieben. Die mRNA- und Proteinspiegel von FOXM1 und CKS1 werden durch E6 und E7 in HPV-positiven Zellen erhöht. Dies erfolgt über eine transkriptionelle Aktivierung der *FOXM1*- und *CKS1B*-Promotoren und wird durch die Hemmung des Tumorsuppressors p53 durch E6 und der Familie der „Pocket-Proteine“ durch E7 vermittelt. Dabei scheint die Interferenz mit dem transkriptionell repressiv wirkenden DREAM-Komplex Teil des Mechanismus zu sein, der zur Aktivierung der *FOXM1*- und *CKS1B*-Promotoren durch E6/E7 beiträgt.

Phänotypisch tragen die erhöhten CKS1-Spiegel zur Proliferation von HPV-positiven Tumorzellen bei und unterdrücken das Auftreten von Seneszenz. Während ein direkter Effekt von FOXM1 auf das zelluläre Wachstum HPV-positiver Zellen nicht beobachtet wurde, schützt FOXM1 HPV-positive Tumorzellen gegenüber genoxtischen Agenzien wie Chemotherapeutika. In wachstumsarretierten HPV-positiven Zellen werden die Spiegel von FOXM1 und CKS1 nicht reduziert, was im Einklang mit der Theorie steht, dass die Aktivierung der beiden Gene durch eine E6/E7-abhängige Interferenz mit dem repressorischen DREAM-Komplex hervorgerufen werden kann.

Diese Erkenntnisse tragen zu einem verbesserten Verständnis der HPV-induzierten Karzinogenese bei und erweitern den Wissenstand im Bezug auf die tiefgreifende

Modulation der molekularen Netzwerke der Wirtszelle durch E6 und E7. Sie zeigen außerdem auf, dass die Hemmung der Expression oder Funktion von FOXM1 und CKS1 eine attraktive Strategie zur Behandlung HPV-positiver Tumore darstellen könnte.

Publications & Presentations

Publications

K. Hoppe-Seyler, J. Mändl, S. Adrian, B. Kuhn, and F. Hoppe-Seyler, "Virus/Host Cell Crosstalk in Hypoxic HPV-Positive Cancer Cells," *Viruses*, vol. 9, no. 7, p. 174, Jul. 2017

S. Adrian, K. Hoppe-Seyler, F. Hoppe-Seyler, "FOXM1 and CKS1 – novel cellular targets of the HPV oncogenes", manuscript in preparation.

Presentations

S. Adrian, K. Hoppe-Seyler, F. Hoppe-Seyler, "FOXM1 and CKS1 – novel cellular targets for the HPV oncogenes", Retreat of the DKFZ Research Program 'Infection, Inflammation and Cancer', 21-23rd May 2017, Rastatt, Germany. Oral Presentation.

S. Adrian, K. Hoppe-Seyler, F. Hoppe-Seyler, "FOXM1 and CKS1 – novel cellular targets of the HPV oncogenes", 28th Annual Meeting of the Society for Virology, 14-17th March 2018, Würzburg, Germany. Poster Presentation.

S. Adrian, K. Hoppe-Seyler, F. Hoppe-Seyler, "FOXM1 and CKS1 – novel cellular targets for the HPV oncogenes", Retreat of the DKFZ Research Program 'Infection, Inflammation and Cancer', 28-30th May 2018, Rastatt, Germany. Oral Presentation.

S. Adrian, K. Hoppe-Seyler, F. Hoppe-Seyler, "FOXM1 and CKS1 – novel cellular targets for the HPV oncogenes", Helmholtz International Graduate School for Cancer Research PhD Retreat, 18-20th July 2018, Weil der Stadt, Germany. Oral Presentation.

S. Adrian, K. Hoppe-Seyler, F. Hoppe-Seyler, "FOXM1 and CKS1 – novel cellular targets of the HPV oncogenes", Helmholtz International Graduate School for Cancer Research PhD Poster Presentation, 12-16th November 2018, Heidelberg, Germany. Poster Presentation.

S. Adrian, K. Hoppe-Seyler, F. Hoppe-Seyler, "FOXM1 and CKS1 – novel cellular targets of the HPV oncogenes", 'Breakthroughs in Cancer Research and Therapy' – 14th Charles Rodolphe Brupbacher Symposium, 30th January – 1st February 2019, Zurich, Switzerland. Poster Presentation.

Acknowledgements

First of all, my thanks go to Prof. Dr. Felix Hoppe-Seyler for letting me conduct this PhD project in his group. Thank you for your personal supervision, the constant support and your valuable feedback at all times. Moreover, I also deeply thank Prof. Dr. Karin Hoppe-Seyler for many helpful discussions and critical insights.

In addition, I would like to thank Prof. Dr. Britta Brügger (University of Heidelberg) for being my first referee, chairing my examination commission and partaking in my TAC meetings with helpful ideas. My gratitude extends to Dr. Marco Binder (DKFZ) and Dr. Steeve Boulant (DKFZ) for taking their time to be part of my examination commission. I would also like to acknowledge Prof. Dr. Frank Rösl (DKFZ) for being a member of my TAC and for valuable comments.

To “my” student Julia Botta, whom I had the pleasure to supervise: I hope you equally enjoyed your time in our group. Thank you very much for joining my project and contributing to this dissertation. I am also very grateful to Ruwen Yang from the group of Prof. Rösl who generously provided me with protein extracts of her NOK cell lines.

A huge “Thank you” goes to the entire group of F065 for the amiable working atmosphere, your helpfulness in all matters and fun beyond the lab. I would especially like to thank Julia Bulkescher, Claudia Lohrey and Angela Holzer for their expert support in all technical questions. To all former and current members of F065, I thank you for the nice time we shared: Johanna Blase, Felicitas Boßler, Julia Braun, Antonia Däschle, Kristin Frensemeier, Anja Herrmann, Sofie Knoll, Bianca Kuhn, Julia Mändl, Tobias Strobel and Dongyung Yang. My gratitude also extends to Diana Schalk for support in administrative matters and Thomas Holz for help with all computer-related problems.

Finally, I need to thank the people who have supported me all the way during this dissertation: my family, my friends and Marcel. To every one of you: thank you for your support at all times and your motivation and encouragement whenever I needed it. I am very lucky to have you in my life.

CHAPTER 1

INTRODUCTION

1 Introduction

1.1 Human papillomavirus (HPV)

Members of the human papillomavirus family are small, non-enveloped double-stranded DNA viruses with a circular genome of about 8 kbp [1]. They infect mucosal and cutaneous surfaces via direct contact and belong to one of the most commonly transmitted infectious agents in humans. In fact, it is estimated that in the United States more than 80% of individuals have acquired at least one sexually-transmitted HPV infection by the age of 45 [2].

To date, more than 200 different HPV types are known, which are categorized into phylogenetic genera of which the alpha (mucosal tropism) and the beta genus (cutaneous tropism) are clinically most relevant and therefore best studied [3].

1.1.1 The HPV lifecycle

Infection with HPV occurs via microlesions in the epithelial surface so that the virus can reach basal cells where it establishes an infection. HPV genome replication requires actively dividing cells which are normally only found in the lower layers of the epithelium [4].

Depending on the HPV type, the HPV genome consists of eight to ten open reading frames (ORFs) which are grouped into an early and a late region. Early genes (E) are required for genome replication and maintenance while the two late genes *L1* and *L2* code for the viral capsid proteins [5]. E1 is a viral DNA helicase which together with the host cell replication machinery realizes viral genome amplification [6]. The E2 protein functions in transcriptional regulation and initiation of DNA replication [7]. E4 is predominantly expressed as an E1^E4 fusion protein and thought to contribute to genome amplification and virus synthesis and release [8]. The cellular activities of the transmembrane protein E5 are not entirely elucidated, however it has been implicated in modulating cellular signaling cascades and immune evasion [9] and is therefore regarded as potentially oncogenic [10]. The E6 and E7 proteins prevent cell cycle exit of the host cell during a productive infection since normally, after leaving the basal membrane to migrate to the epithelial surface, keratinocytes would start to differentiate and terminally end their replication. E6 and E7, however, inactivate proliferation-

suppressing host cell proteins and thus drive continuing replication (see also 1.2.2). The HPV lifecycle is completed when the virus is assembled in the upper epithelial layer and shed from the epithelial surface [1].

Initial and productive infections with HPV are most often cleared immunologically without causing apparent symptoms [11]. However, in some cases the viral genome can be maintained episomally at very low copy numbers in infected cells, a state called latency or persistent infection, from where it may be reactivated years to decades later [12].

1.2 HPV and cancer

Harald zur Hausen and his group were the first to demonstrate the transforming potential of a persistent HPV infection and its role in the development of cervical cancer [13, 14]. Since then, it was established that so-called high-risk HPV types cause almost 100% of cervical cancers and significant fractions of other anogenital cancers such as anal, vulvar or penile carcinomas [3]. In addition, a growing proportion of head and neck squamous cell carcinomas (HNSCC), especially of the oropharynx, are attributed to HPV. Carcinogenic (= high-risk) HPV types of the alpha genus include HPV16, -18, -31, -33, -35, -39, -45, -52, -58 and -59 [3]. Besides, a contribution of beta-HPVs to non-melanoma skin cancer is discussed [15].

In total, more than 600000 new cancer cases per year are caused by infections with mucosal HPV types. This amounts to 4.5% of the global cancer incidence [16].

1.2.1 Pathogenesis of cervical cancer

In rare cases, persistent infection with HPV can give rise to carcinomas through a multi-step process which is mainly driven by the viral oncogenes *E6* and *E7.* HPV-induced cervical carcinogenesis typically requires several decades from the first infection until the onset of cancer, during which an increasing number of mutations accumulate in the host cell. Therefore, cervical cancer is most often diagnosed in women beyond 45 years of age.

At the uterine cervix, pre-cancerous lesions can be detected years before malignancy is established. They are termed cervical intraepithelial neoplasia (CIN) and are classified from grade 1 to 3 according to their increasing state of dedifferentiation and enhanced

risk of developing invasiveness [11]. Notably, most CIN1 lesions regress spontaneously and only very few cases progress to CIN2-3 and later to cancer (see figure 1). During the progression from CIN2 to CIN3, viral genome integration into the host chromosome can occur [17]. This is typically associated with the loss of many viral genes, while the oncogenes *E6* and *E7* are regularly retained [18]. The genome integration of oncogenic HPVs can result in further elevated *E6* and *E7* expression, however also lesions with episomally-maintained HPV genomes can be characterized by expressing increased E6 and E7 levels during the progression of transformation [1].

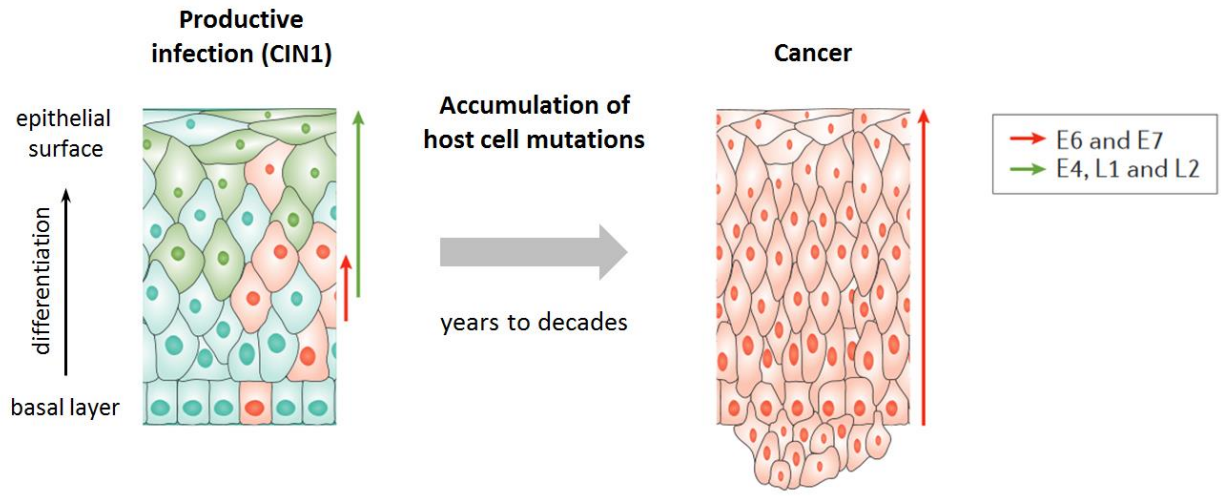

Figure 1: Progression from a productive HPV infection to invasive cancer. In benign lesions, E6 and E7 are primarily expressed in the basal and parabasal epithelial layers to stimulate host cell proliferation throughout the differentiation programme. In surficial layers, E4 and late proteins are predominantly expressed to prepare virus assembly and shedding. However, during the progression to cancer, E6/E7 expression becomes more and more deregulated while the expression of other viral proteins is usually suppressed. Figure modified from [3].

1.2.2 Oncogenic properties of E6 and E7

E6 and E7 are rather small viral proteins of ca. 150 and 100 amino acids, respectively, that produce and sustain the malignant phenotype of HPV-driven cancers. It has been shown that overexpression of E6/E7 is sufficient to cause immortalization of keratinocytes *in vitro* [19, 20] and E6/E7 suppression in cervical cancer cell lines leads to a rapid and efficient induction of senescence, an irreversible proliferative stop [21, 22]. Hence, it was a central dogma that *E6* and *E7* are required to be expressed in cervical carcinoma cells at all times, making them so-called "oncogene-addicted". Notably in recent years an exception emerged in tumor hypoxia, where low intratumoral

oxygen levels downregulate E6/E7 expression. Yet under this condition, the cells evade senescence and evoke a reversible state of cellular dormancy [23, 24, 25].

E6 and *E7* are transcribed from a common promoter into a bicistronic mRNA which then yields either of the two gene products after a complex splicing process [26]. Both oncoproteins induce and support tumorigenesis through a variety of functions and interaction partners and together promote all of Hanahan's and Weinberg's 'hallmarks of cancer', being (I) sustaining proliferative signaling, (II) evading growth suppressors, (III) activating invasion and metastasis, (IV) enabling replicative immortality, (V) inducing angiogenesis and (VI) resisting apoptosis [27, 28].

E7's primary function is attributed to the stimulation of host cell proliferation, mainly through its binding to the members of the pocket protein family, pRb, p130 and p107. This results in the displacement of other binding partners from the pocket proteins, such as the proliferation-inducing transcription factor E2F1 which is typically controlled through and inactivated by association with pRb [29]. This uncontrolled proliferation would usually result in the activation of checkpoint proteins such as p53 which then guide the cell towards apoptosis, a controlled form of cell death, or senescence, thereby eliminating it from the pool of proliferating cells.

However, in HPV-positive cells, p53 is inactivated by the E6 oncoprotein: E6 interacts with the E3-ubiquitin ligase E6-AP and p53 to form a heterotrimer which enables the proteasomal degradation of p53 [30]. The induction of apoptosis or senescence is thereby efficiently suppressed. In addition, E6 proteins of the high-risk HPV types also contain a PDZ binding motif at their C-terminal end. Thus, in contrast to low-risk type E6 proteins, they can modulate a multitude of cellular proteins containing PDZ domains which is also thought to contribute significantly to the transforming potential of E6 [31].

Other effects of E6/E7 expression include epigenetic alterations, changes in miRNA expression patterns and the induction of genomic instability [32, 33]. E6 and E7 therefore cooperate to strongly enhance proliferation in HPV-positive cells while at the same time inactivating key tumor suppressor pathways (see figure 2).

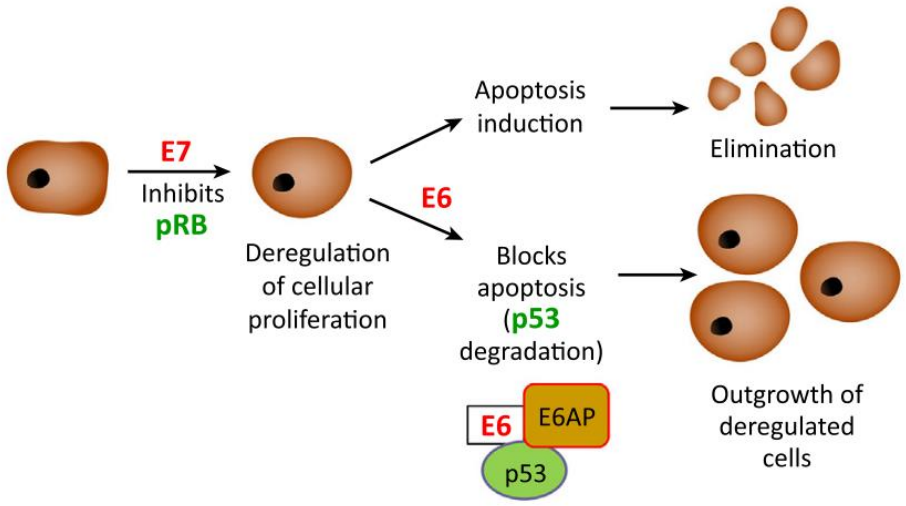

Figure 2: The HPV oncoproteins E6 and E7 cooperate in tumorigenesis. Cellular proliferation is deregulated by the inhibition of pRb through E7. The aberrant cellular behaviour would normally lead to the induction of apoptosis (or senescence; not shown) by p53 upregulation. However in the presence of E6, p53 is degraded leading to a blockage of apoptosis and thereby allowing the outgrowth of deregulated cells. Figure from [34].

1.2.3 Prevention and treatment of cervical cancer

Due to the large time frame between the establishment of detectable forms of pre-cancer and the progression to carcinoma, monitoring and if necessary treatment of CIN lesions has proven high efficiency for the prevention of cervical cancer. Regular screening programs for women have been enabled and led to a drastic decrease in cervical cancer numbers in developed countries [35]. For decades, the Pap smear (named after its inventor George Papanicolaou) has been the gold standard for early detection of cervical lesions, but is now more and more replaced by the more accurate HPV DNA testing [36].

After the discovery of HPV as the causative agent for cervical cancer, prophylactic vaccines based on virus-like particles comprised of the L1 capsid protein have been developed. To date, three different formulations are available: Cervarix by GlaxoSmithKline protects against infection with HPV16 and -18 which together account for more than 70% of cervical carcinomas [37]. Gardasil (Merck) additionally confers protection against the two low-risk types HPV6 and -11 which are the main causes of genital warts [38]. A new nonavalent vaccine, Gardasil9 (Merck), additionally immunizes against infection with HPV31, -33, -45, -52 and -58 and is thereby hoped to prevent more than 90% of cancer-linked HPV infections [39].

If prevention failed and cancer has arisen, surgical excision of the tumor and adjuvant radio- and chemotherapy is the primary choice of treatment.

1.2.4 Why study additional HPV target genes?

The existence of efficient prophylactic HPV vaccines makes cervical cancer a disease that is, in theory, completely preventable. Nevertheless, incidence rates of cervical and other HPV-associated cancers are estimated to continue to rise globally over the next years due to the increasing population worldwide [36]. Overall vaccination rates are low, even in industrialized nations, and low-income countries often lack the infrastructure to provide comprehensive vaccination and screening programs. Yet here, HPV prevalence in the population is particularly high [36]. Moreover, the existing vaccines are purely prophylactic and offer no profit for individuals who have already acquired a persistent infection. In the light of ca. 250000 deaths annually attributed to cervical cancer (in 2012) the need for new therapeutic strategies against HPV-driven cancers remains high [3].

While E6/E7 would, in principle, represent ideal antigens for a therapeutic vaccination approach or other HPV oncogene-targeting therapies, so far no E6/E7-specific treatment has reached the market. The identification and characterization of novel downstream targets of E6/E7 should therefore not only result in a better understanding of HPV-induced tumorigenesis but could also lead to the discovery of potential HPV-linked cellular vulnerabilities that might be exploited therapeutically.

1.2.5 Transcriptome analyses for the identification of novel HPV targets

In order to gain a deeper comprehension of HPV-driven carcinogenesis, Kuner *et al* have performed a transcriptome-based microarray in HPV18-positive HeLa cells, where *E6/E7* had been knocked down by RNA interference (RNAi) [40]. Differentially regulated genes under these conditions possibly constitute cellular targets of the HPV oncogenes, since they react to changes in HPV oncogene expression. Upon *E6/E7* knockdown, 648 genes were found to be differentially expressed, of which 360 were downregulated and 288 upregulated.

FOXM1 and *CKS1B* are two cellular genes that showed a repression of 50% and 70% respectively at their mRNA expression levels, indicating that E6/E7 expression could be linked to the activation of both genes. This notion is of interest since both *FOXM1* and *CKS1B* have been discussed before to possess oncogenic potential, making them

interesting putative targets for E6/E7 during HPV-induced carcinogenesis. Additionally, *CKS1B* expression was found to be stimulated by FOXM1 [41], positioning it as a potential downstream target of FOXM1 and thereby possibly connecting both genes in a common pathway. *FOXM1* and *CKS1B* were therefore chosen as promising candidates for the study of novel HPV target genes and the cellular consequences of their modulation by E6/E7.

1.3 The Forkhead Box Transcription Factor M1 – FOXM1

FOXM1, also known as Trident, FKHL-16, MPP2 or HFH-11, is a member of the evolutionary conserved forkhead box family of transcription factors that all share similarities in their so-called 'winged helix' DNA binding domain [42]. FOXM1 is composed of a central DNA-binding domain, a strong C-terminal transactivation domain and a N-terminal autoinhibitory domain [43–45]. Differential splicing of the *FOXM1* mRNA gives rise to three isoforms, termed FOXM1a, -b and -c, of which FOXM1b and FOXM1c are transcriptionally active and FOXM1a is considered transcriptionally inactive [45, 46].

FOXM1 expression is regarded as being strictly proliferation-dependent [47]. Indeed, detectable levels of FOXM1 mRNA or protein are only found in embryonic or strongly proliferating adult tissues, but not in quiescent or terminally differentiated cells [48–50]. In addition, FOXM1 levels are extremely low in cells that have been arrested by serum starvation or undergone senescence [48, 51]. In proliferating cells, FOXM1 expression is cell cycle-dependent, with an upregulation of FOXM1 expression starting in late G1 phase and peaking at the G2/M phase transition [52]. The same dynamic is described for FOXM1 activity which results from increasing multi-site phosphorylation during progression of the cell cycle, thereby relieving repression of the transactivation domain by the FOXM1 autoinhibitory domain [53–55].

While some research groups have proposed the existence of a FOXM1 autoregulatory loop by which FOXM1 induces and potentiates its own transcription [56, 57], others could not verify this proposition [58]. It is however well established that FOXM1 levels are transcriptionally repressed by p53 and activated by E2F1 after its release from pRb [59–63]. These observations are in line with FOXM1's central role in the cell

cycle-dependent MuvB-B-Myb-FOXM1 complex (MMB-FOXM1) to activate timely transcription of G2/M phase genes [64].

FOXM1 was found indispensable for embryonic development, since *FOXM1*$^{-/-}$ knockout mice die before birth with severe developmental defects in heart, liver and lung [52, 65, 66]. *FOXM1* knockdown in primary mouse embryonic fibroblasts (MEFs) resulted in heavy polyploidy, delayed entry into mitosis and disturbed chromosome segregation [67]. These results underline the essential role for FOXM1 in coordinating cell cycle progression, specifically of the G2/M phase transition.

1.3.1 FOXM1 in cancer

Highly elevated levels of FOXM1 transcript and protein have been found in tumors originating from many different tissues, including a. o. breast, liver, pancreatic, colorectal, lung, head and neck and cervical cancers [68]. High FOXM1 levels frequently correlate with a more severe course of disease, advanced tumor stage and a significantly worsened clinical prognosis [69]. While all three splice variants were shown to be equally upregulated in cancer, a differential contribution of single isoforms to the oncogenic phenotype is discussed, however with inconsistent results [58, 70, 71]. Overall, FOXM1 is one of the most commonly overexpressed genes across different human tumor entities [72]. Correspondingly, it forms part of the CIN25 gene signature that predicts outcome for multiple cancer types based on the expression of 25 genes related to chromosomal instability and of the 'cervical cancer proliferation cluster' for the prediction of early progression of cervical carcinomas [73, 74]. In some reports, an 'addiction' of proliferating tumor cells to FOXM1 is postulated [75, 76].

FOXM1 exerts its tumorigenic properties via the modulation of a multitude of cellular processes. Being under the control of two tumor suppressors that are frequently mutated or otherwise inactivated in cancers, p53 and pRb, regulation of FOXM1 is usually aberrant in transformed cells. Mutant p53 was found to elevate FOXM1 expression, in contrast to its wildtype counterpart which has a repressive effect on the *FOXM1* promoter [77, 78]. Apart from its general proliferation-promoting effect, FOXM1 also further deregulates cellular proliferation, for example via activation of the oncogene *MYC* [79, 80]. Moreover, many components of the DNA damage repair (DDR) machinery are reported FOXM1 targets, resulting in enhanced DDR which can increase resistance to apoptosis, for example in response to treatment with chemotherapeutic agents [59, 81–84]. Furthermore, FOXM1 is described to potentially confer replicative immortality by

the suppression of senescence and thus stem cell-like properties to FOXM1-overexpressing cells [51, 85]. The vascular endothelial growth factor (VEGF) is another FOXM1 target gene, linking FOXM1 to the stimulation of angiogenesis [86, 87]. In addition, high FOXM1 expression was found to increase invasion and metastasis and promote epithelial-mesenchymal transition, for instance via upregulation of the matrix metalloproteinases MMP2 and -9 [88, 89]. Thus, similar to the HPV oncogenes, *FOXM1* also promotes all hallmarks of cancer and can be regarded as a *bona fide* cellular oncogene [90].

A tumor-promoting role for FOXM1 has also been discussed in the pathogenesis of cervical cancer: Modulation of FOXM1 levels by the HPV oncogenes has been reported, with different modes of action observed: Lüscher-Firzlaff *et al* proposed a direct interaction between HPV16 E7 and FOXM1 which increases transactivational activity of FOXM1 [91] while Jaiswal *et al* report a stabilization of FOXM1 protein levels by E7 expression, due to the inhibition of FOXM1 SUMOylation through E7 [92]. In contrast, two other publications show an activation of FOXM1 by E6, but not E7, in oral keratinocytes [93, 94]. Interestingly, cellular FOXM1 levels increase strongly from normal cervical epithelium over CIN lesions to squamous cell carcinoma [95].

1.4 The cyclin-dependent kinases regulatory subunit 1B –CKS1

The family of CKS proteins is evolutionary highly conserved in eukaryotes and recognized as an important regulator of orderly cell cycle progression. Its first member was identified in the fission yeast *Schizosaccharomyces pombe* and termed Suc1 (suppressor of cdc2) [96]. In humans two orthologues, CKS1 (gene name: *CKS1B*) and CKS2, have been identified that both are 79 amino acids long and share a sequence homology of 81% [97]. Although they have been found to substitute for each other in murine knockout studies [98], they nevertheless also have additional independent functions [99].

Both CKS proteins were found to bind tightly to cyclin-dependent kinases (CDKs) and are thought to stimulate their activities. However, the exact mechanism of CDK modulation by CKS proteins in mammals remains elusive. CKS1 and CKS2 are indispensable for proper cell cycle progression [100], as can also be seen from *CKS1B*$^{-/-}$ *CKS2*$^{-/-}$ double knockout mice which die very early during embryogenesis [98]. CKS

mRNA and protein levels start to rise in late G1 with a first peak before the entry into S phase. A second peak occurs at the transition from G2 to M phase [97, 101].

In addition, CKS1 interacts with the F-Box-protein Skp2 in the Skp1-Cullin1-F-box protein (SCF) ubiquitin ligase complex. This SCF^{Skp2} complex requires CKS1 as an adaptor protein to bind and ubiquitinate its targets, the most prominent being the cell cycle inhibitor p27 [102, 103]. This leads to the proteasomal degradation of ubiquitinated p27 at the G1/S phase transition and therefore timely progression of the cell cycle. Other ubiquitination targets of SCF^{Skp2}-CKS1 include p21 and p130 [104, 105] which both have important functions in cell cycle regulation as well. This role of CKS1 is not shared by CKS2.

A *CKS1*$^{-/-}$ knockout does not lead to lethality in mice, although they have a smaller body size that is attributed to reduced cell division as a result of p27 accumulation [103]. Mouse embryonic fibroblasts devoid of CKS1 also show a lower proliferation and undergo premature senescence [103]. But also p27-independent functions of CKS1 during cell cycle regulation have been demonstrated [106]. Additionally, regulatory roles of CKS1 as a transcriptional activator and in growth signaling have also been discussed [107, 108].

1.4.1 CKS1B as a potential proto-oncogene

CKS1B transcript and protein levels are elevated in many human cancers, such as gastric, colorectal, hepatocellular, breast, bladder and oral squamous cell carcinomas a. o. [109]. This overexpression is generally linked to a worse prognosis which is attributed to CKS1's proliferation-promoting effects [110]. *CKS1B* is therefore discussed as a cellular proto-oncogene which when deregulated contributes to tumorigenesis [111, 112].

CKS1B knockdown inhibits proliferation and induces apoptosis in cell lines derived from lung, breast and liver cancers [112, 113, 114]. *Vice versa*, elevated levels of CKS1 lead to failure of the intra-S-phase checkpoint in response to replication stress, which could support the expansion of (pre-)malignant cells [115]. This may pose a potential therapeutic vulnerability of CKS1-overexpressing cancer cells, as a selective sensitization to DNA damaging agents that induce replication stress (such as 5-fluorouracil or methotrexate) was demonstrated [116, 117].

It is not well understood what causes the elevated CKS1 expression in different types of cancers. An increase of *CKS1B* promoter activity has been shown in response to the *MYC* oncogene in B-cell lymphoma in mice, although the promoter lacks a recognized Myc

binding site [118]. Upregulation of *CKS1B* by the FOXM1 transcription factor and a repressive effect of p53 have been reported as well [41, 101].

1.5 Research Objectives

Despite considerable advances in the fields of prevention and treatment of HPV-associated cancers, there remains an urgent need for a better understanding of the molecular mechanisms of HPV-driven carcinogenesis. A previous transcriptome analysis raised the possibility that *FOXM1* and *CKS1B* may represent new cancer-linked cellular targets for activation by the HPV oncogenes.

This study therefore aims at

(I) validating whether and how *FOXM1* and *CKS1B* are modulated by the E6/E7 oncoproteins. *E6/E7* knockdown and overexpression studies in cervical cancer cells and immortalized keratinocytes will be conducted and the resulting effects on *FOXM1* and *CKS1B* expression will be assessed.

(II) analyzing a possible transcriptional regulation of the *FOXM1* and *CKS1B* promoters by the HPV oncogenes, using luciferase reporter constructs.

(III) elucidating if FOXM1 and CKS1 are situated downstream of one another in cervical cancer cells or whether they constitute independent target genes of HPV.

(IV) characterizing the phenotypic effects of FOXM1 and CKS1 activation in cervical cancer cells. This will include knockdown studies followed by proliferation and cell death assays, such as cell cycle analyses, senescence assays, apoptosis detection, colony formation assays and live-cell imaging. In addition, a special focus will be laid upon the cellular effects of FOXM1 modulation under conditions of DNA damage.

Overall, the present study aims to elucidate the underlying mechanisms and functional consequences of the E6/E7-linked elevation of FOXM1 and CKS1 expression in HPV-positive tumor cells. This should improve our concepts of the

molecular mechanisms of HPV-induced carcinogenesis and may pave the way for new therapeutic options.

CHAPTER 2

RESULTS

2 Results

2.1 *FOXM1* and *CKS1B* as new candidate target genes of HPV

A transcriptome array identified *FOXM1* and *CKS1B* as new candidate target genes of the HPV oncoproteins in cervical cancer since they exhibited significantly repressed mRNA levels as a response to *E6/E7* knockdown in HeLa cells [40]. This would suggest that *FOXM1* and *CKS1B* are upregulated upon E6/E7 expression in HPV-positive cancer cells.

2.1.1 FOXM1 and CKS1 are downregulated upon *E6/E7* knockdown

First, I aimed at validating the results from the microarray by independent experimental assays. *E6* and *E6/E7* knockdowns using siRNAs in three different HPV-positive cervical cancer cell lines were performed and FOXM1 and CKS1 expression was evaluated at the protein and the mRNA level.

E6 and E7 are derived from a common transcript and their mRNA is subjected to a complex splicing process before yielding the respective gene products. While conjunctive knockdown of *E6/E7* or knockdown of *E6* alone have been achieved, so far it has been technically not feasible to specifically knock down *E7* alone [119, 120]. Conclusions concerning the effects of *E7* silencing alone may therefore only be indirectly drawn from a combination of experiments conducting *E6* and *E6/E7* knockdowns and therefore need to be interpreted with some caution.

As shown in figure 3A, depletion of E6/E7 by RNAi caused a strong downregulation of FOXM1 and CKS1 protein levels in both HPV18-positive HeLa and HPV16-positive SiHa cells, as detected by immunoblot analyses. On the contrary, FOXM1 and CKS1 levels were not affected by *E6* knockdown alone in HeLa cells and only showed a slight reduction in SiHa cells under these conditions. These results were mirrored on the mRNA level, as seen in RT-qPCR experiments (fig. 3B). Successful repression of *E6* or *E6/E7* was verified by specific antibodies and the reconstitution of p53 (fig. 3A) and on the RNA level by the use of specific primer pairs for E6 or E6/E7 transcripts (fig. 3B).

By use of the HeLa “p53 null” cell line which stably expresses an shRNA against p53 [121] and efficiently silences the *TP53* gene (fig. 3A), a requirement for p53 reconstitution to mediate FOXM1 or CKS1 downregulation could be precluded: FOXM1

or CKS1 protein and RNA levels in the *TP53* knockdown cell line reacted with the same expression patterns as HeLa cells in which *TP53* was not silenced (fig. 3A, B).

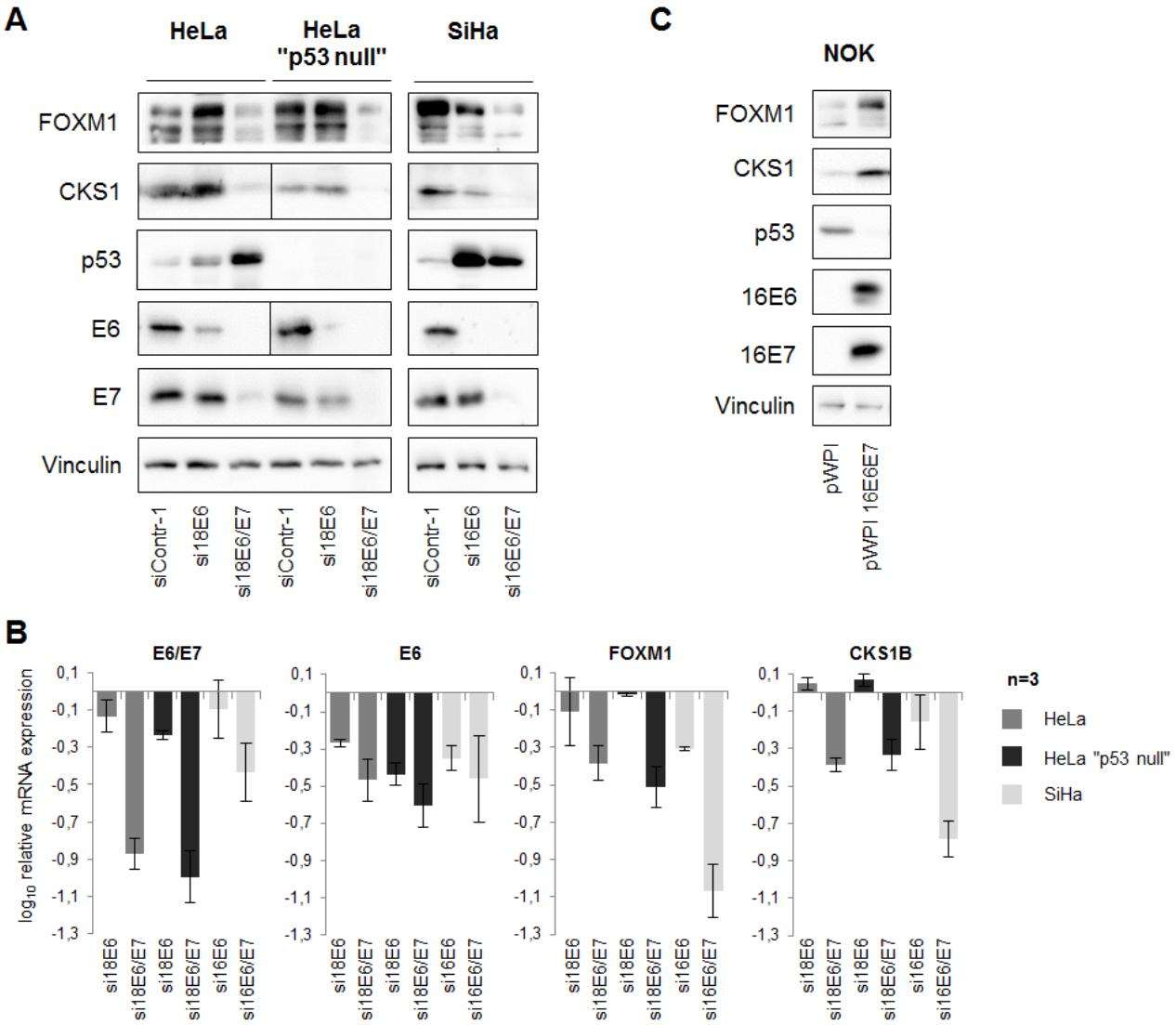

Figure 3: FOXM1 and CKS1 levels are upregulated by E6/E7 expression. A, B: HeLa, HeLa "p53 null" and SiHa cells were treated with siRNAs against E6 or E6/E7. Protein levels were determined by Western blot analyses (A). Relative mRNA expression of *E6/E7, E6, FOXM1* and *CKS1B* was determined using RT-qPCR; shown is the $\log_{10}$ of the mean expression relative to siContr-1 (=0; not depicted) with standard deviations of 3 independent experiments (B). siContr-1: control siRNA. **C:** Stably transduced NOK cells were analysed for their protein levels by Western blot. Vinculin: loading control.

2.1.2 E6/E7 increase expression of FOXM1 and CKS1 in keratinocytes

If *FOXM1* and *CKS1B* are indeed target genes of E6/E7 and are repressed by *E6/E7* silencing, then ectopic expression of E6/E7 in HPV-negative cells should result in upregulation of the two genes. To that end, human telomerase reverse transcriptase

(hTERT)-immortalized normal oral keratinocytes (NOKs), which had been stably transduced with HPV16E6/E7, were analysed for their FOXM1 and CKS1 protein levels. This model system is of particular interest and significance, since mucosal keratinocytes constitute the primary host cells for high-risk HPV infection [122]. As recognizable from figure 3C, FOXM1 and CKS1 levels were clearly increased after expression of HPV16 E6 and E7 in NOKs. This observation further supports the assumption that *FOXM1* and *CKS1B* represent novel target genes of HPVE6/E7 and are activated by the viral oncogenes.

2.2 FOXM1 and CKS1 are transcriptional targets of E6 and E7

2.2.1 The *FOXM1* promoter is activated by E6 and E7

To further analyse the effect of E6 and E7 expression on FOXM1, *luciferase* reporter assays were conducted in order to assess a possible effect on the *FOXM1* transcriptional reporter. Two promoter constructs of *FOXM1* have been tested, the 2.4 kbp full-length promoter termed pGL3-FOXM1long, and a shorter, ca. 300 bp variant named pGL3-FOXM1 (fig. 4A). Both reporters showed considerable activity over the pGL3 basic backbone, with pGL3-FOXM1 being much stronger activated (to ca. 100-fold) than pGL3-FOXM1long, which might be due to the existence of potential negative regulatory elements in the longer fragment.

Next, the reporter constructs were employed for *E6* and *E6/E7* knockdown experiments in HeLa to test for their transcriptional activity upon viral oncogene repression. Mirroring the effects on protein and mRNA level presented in figure 3, the pGL3-FOXM1 promoter construct showed a strong decline in promoter activity after *E6/E7* knockdown, while it was unaffected by *E6* knockdown alone (fig. 4B). A similar tendency was observed using pGL3-FOXM1long as reporter, however the effects were weaker, potentially due to the much lower basal promoter activation of the construct. Therefore, pGL3-FOXM1 was chosen as *FOXM1* promoter construct for further experiments. Also, previous analyses by Korver *et al* had demonstrated that the pGL3-FOXM1 promoter fragment retains inducibility during cell cycle progression, just as pGL3-FOXM1long, and may therefore be regarded as containing the essential promoter regions of *FOXM1* [42].

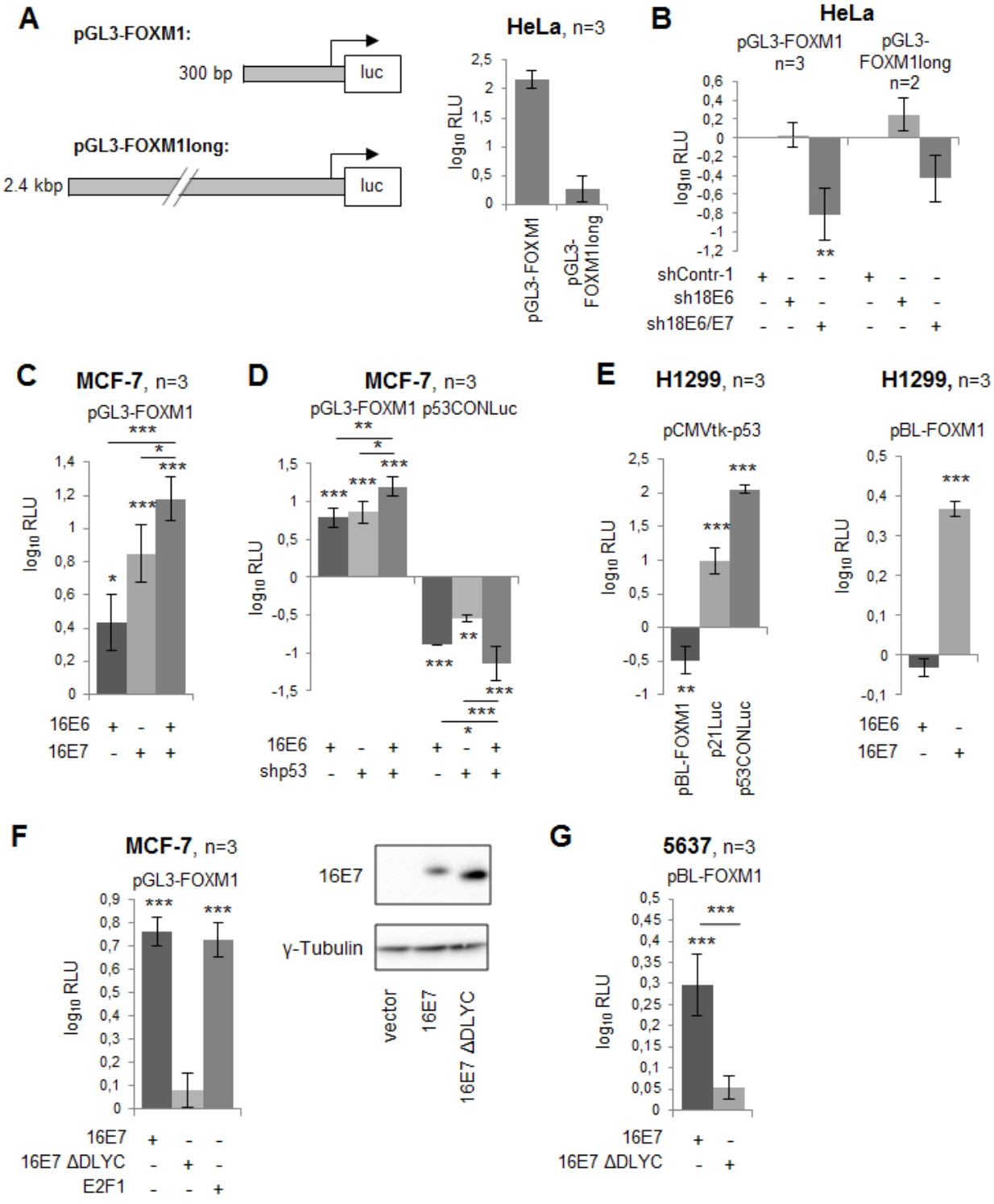

Figure 4: The *FOXM1* promoter is responsive to activation by E6 and E7. A: Schematic representation of the two promoter constructs pGL3-FOXM1 and pGL3-FOXM1long and their basal expression levels in HeLa in luciferase reporter assays; control for normalization: pGL3 basic. **B:** Luciferase reporter assays of pGL3-FOXM1 and pGL3-FOXM1long in HeLa co-transfected with pSUPER-shContr-1, pSUPER-sh18E6 or pSUPER-sh18E6/E7; control for normalization: pGL3-FOXM1 or pGL3-FOXM1long + pSUPER-shContr-1. shContr-1: control shRNA. **C:** Luciferase reporter assays of pGL3-FOXM1 in MCF-7 co-transfected with pBCH-16E6 and/or pCMV-16E7-HA/flag; control for normalization: *(continued on next page)*

Having shown that the *FOXM1* promoter is responsive to *E6/E7* knockdown, overexpression experiments of E6 and E7 in HPV-negative cells were performed next. To that end, MCF-7 breast cancer cells were chosen, because they are wildtype for p53 and no mutations in either of the three pocket proteins pRb, p130 and p107, the main downstream targets of E7, have been described [123]. pGL3-FOXM1 was significantly activated by ectopic expression of 16E6, 16E7 or both oncogenes in MCF-7 cells (fig. 4C). Interestingly, whereas the activity of the *FOXM1* promoter was not affected by knockdown experiments specifically targeting *E6* (fig. 4B), ectopic E6 expression alone was sufficient to activate the *FOXM1* promoter. The combined overexpression of E6 and E7 yielded an over-additive activation in comparison to the single oncoproteins.

In order to elucidate which intracellular pathways mediate promoter activation by E6, a shRNA against p53 was employed. Knockdown of *TP53* led to a similar activation as overexpression of E6 in MCF-7 (fig. 4D), arguing for a repressive effect of p53 on the *FOXM1* promoter which is relieved by the introduction of E6. Notably, concomitant silencing of *TP53* and expression of E6 resulted in significantly higher *FOXM1* promoter activation in comparison to the single constructs. The p53CONLuc reporter was used to verify successful downregulation of p53 (fig. 4D). This plasmid carries a p53 consensus binding site upstream of the *luciferase* gene [124]. Also here, simultaneous expression of

---

(Figure legend to fig. 4 continued) pGL3-FOXM1 + pCMV-HA/flag + pBCH. **D:** Luciferase reporter assays of pGL3-FOXM1 or pGUP.PA.8-p53CONLuc in MCF-7 co-transfected with pBCH-16E6 and/or pSUPER-shp53; control for normalization: pGL3-FOXM1 or pGUP.PA.8-p53CONLuc + pSUPER-shContr-1 + pBCH. shContr-1: control shRNA. **E, left panel:** Luciferase reporter assays of pBL-FOXM1, p21Luc or pGUP.PA.8-p53CONLuc in H1299 co-transfected with pCMVtk-p53; control for normalization: pBL-FOXM1, p21Luc or pGUP.PA.8-p53CONLuc + pCMVtk. **E, right panel:** Luciferase reporter assays of pBL-FOXM1 in H1299 co-transfected with pBCH-16E6 or pCMV-16E7-HA/flag; control for normalization: pBL-FOXM1 + pBCH or pCMV-16E7-HA/flag. **F:** Luciferase reporter assays of pGL3-FOXM1 in MCF-7 co-transfected with pCMV-16E7-HA/flag, pCMV-16E7ΔDLYC-HA/flag or pCMV-E2F1; control for normalization: pGL3-FOXM1 + pCMV-HA/flag. Western blot of 16E7 overexpression in MCF-7, γ-tubulin: loading control. **G:** Luciferase reporter assays of pBL-FOXM1 in 5637 co-transfected with pCMV-16E7-HA/flag or pCMV-16E7ΔDLYC-HA/flag; control for normalization: pBL-FOXM1 + pCMV-HA/flag. Given is the $\log_{10}$ of the mean RLUs (relative luciferase units) relative to the respective control (=0; usually not depicted). Error bars represent standard deviations. Asterisks indicate statistically significant differences to the respective control as determined by one-way ANOVA (***$p < 0.001$, **$p < 0.01$, *$p < 0.05$).

shp53 and E6 decreased activity of p53CONLuc more efficiently than either construct alone, indicating that the cellular p53 level was further decreased by the double transfection.

The p53-negative non-small cell lung cancer (NSCLC) cell line H1299 was used to further characterize the effect of p53 expression on the *FOXM1* transcriptional region. This cell line carries a homozygous partial deletion of *TP53* and does not express any p53 protein [125]. Since, for unknown reasons, the pGL3 basic backbone was found to respond considerably to p53 in overexpression experiments in H1299 cells, the *FOXM1* promoter construct was cloned into the pBL backbone [126] which is much less p53-responsive (data not shown), yielding pBL-FOXM1. Overexpression of p53 in H1299 cells inhibited pBL-FOXM1 activity, further strengthening the notion that the *FOXM1* promoter can be repressed by p53 (fig. 4E). Under the same experimental conditions, two positive controls for p53-mediated transactivation, the p53-responsive reporter constructs p21Luc and p53CONLuc were highly upregulated. The absence of p53 in H1299 was also linked to the inability of 16E6 to activate pBL-FOXM1, while the activating effect of 16E7 was preserved (fig. 4E). Collectively, these data indicate that the E6 oncoprotein is able to activate transcription of the *FOXM1* gene by inducing the degradation of p53, whereby p53's repressive effect on the *FOXM1* promoter is alleviated.

The E7 oncoprotein sequesters pocket proteins like pRb or p130, thereby preventing them to bind to their targets, where they usually have inhibitory effects. Notably, FOXM1 promoter activation by E7 in MCF-7 cells was abrogated when the pocket protein-binding-deficient mutant 16E7ΔDLYC was expressed instead of wildtype 16E7 (fig. 4F). To exclude that decreased *FOXM1* promoter stimulation by 16E7ΔDLYC was due to a lower expression level of the mutant, protein expression of 16E7 and 16E7ΔDLYC was assessed by Western blot.

A main target of pRb is the pro-proliferative transcription factor E2F1 [29]. Expression of E7 typically leads to an activation of E2F1 target genes, because E2F1 is released from pRb when the pocket protein is bound by E7. Indeed, the *FOXM1* promoter was found responsive to overexpression of E2F1 (fig. 4F). However, also pocket proteins other than pRb appear able to mediate *FOXM1* promoter activation via E7: In the pRb-negative bladder cancer cell line 5637, increased activity of the reporter construct was still conferred by E7 expression and appeared to require the ability to bind to pocket

proteins, since *FOXM1* promoter activation was abrogated upon mutation of the pocket protein binding domain of E7 (fig. 4G).

In conclusion, the *FOXM1* promoter was shown to be responsive to activation by the HPV oncogenes *E6* and *E7*. Activation by E6 is hereby likely mediated by inducing the degradation of p53, which mitigates the repressive effect of p53 on the *FOXM1* transcriptional promoter. While the pRb-E2F1 axis certainly plays a role in inducing *FOXM1* transcriptional activity via E7, also the interference with the function of the other pocket proteins, p130 and p107, can mediate E7-induced promoter activation.

2.2.2 The *CKS1B* promoter is activated by E6 and E7

To analyse the regulation of the *CKS1B* promoter, a 550 bp fragment upstream of the *CKS1B* transcription start site was cloned from HeLa genomic DNA into the pBL reporter plasmid, thereby obtaining pBL-CKS1B. (The detailed cloning strategy is delineated in Materials & Methods, section 4.4.3.) pBL-CKS1B was tested for its activity in HeLa and yielded luciferase values 100-200 times above the pBL basic vector (data not shown).
As depicted in figure 5A, pBL-CKS1B was significantly inhibited after *E6/E7* knockdown, while *E6* knockdown led to a slight but insignificant upregulation of the promoter activity. *Vice versa*, pBL-CKS1B was stimulated by overexpression of 16E6, 16E7 or both in MCF-7 (fig. 5B). Collectively, these data indicate that the HPV oncogenes can activate the *CKS1B* promoter. Concurrent expression of E6 and E7 resulted in an additive effect on promoter activation (fig. 5B).

Upregulation of pBL-CKS1B by E6 was mimicked by knockdown of *TP53* (fig. 5C), indicating the p53 downregulation leads to the stimulation of the CKS1B promoter. Concomitant expression of E6 and shp53 resulted in significantly higher luciferase values of the pBL-CKS1B construct than E6 or shp53 expression alone. Interestingly, and in contrast to the *FOXM1* promoter, the *CKS1B* promoter remained inducible by E6 overexpression in the absence of p53 in H1299 cells (please compare fig. 5D and fig. 4E). These findings suggest that the E6-mediated activation of *CKS1B* expression is not necessarily only induced via p53 downregulation, which could be a cell-line specific effect. However, degradation of p53 by E6 still has an activating effect on pBL-CKS1B (fig. 5C).

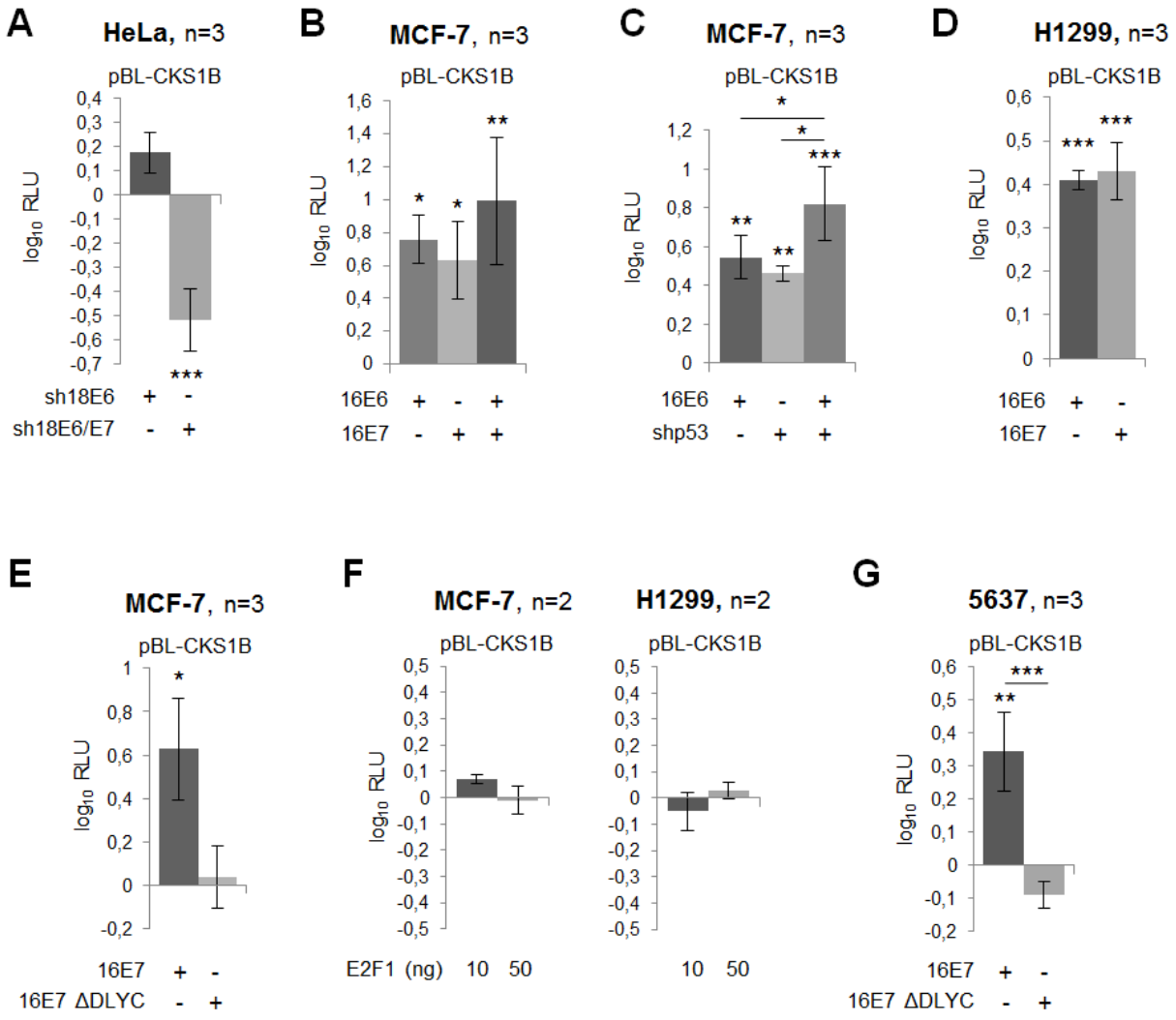

Figure 5: The transcriptional promoter of *CKS1B* is activated by E6 and E7. A: Luciferase reporter assays of pBL-CKS1B in HeLa co-transfected with pSUPER-sh18E6 or pSUPER-sh18E6/E7; control for normalization: pBL-CKS1B + pSUPER-shContr-1. shContr-1: control shRNA. **B:** Luciferase reporter assays of pBL-CKS1B in MCF-7 co-transfected with pBCH-16E6 and/or pCMV-16E7-HA/flag; control for normalization: pBL-CKS1B + pBCH + pCMV-HA/flag. **C:** Luciferase reporter assays of pBL-CKS1B in MCF-7 co-transfected with pBCH 16E6 and/or pSUPER-shp53; control for normalization: pBL-CKS1B + pBCH + pSUPER-shContr-1. shContr-1: control shRNA. **D:** Luciferase reporter assays of pBL-CKS1B in H1299 co-transfected with pBCH-16E6 or pCMV-16E7-HA/flag; control for normalization: pBL-CKS1B + pBCH or pCMV-HA/flag. **E:** Luciferase reporter assays of pBL-CKS1B in MCF-7 co-transfected with pCMV-16E7-HA/flag or pCMV-16E7ΔDLYC-HA/flag; control for normalization: pBL-CKS1B + pCMV-HA/flag. For equivalent expression of 16E7 and 16E7ΔDLYC, see fig. 4F. **F:** Luciferase reporter assays of pBL-CKS1B in MCF-7 or H1299 co-transfected with 10 or 50 ng pCMV-E2F1; control for normalization: pBL-CKS1B + pCMV-HA/flag. **G:** Luciferase reporter assays of pBL-CKS1B in 5637 co-transfected with pCMV-16E7-HA/flag or pCMV-16E7ΔDLYC-HA/flag; control for normalization: pBL-CKS1B + pCMV-HA/flag. Given is the $\log_{10}$ of the mean RLUs (relative luciferase units) relative to the respective control (=0; not depicted). Error bars represent standard deviations. Asterisks indicate statistically significant differences to the respective control as determined by one-way ANOVA (***$p < 0.001$, **$p < 0.01$, *$p < 0.05$).

CKS1B promoter activation via E7 likely depends on pocket protein binding as the pocket protein binding mutant 16E7ΔDLYC failed to stimulate the *CKS1B* promoter (fig. 5E). Unlike the *FOXM1* promoter however, the *CSK1B* promoter was not responsive to E2F1 expression (fig. 5F). This was tested in MCF-7 and H1299 cells and by using different amounts of the E2F1 overexpression plasmid, including the conditions that had conferred activation of the *FOXM1* promoter construct (fig. 4F). The pRb-E2F1 axis therefore apparently does not mediate promoter activation of *CKS1B* by E7. In line with this notion, the *CKS1B* promoter was also activated by E7 in the pRb-deficient cell line 5637. Yet, this process still appears to depend on the pocket protein binding capacity of E7 since the *CKS1B* promoter activation was abrogated upon mutation of the pocket protein binding domain in E7 (fig. 5G).

Recapitulating, the HPV oncoproteins E6 and E7 confer promoter activation of *CKS1B*. While activation by E6 occurs via p53-dependent and potentially also –independent functions thereof, activation by E7 is mediated by binding to the pocket proteins p130 and p107 and probably does not require the pRb-E2F1 axis.

These findings also offer a possible explanation why a downregulation of FOXM1 and CKS1 was not observed in HPV-positive cell lines after *E6* knockdown alone (see fig. 3), while overexpression of only E6 was capable of activating both the *FOXM1* and the *CKS1B* promoter in HPV-negative cells: Since E7 levels remain largely unchanged after a specific *E6* knockdown, the activating stimulus exerted by E7 is preserved and may superimpose the effect of *E6* silencing.

2.3 CKS1 expression regulation by E6/E7 is independent of FOXM1

Several reports describe *CKS1B* as a downstream target gene activated by FOXM1, usually based on the observation that *CKS1B* mRNA was found to decline after FOXM1 depletion [41, 57, 127]. To investigate this possible connection, siRNAs against FOXM1 and CKS1 were employed. Potent downregulation of the respective targets was achieved on protein and transcript level (fig. 6A and B). Expectedly, while silencing of *CKS1B* resulted in an accumulation of its degrading target p27, FOXM1 levels stayed unaffected (fig. 6A). *Vice versa* neither *CKS1B* mRNA nor protein expression was altered by *FOXM1*

knockdown. Also the p27 protein level remained unchanged after FOXM1 depletion. A weak but significant downregulation of *CKS1B* promoter activity was observed after *FOXM1* knockdown in reporter assays (fig. 6C), but this effect was not mirrored by changes at the endogenous CKS1 mRNA or protein level. Furthermore, silencing of *FOXM1* did not impair *CKS1B* promoter stimulation by E6 and E7 overexpression in MCF-7 cells (fig. 6C). Collectively, these data indicate that FOXM1 is dispensable for the activation of the *CKS1B* promoter by the HPV oncogenes. The CKS1 expression level in HPV-positive cancer cells therefore seems to mainly depend on E6/E7 expression, independent of FOXM1. This notion is further corroborated by the different mechanisms of promoter activation by E6/E7 for *FOXM1* and *CKS1B* unravelled in the preceding experiments.

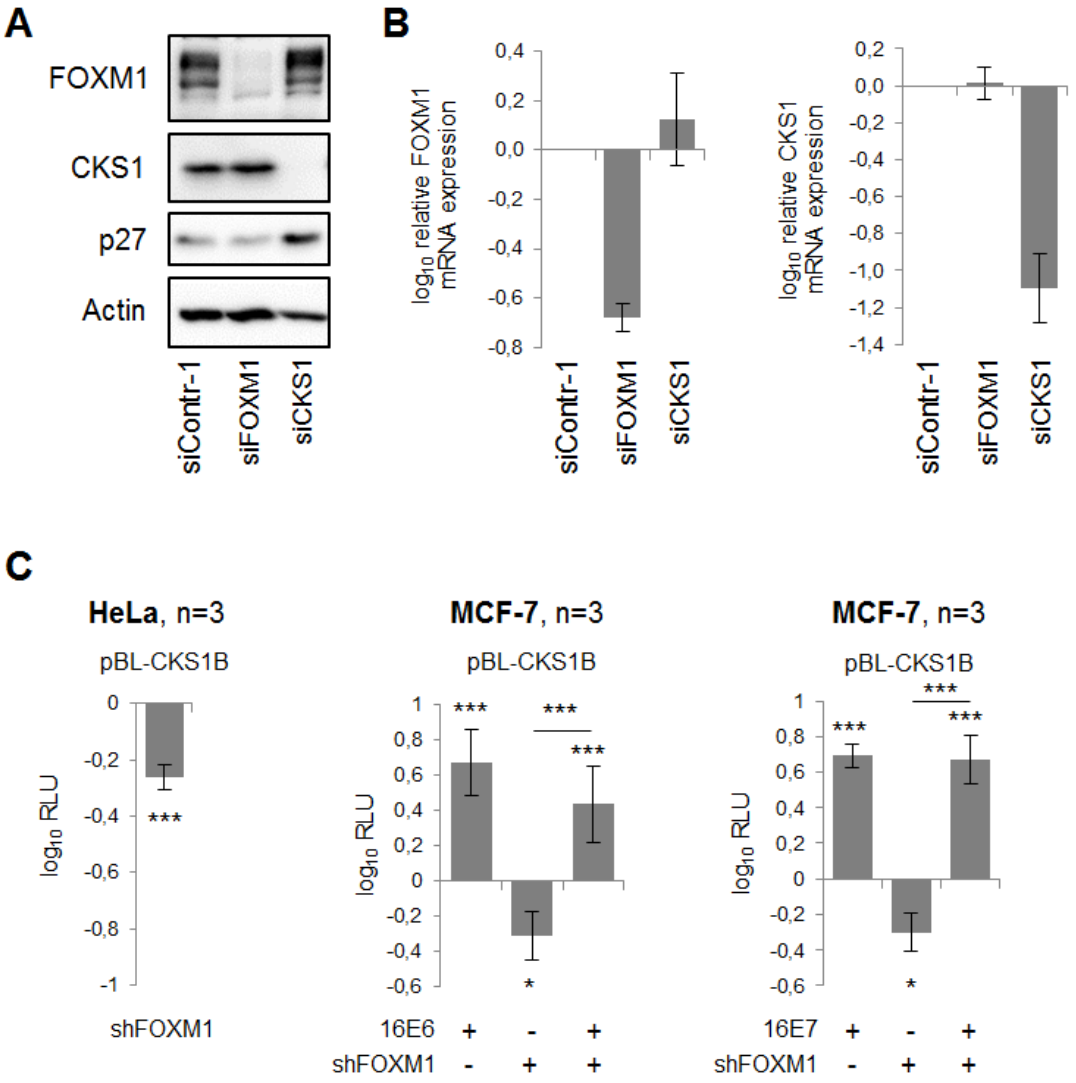

Figure 6: *CKS1B* and *FOXM1* are independently regulated target genes of E6/E7. A, B: Western blot (A) or RT-qPCR (B) of *FOXM1* or *CKS1B* knockdown by siRNAs in HeLa. Actin: loading control. Shown is the $\log_{10}$ of the mean expression relative to siContr-1 (=0) with standard deviations of 2 (FOXM1 mRNA)/3 (CKS1B mRNA) independent experiments. siContr-1: control siRNA. **C, left panel:** Luciferase reporter assays of pBL-CKS1B in HeLa co-transfected with pSUPER-shFOXM1-2/3 (=shFOXM1); control for normalization: pBL-CKS1B + pSUPER-shContr-1. **C, middle panel:** Luciferase reporter assays of pBL-CKS1B in MCF-7 co-transfected with pBCH-16E6 and/or pSUPER-shFOXM1-2/3 (= shFOXM1); control for normalization: pBL-CKS1B + pBCH + pSUPER-shContr-1. **C, right panel:** Luciferase reporter assays of pBL-CKS1B in MCF-7 co-transfected with pCMV-16E7-HA/flag and/or pSUPER-shFOXM1-2/3 (=shFOXM1); control for normalization: pBL-CKS1B + pCMV-HA/flag + pSUPER-shContr-1. Given is the $\log_{10}$ of the mean RLUs (relative luciferase units) relative to the respective control (=0; not depicted). shContr-1: control shRNA. Error bars represent standard deviations. Asterisks indicate statistically significant differences to the respective control as determined by one-way ANOVA (***$p < 0.001$, *$p < 0.05$).

2.4 CKS1 is required for cell cycle progression and senescence suppression in HPV-positive cells

Since cellular CKS1 and FOXM1 levels are increased by E6/E7 expression, it is of high interest to study the impact of this upregulation in cervical cancer cells and to identify whether and how this contributes to their malignant phenotype.

To investigate the effects of CKS1 upregulation by E6/E7, the cellular phenotype after *CKS1B* knockdown was characterized. To that end, three different shRNAs were employed independently to minimize the risk of studying off-target effects. All three shRNAs shCKS1_1, -_2 and -_3 efficiently downregulated CKS1 expression on protein and RNA level and expectedly resulted in the upregulation of the p27 cell cycle inhibitor (fig. 7A). Accordingly, knockdown of *CKS1B* accumulated HeLa cells at the G1/S phase transition in the cell cycle, with cells in G1 phase increasing from 53.2% in control cells to up to 79.1% in shCKS1-treated cells (fig. 7B). In addition, the number of senescent cells increased in CKS1-depleted cells, as verified by the positive staining of the well-established senescence marker senescence-associated β-galactosidase (SA β-Gal) (fig. 7C).

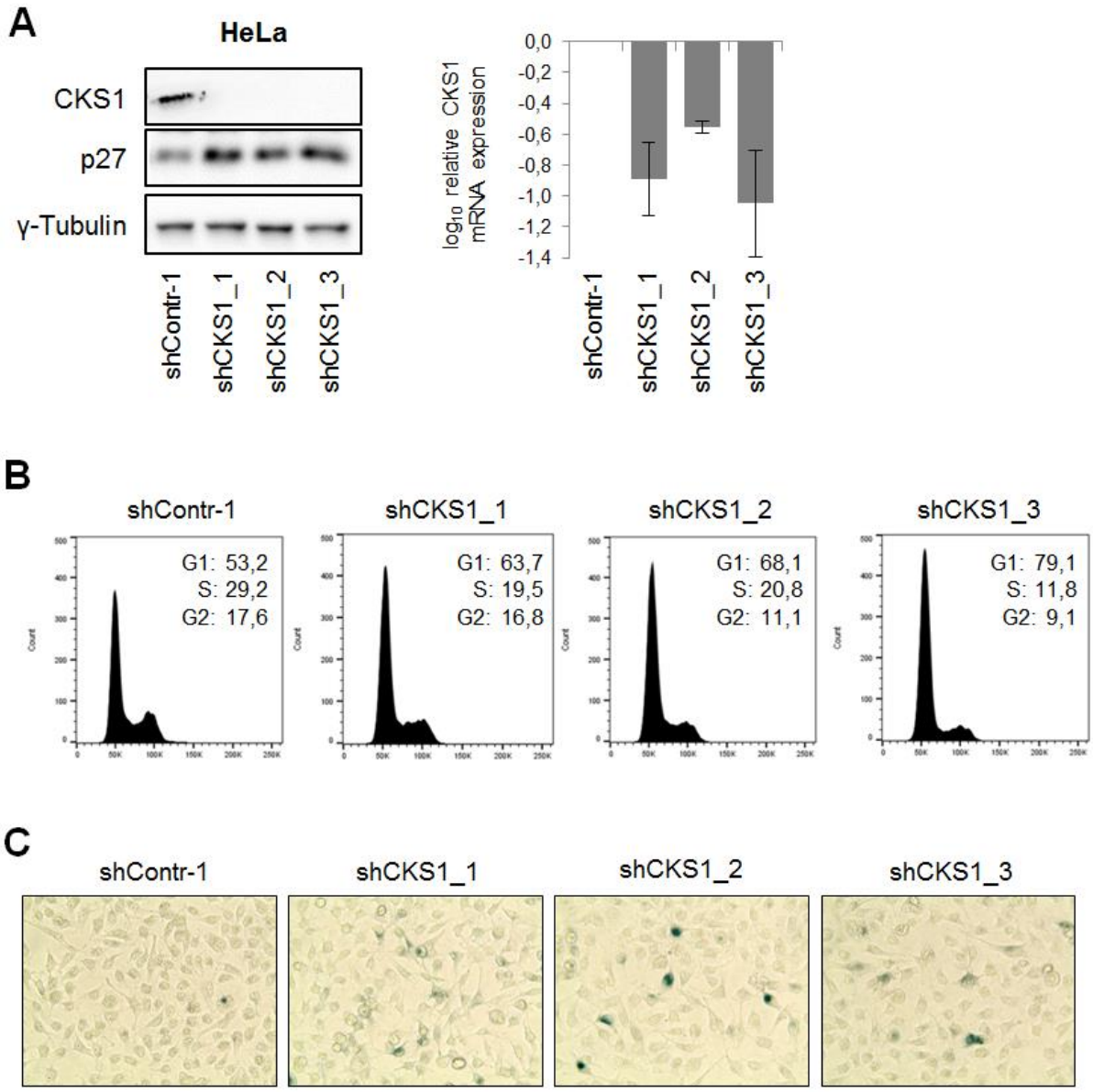

Figure 7: *CKS1B* knockdown in HeLa leads to cell cycle arrest and senescence induction. A: Western blot (left) and RT-qPCR (right) analyses of HeLa cells after *CKS1B* knockdown. γ-tubulin: loading control. Shown is the $\log_{10}$ of the mean expression relative to shContr-1 (=0) with standard deviations of 3 independent experiments. **B:** Cell cycle analyses of HeLa cells after *CKS1B* knockdown. Cell cycle phase distributions are given in %. **C:** SA β-Gal assay of HeLa cells after *CKS1B* knockdown. Split ratios: 1:10 for shContr-1; 1:5 for shCKS1_1, -_2, and -_3. shContr-1: control shRNA.

The same phenotype was observed in SiHa cells using siRNA-mediated *CKS1B* knockdown: CKS1-depleted cells showed a cell cycle arrest at the G1/S phase transition (fig. 8A) which resulted in the efficient induction of senescence, as indicated in figure 8B.

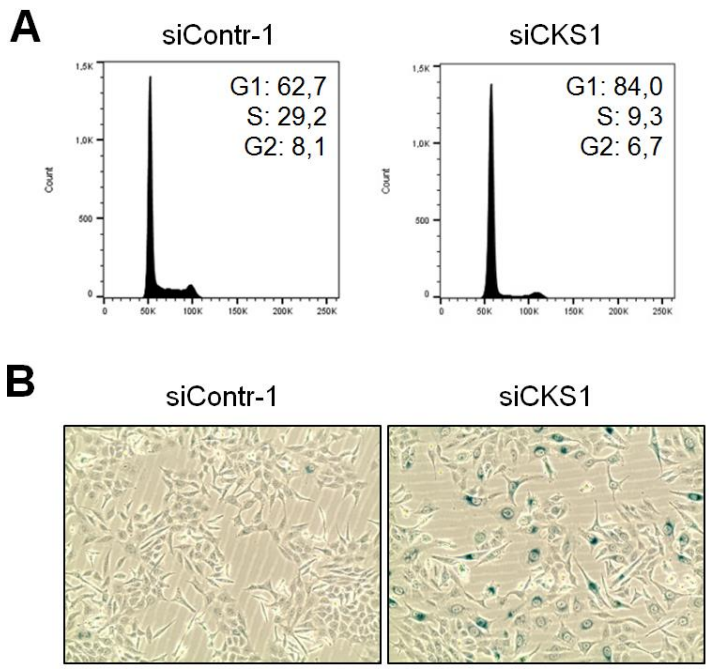

Figure 8: *CKS1B* knockdown in SiHa leads to cell cycle arrest and senescence induction. A: Cell cycle analyses of SiHa cells after *CKS1B* knockdown. Cell cycle phase distributions are given in %. **B:** SA β-Gal assay of SiHa cells after *CKS1B* knockdown. Split ratios: 1:10 for siContr-1; 1:5 for siCKS1. **A, B:** Shown is one representative replicate of 2 independent experiments. siContr-1: control siRNA.

The diminished proliferative capacity after *CKS1B* knockdown was also confirmed in colony formation assays (CFAs). Here, cells were subjected to *CKS1B* knockdown over a longer time period. Episomal maintenance of the shRNA expression vector (pCEP4sh) targeting *CKS1B* was ensured by selection with the antibiotic hygromycin B (HYG). *CKS1B* knockdown in each HeLa, SiHa and CaSki cells resulted in a strongly decreased number of outgrowing colonies, indicative of impaired colony formation capacity in comparison to control transfected cells (fig. 9).

In conclusion, cervical cancer cells require CKS1 for cell cycle progression, a failure of which leads to a cell cycle arrest in the G1 phase and the induction of senescence. Thus, the increase of *CKS1B* expression induced by E6/E7 has pro-proliferative and senescence-suppressing potential in HPV-positive cancer cells, thereby providing a growth advantage.

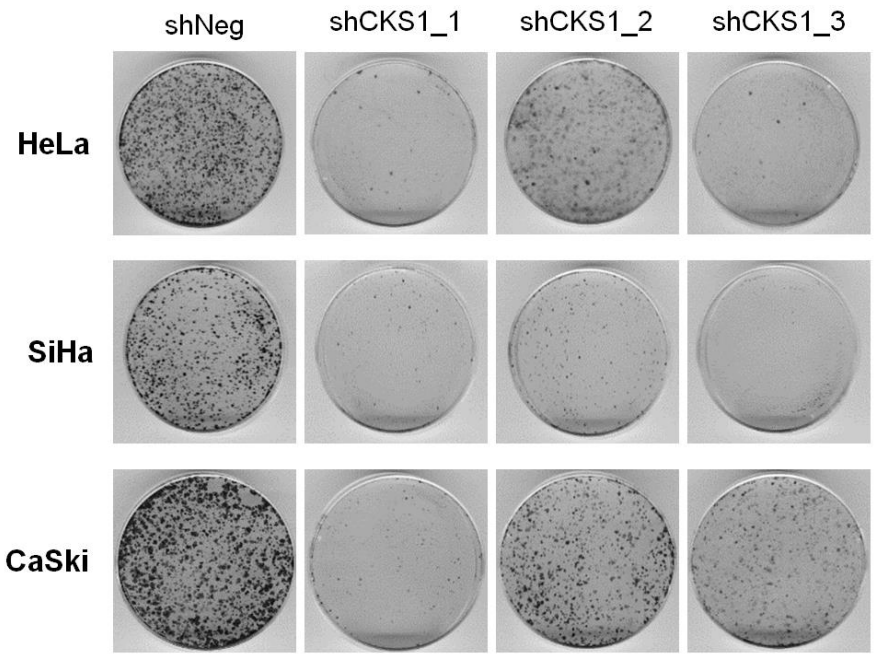

Figure 9: *CKS1B* knockdown decreases colony formation capacity. HeLa, SiHa and CaSki cells were subjected to *CKS1B* knockdown and proliferation was monitored in CFAs. HYG concentration: HeLa 200 µg/mL; SiHa 250 µg/mL; CaSki 100 µg/mL. Shown is one representative replicate of 2 independent experiments. shNeg: control shRNA.

2.5 FOXM1 is required for DNA damage repair in HPV-positive cells

2.5.1 Proliferation of cervical cancer cells is not impaired by *FOXM1* knockdown

Next, the possible consequences of FOXM1 upregulation by E6/E7 were studied in HeLa cells using three different shRNAs for FOXM1 downregulation.

Efficient downregulation of FOXM1 by shFOXM1_1, -_2, and -_3 was achieved on the protein and transcript level (fig. 10A). However, neither alterations in cell cycle distribution (fig. 10B), nor the induction of senescence (fig. 10C) or apoptosis (fig. 10D) could be detected. Corresponding results were obtained in SiHa cells (see supplemental figure 1 in the appendix). These data indicate that the proliferation of cervical cancer cells is unaffected by FOXM1 downregulation.

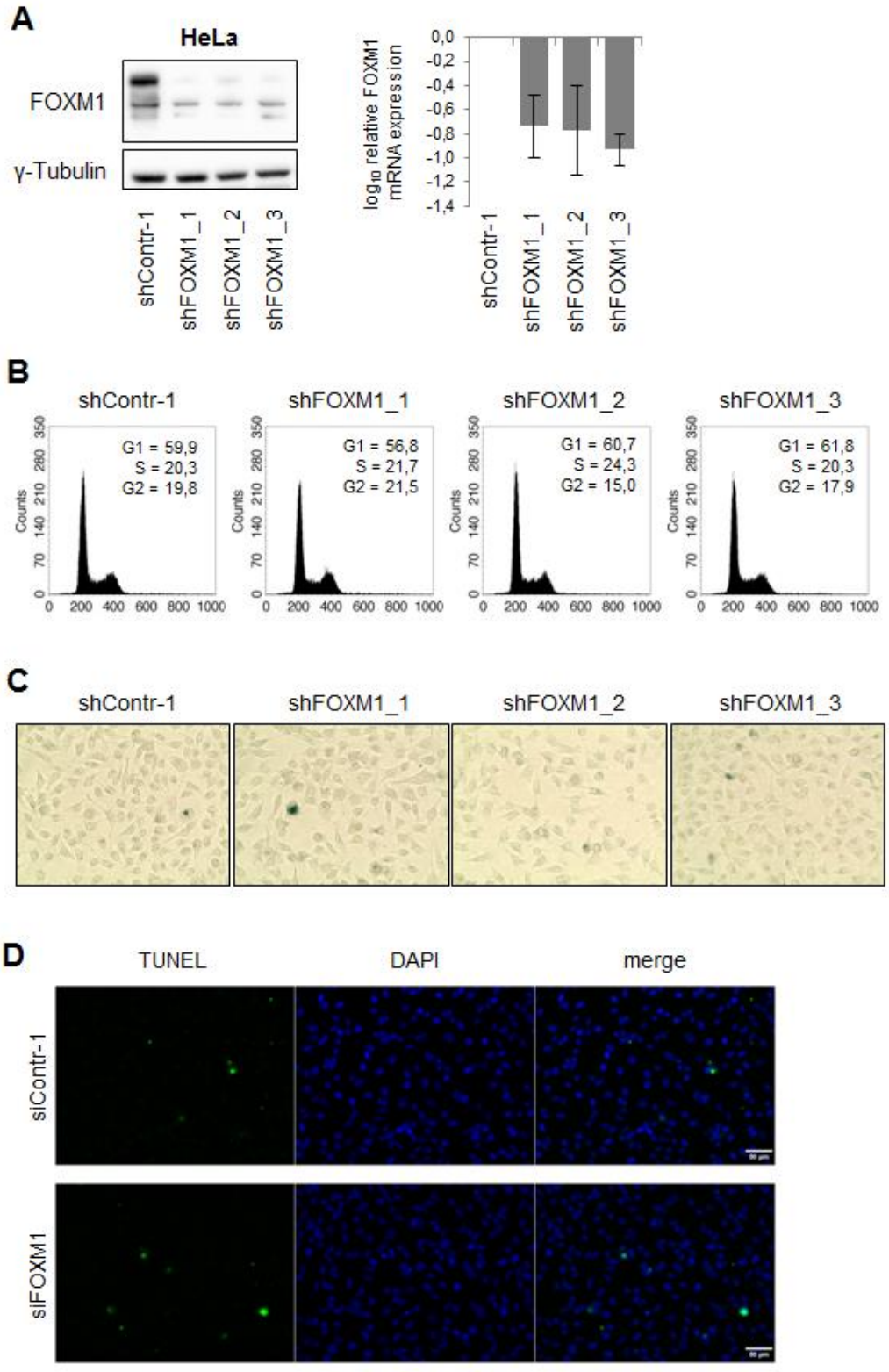

Figure 10: Characterization of the cellular phenotype after *FOXM1* knockdown in HeLa. A: Western blot (left) and RT-qPCR (right) analyses of HeLa cells after *FOXM1* knockdown. γ-tubulin: loading control. Shown is the $\log_{10}$ of the mean expression relative to shContr-1 (=0) with standard deviations of 2 independent experiments. **B:** Cell cycle analyses of HeLa cells after *FOXM1* knockdown. Cell cycle phase distributions are given in %. **C:** SA β-Gal assay of HeLa cells after *FOXM1* knockdown. Split ratio: 1:10. **D:** TUNEL staining in HeLa cells after *FOXM1* knockdown. Scale bar: 50 µm. **B-D:** Shown is one representative replicate of 2 independent experiments. shContr-1: control shRNA, siContr-1: control siRNA.

In order to monitor cellular proliferation after *FOXM1* knockdown more closely over a prolonged time period and in multiple cell lines, the IncuCyte Live-Cell Analysis System was utilized. For a more accurate evaluation, stably transfected cell lines with the red fluorescent protein mCherry tagged to histone 2B (termed "mCherry H2B") were used when available. Use of these cell lines allows for the calculation of actual cell numbers (as each cell carries a red fluorescent nucleus) in contrast to the customary interpretation of confluency percentages by the analysis software.

As can be recognized from figure 11A, cellular proliferation remained unchanged by *FOXM1* knockdown in HeLa mCherry H2B and CaSki mCherry H2B cells. Image acquisition was started 24 h after transfection and typically carried on over an observation period of 100-120 h. This time frame widely exceeds the usual evaluation point 72 h *post* transfection for knockdown experiments. The maintained downregulation of FOXM1 by siRNA for 120 h *post* transfection was verified in immunoblots for HeLa, HeLa "p53 null" and CaSki cells (see supplemental figure 2 in the appendix).

To validate whether the residual p53 in cervical cancer cells plays a role in the cellular response to FOXM1 depletion, the HeLa "p53 null" cell line was also employed for analyses in the live-cell imaging system. Here, an interesting observation was made: Whether or not *FOXM1* knockdown affected proliferation in HeLa "p53 null" depended on whether the stock culture had been grown in medium containing the antibiotic G418 the week before experiments were conducted (fig. 11B). In specific, the stock culture of this cell line is usually kept under selection with G418 to ensure stable expression of the shRNA against p53. During experiments, the antibiotic is omitted from the cell culture medium. However, HeLa "p53 null" cells that came freshly from the G418-containing medium and were seeded for experiments in G418-free medium, displayed a growth disadvantage when FOXM1 was knocked down in comparison to control siRNA-treated cells (fig. 11B, right panel). In contrast, if the stock culture had been kept in G418-free medium for at least one week before experiments were started, no difference in proliferation by *FOXM1* knockdown was observed (fig. 11B, left panel), just as in HeLa mCherry H2B and CaSki mCherry H2B. Maintained downregulation of p53 in cells cultured without G418 selection was monitored by immunoblot, shown in figure 11C. Also, no significant effect of G418 on basal FOXM1 levels was observed.

As demonstrated by the experiments presented in figures 10 and 11, FOXM1 is obviously dispensable for proliferation in cervical cancer cells. This effect is independent

of p53. These findings are in notable contrast to the literature where FOXM1 is generally regarded as an inducer of proliferation in a variety of cell types including cervical cancer [95, 128–130].

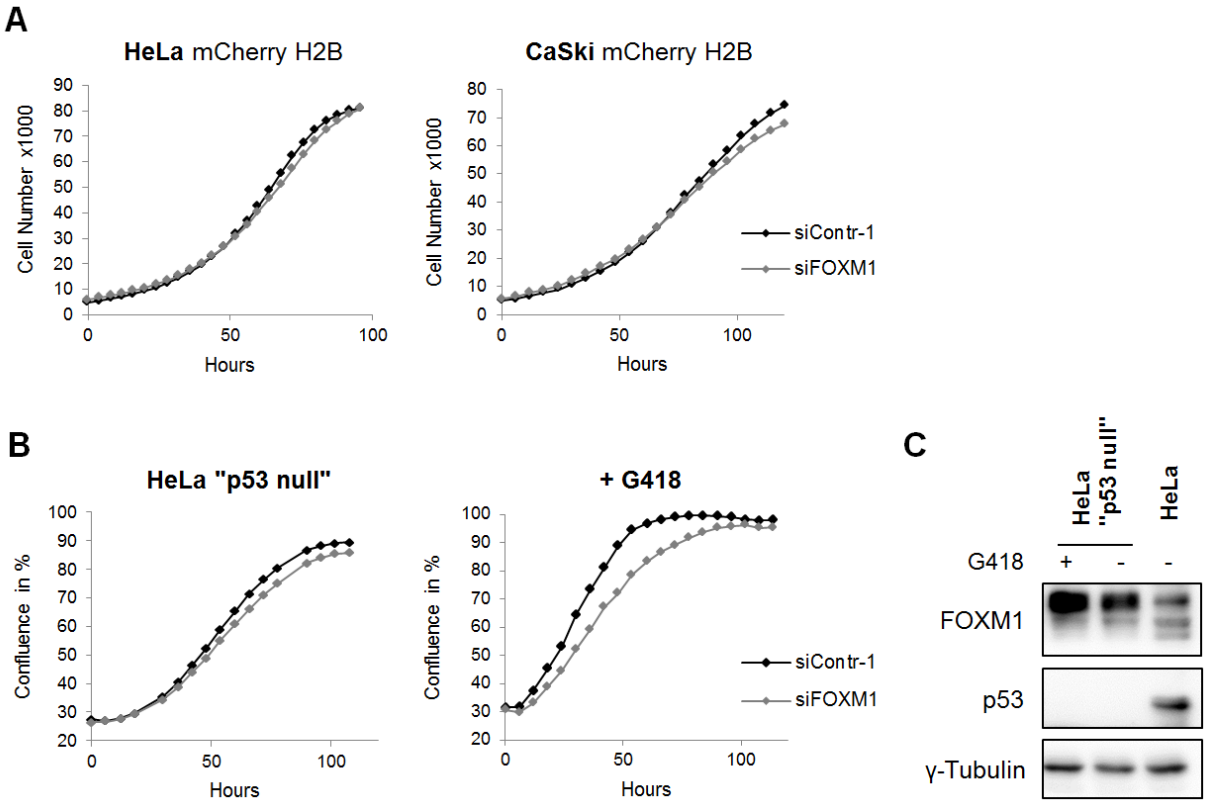

Figure 11: Proliferation of cervical cancer cell lines is unaffected by *FOXM1* knockdown. A: Proliferation of HeLa mCherry H2B and CaSki mCherry H2B was monitored after *FOXM1* knockdown in the IncuCyte Live-Cell Analysis System. **B:** Proliferation of HeLa "p53 null" that had been cultured without (left) or with (right) G418 in their stock culture medium, was monitored after *FOXM1* knockdown in the IncuCyte Live-Cell Analysis System. Data produced jointly with Julia Botta. **A, B:** Image acquisition was started 24 h after transfection. siContr-1: control siRNA. **C:** Immunoblot analysis verifying the maintained downregulation of p53 in HeLa "p53 null" cultured without G418 for 3 weeks. Data produced jointly with Julia Botta. γ-tubulin: loading control.

CFAs are another way of studying the proliferative capacity of cells over a longer period of time (typically 1.5 – 3 weeks from transfection to colony fixation). Although the growth curves of HeLa and CaSki cells had demonstrated no inhibitory effect of FOXM1 downregulation on their proliferation, the number of colonies outgrowing in the CFA was markedly reduced (fig. 12). SiHa cells on the other hand, showed no reduced colony formation capacity after *FOXM1* silencing.

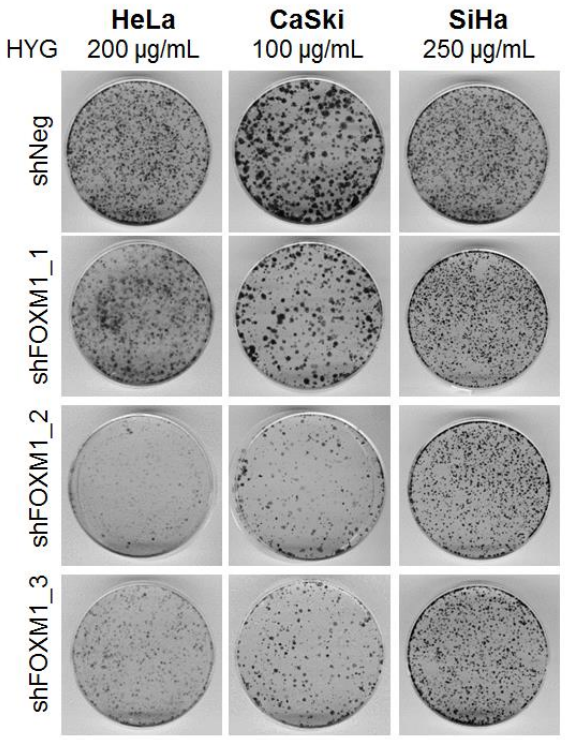

Figure 12: *FOXM1* knockdown decreases colony formation capacity in HeLa and CaSki. HeLa, CaSki and SiHa cells were subjected to *FOXM1* knockdown and proliferation was monitored in CFAs. HYG concentration is given in the figure. Shown is one representative replicate of 2 independent experiments. shNeg: control shRNA.

These CFAs are carried out in the presence of HYG, an antibiotic that inhibits protein biosynthesis in pro- and eukaryotes [131], to select for plasmid maintenance and therefore stable shRNA expression. As has been observed before for G418 in the HeLa "p53 null" cells, decreased colony formation capacity after *FOXM1* knockdown could therefore possibly be linked to HYG selection.

Both HYG and G418 are mainly known and used for their antibiotic properties, caused by inhibition of protein translation. However, there are indications in the literature that both substances could also induce DNA damage in treated cells [132, 133]. Even though G418 was removed from the medium before experiments were started, long-term cultivation with the compound could have possibly resulted in an accumulation of DNA damage lesions. Could the growth-inhibitory effect of *FOXM1* knockdown under these conditions be the consequence of DNA damage?

2.5.2 *FOXM1* knockdown sensitizes cervical cancer cells to DNA damage

To test the above-mentioned hypothesis, HPV-positive cells were subjected to *FOXM1* knockdown and concomitant treatment with different DNA damaging agents (including HYG) and proliferation was monitored in the IncuCyte Live-Cell Analysis System over several days. Camptothecin (CPT), doxorubicin (DOX) and cisplatin (*cis*-diamminedichloridoplatinum, CDDP) are all clinically relevant chemotherapeutics that induce DNA damage via different modes of action: CPT is an inhibitor of topoisomerase I by covalently binding to the enzyme, DOX intercalates with DNA and thereby inhibits topoisomerase II and CDDP forms intrastrand bulky adducts at the DNA. CDDP is a first-line chemotherapeutic in the treatment of cervical cancers and topotecan and irinotecan, two derivatives of CPT, are also approved for cervical cancer therapy.

Figure 13 shows growth curves of HeLa, HeLa "p53 null" and CaSki cells after knockdown of *FOXM1* and concomitant treatment with HYG, CPT, DOX or CDDP. In all cases, while FOXM1-depleted cells proliferated at the same rate as control cells if untreated, a growth reduction after treatment with DNA damaging agents was observed. Low, sub-lethal doses of the drugs were chosen to enable largely unaffected proliferation of control cells in contrast to *FOXM1* knockdown cells. The challenge with DNA damaging agents was therefore shown to selectively target FOXM1-depleted cells and impair their proliferation. These observations may explain why HeLa and CaSki cells showed reduced colony outgrowth after *FOXM1* knockdown in CFAs performed under HYG selection and why HeLa "p53 null" cells that came freshly from G418-containing medium are sensitive to FOXM1 depletion.

The presented results point to a significant involvement of FOXM1 in the DNA damage response (DDR) of HPV-positive cancer cells. A contribution of p53 to this regulation appears unlikely, since the "p53 null" HeLa cells are equally affected as HeLa cells that express p53. These findings are also of potential clinical interest since they indicate that the E6/E7-induced increase in FOXM1 expression may contribute to the resistance of HPV-positive cancer cells towards genotoxic chemotherapy.

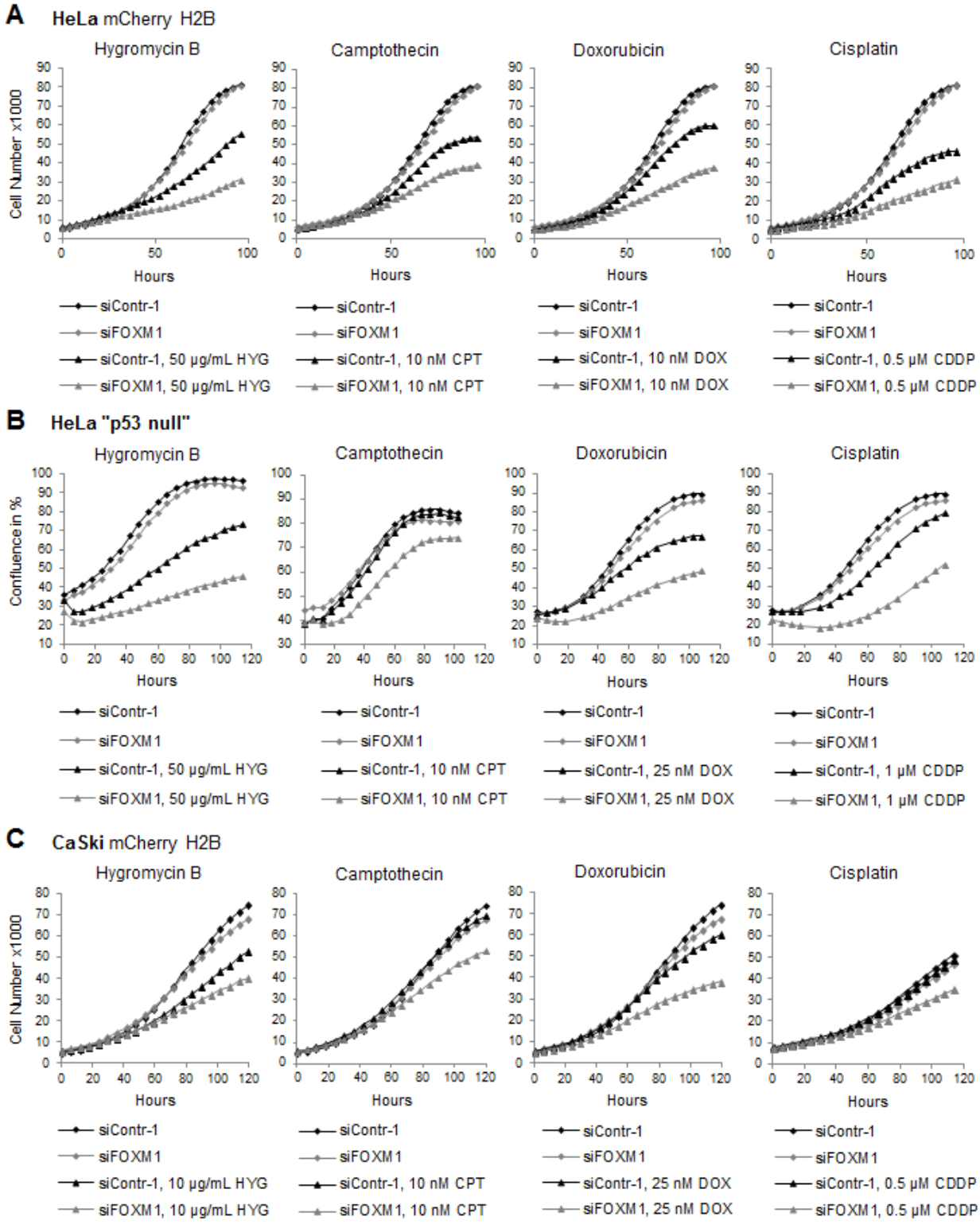

Figure 13: DNA damaging agents selectively impair proliferation of *FOXM1* knockdown cells. HeLa (**A**), HeLa "p53 null" (**B**) and CaSki (**C**) were transfected with siFOXM1 or siContr-1 and treated with different DNA damaging agents at the indicated concentrations. Data acquisition was performed with the IncuCyte Live-Cell Analysis System and started with the addition of the drugs 24 h after transfection. HeLa "p53 null" cells had been cultivated without G418 for at least one week before the start of experiments. siContr-1: control siRNA. **B:** Data produced jointly with Julia Botta.

Interestingly, while this phenomenon applied consistently to the three cell lines described in figure 13, no increased sensitivity to DNA damaging agents was noticed in FOXM1-depleted SiHa cells (fig. 14). This observation is in line with the results from the CFA, where *FOXM1* knockdown under HYG selection also did not impair colony formation capacity in SiHa cells. The role of *FOXM1* knockdown in mediating sensitivity to DNA damaging agents therefore seems to be influenced by cell-type specific differences.

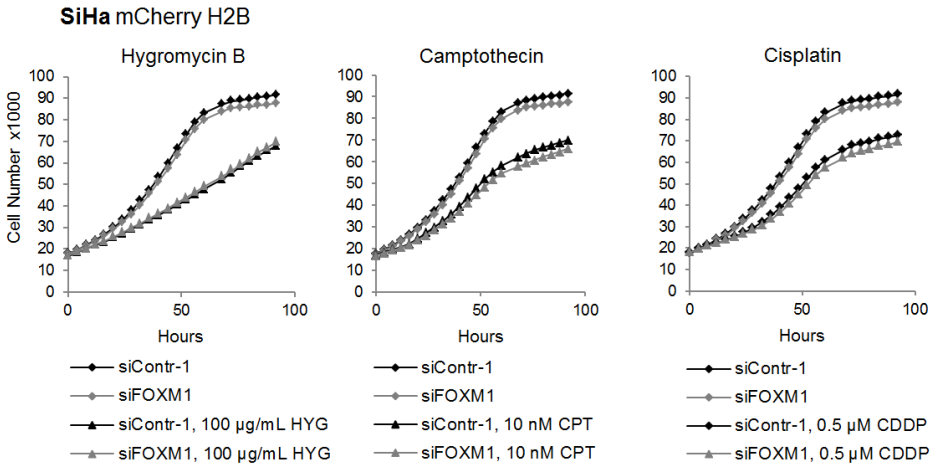

Figure 14: Proliferation of SiHa cells is not affected by *FOXM1* knockdown under DNA damage. SiHa were transfected with siFOXM1 or siContr-1 and treated with different DNA damaging agents at the indicated concentrations. Data acquisition was performed with the IncuCyte Live-Cell Analysis System and started with the addition of the drugs 24 h after transfection. Shown is one representative replicate of 2 independent experiments. siContr-1: control siRNA.

In order to verify that treatment with the different compounds indeed led to an accumulation of DNA damage lesions in *FOXM1*-silenced cells, immunofluorescent staining for the DNA damage marker γ-H2AX was performed. Phosphorylation of the histone 2AX at Ser139 (yielding γ-H2AX) is a very sensitive marker for the detection of double-strand breaks (DSBs) in the DNA [134]. With the use of a phospho-specific antibody in immunofluorescence, distinct γ-H2AX foci can be detected, indicative of DNA damage sites.

Figure 15 shows a clear increase of γ-H2AX signal in *FOXM1* knockdown HeLa cells treated with 10 nM CPT or 10 nM DOX for 48 h in comparison to control cells. The dosages employed were the same as for the proliferation studies. *FOXM1* knockdown *per se* did not induce accumulation of the DNA damage marker.

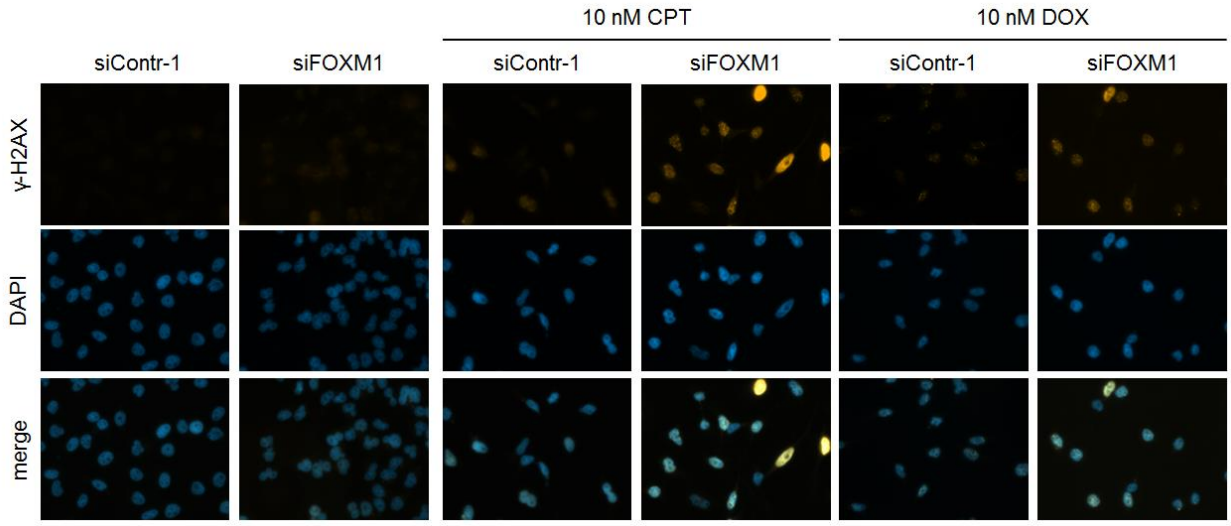

Figure 15: γ-H2AX foci accumulate in *FOXM1* knockdown cells after DNA damage treatment. HeLa were subjected to *FOXM1* knockdown and treated with 10 nM CPT or 10 nM DOX 24 h after the transfection, for 48 h. Cells were stained for γ-H2AX and DAPI by immunofluorescence.siContr-1: control siRNA.

Thus, FOXM1 can enhance resistance of cervical cancer cells to genotoxic agents. While proliferation itself is unaffected by FOXM1 depletion, cells lacking FOXM1 fail to effectively repair DSBs caused by different means of DNA damage. The accumulation of DNA lesions is likely the cause for impaired proliferation of *FOXM1* knockdown cells after treatment with low doses of chemotherapeutics.

2.6 FOXM1 in proliferative arrest

FOXM1 is generally regarded as being a strictly proliferation-dependent transcription factor [48, 49, 135]. To test whether FOXM1 repression after *E6/E7* knockdown is rather a secondary effect due to the proliferative halt induced by *E6/E7* silencing in HPV-positive cancer cells, it was of interest to see how FOXM1 levels react to a proliferation arrest in HPV-positive cells under conditions of continuous E6 and E7 expression.

The compound hydroxyurea (HU) was employed to achieve efficient cell cycle arrest under conditions where viral oncoprotein expression levels remained unaltered. HU is an inhibitor of the enzyme ribonucleotide reductase that supplies the cellular deoxyribonucleoside triphosphate (dNTP) pool by catalysing the conversion of ribonucleoside diphosphates (NDPs) to deoxyribonucleoside diphosphates (dNDPs). HU

treatment therefore leads to depletion of the dNTP pool and typically arrests cells at the G1/S border of the cell cycle.

HeLa and SiHa cells were treated with 1 mM HU for 48 h. Interestingly, the proliferation arrest induced by HU did not decrease FOXM1 (or CKS1) levels in either HeLa or SiHa cells (fig. 16A, B). Rather, FOXM1 protein levels were increased in both cell lines. At the same time, E7 levels stayed unaltered by the treatment. (In general, E6 protein levels were not found to react differently from E7 and were therefore not always probed in the Western blots.) Effective cell cycle arrest under HU treatment was verified by EdU assays and assessment of cell cycle profiles (fig. 16A, B). HU-treated HeLa cells did not incorporate any EdU any more over the 2 h-incubation period, indicative of an efficient cell cycle arrest. The cell cycle profile showed a clear decrease of cells in G2 phase which led to increases in G1 and S phase. While the majority of cells was arrested in G1 phase, some have entered S phase were they failed to complete DNA replication due to the missing dNTPs.

In contrast, quite a high proportion of SiHa cells (48.7%) were found EdU-positive in comparison to 18.6% in unarrested cells. However, the distribution of cells in the dot plot and the cell cycle profile varied widely between HU-treated and untreated SiHa cells. Apparently after HU treatment, most cells have still entered the S phase and started DNA replication which they failed to complete because the dNTP pool was depleted. Upon addition of EdU, cells which are already stuck in the S phase were therefore still capable of incorporating the thymidine analogue and turn weakly EdU-positive. The cell cycle profile corroborates an S phase arrest by HU in SiHa cells.

In conclusion, HeLa and SiHa cells were arrested after treatment with 1 mM HU, yet in both cell lines, CKS1 and FOXM1 levels were not reduced or even upregulated. This is in contrast to the notion that FOXM1 expression is thought to be strictly proliferation-dependent. To receive a better understanding of the responses of FOXM1 and CKS1 to cell cycle arrest and whether these depend on E6/E7 expression, HeLa and SiHa cells were arrested by the means of additional anti-proliferative agents: Mimosine is a non-proteinogenic amino acid that induces cell cycle arrest in the late G1 phase. Excess of the nucleotide thymidine also inhibits the activity of ribonucleotide reductase, arresting cells at the G1/S phase transition or during S phase [136]. Nocodazole is a microtubule polymerization inhibitor and therefore prevents cells from completing mitosis. Efficient blocking of cell cycle progression with these compounds in HeLa cells under the given experimental conditions has been shown by Leitz *et al* [137].

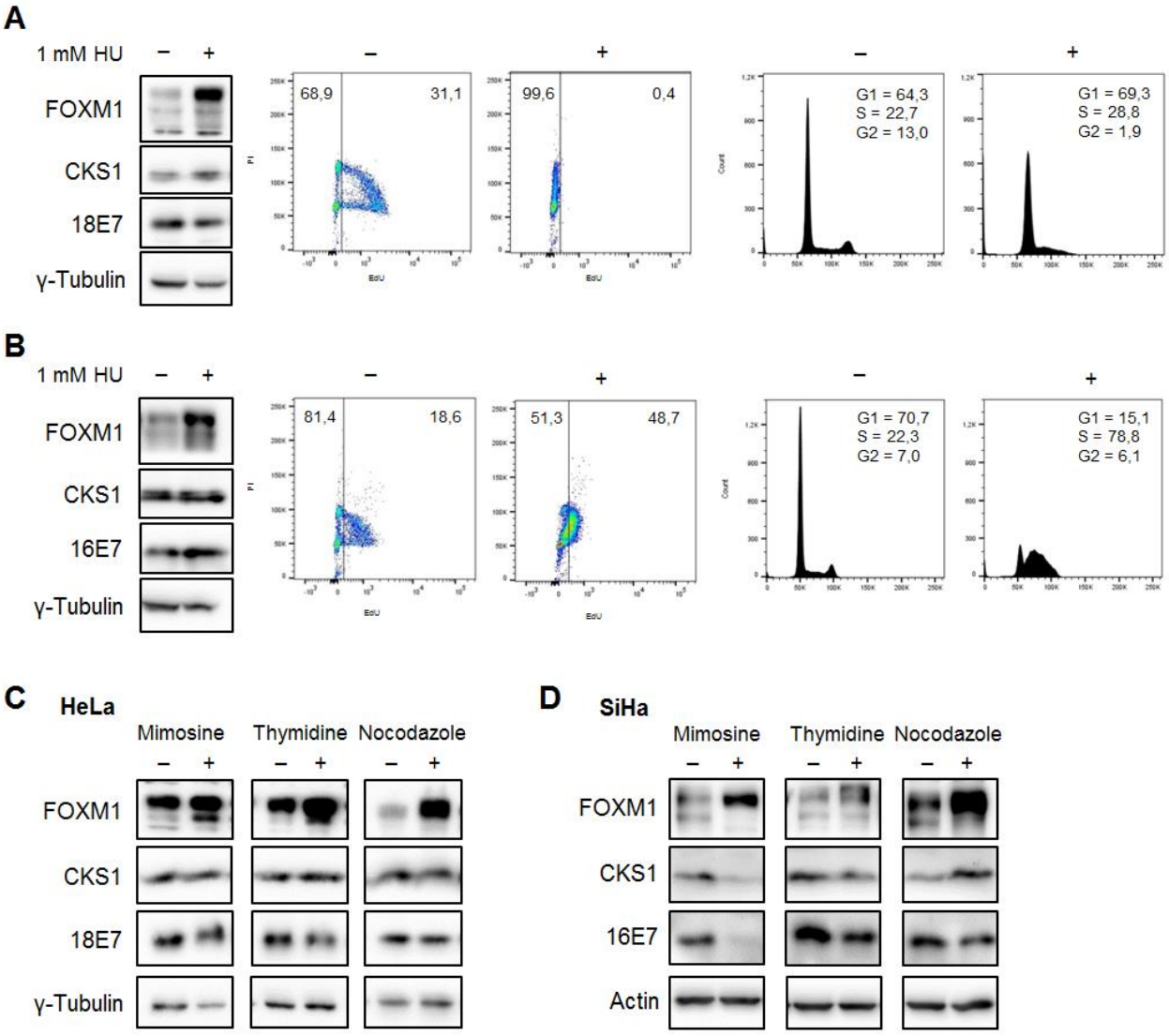

Figure 16: FOXM1 and CKS1 expression is not proliferation-dependent. A, B: HeLa (A) and SiHa (B) were treated with 1 mM HU for 48 h and then harvested for protein extraction or EdU assay. For EdU assay, one representative replicate of 2 independent experiments is shown. **C, D:** Immunoblots of HeLa (C) or SiHa (D) cells treated with 400 µM mimosine, 2 mM thymidine, 0.04 µg/mL nocodazole or the respective solvent control for 24 h (HeLa) or 48 h (SiHa). γ-tubulin, Actin: loading controls.

After incubation with the different cell cycle inhibitors, FOXM1 levels were not decreased but rather increased, at least slightly, in all treatments for HeLa and SiHa cells (fig. 16C, D). CKS1 levels remained largely unchanged, with the exception of mimosine treatment in SiHa cells, were they were found to decline. This latter effect was accompanied by a downregulation of E7 by this treatment. Under all other experimental conditions, HPV18 or -16 E7 levels were not affected by the arrest. Hence, the

experiments with the different anti-proliferative agents collectively support the notion that in HPV-positive cancer cell lines, sustained expression of FOXM1 and CKS1 is not dependent on actively proliferating cells. This effect was largely conserved regardless of the cell cycle inhibitor chosen for treatment.

It was noted that during cell cycle-inhibiting treatments, the higher molecular weight species in the band pattern of the FOXM1 antibody signal accumulated to a greater degree. While the identity of the different bands produced in Western blot for FOXM1 is not ultimately resolved, they could potentially result from different post-translational modifications such as phosphorylations a. o. [138].

Is the unexpected upregulation of FOXM1 expression in proliferation arrest a phenomenon specific to HPV-positive or other tumor cells? To answer this question, HU treatment was performed on HPV-positive cervical cancer cell lines as well as on HPV-negative cell lines from other cancer entities and primary fibroblasts. A range of different dosages and treatment periods was analysed. Figure 17A shows that FOXM1 expression was elevated in HPV-positive cells after HU treatment, also at higher doses of HU or longer treatment periods in comparison to figure 16. This phenomenon appears to be p53-independent as shown by analysis of the HeLa “p53 null” cells. In contrast, FOXM1 levels in the primary fibroblasts Fib101 and CxF6 clearly decreased after prolonged proliferative arrest (fig. 17B). Concordantly, also HPV-negative MCF-7 and H1299 cancer cell lines showed a decline in FOXM1 protein levels. That the effect of increased FOXM1 levels after proliferation arrest is however not necessarily a HPV-dependent phenomenon, is demonstrated by the HPV-negative bladder cancer cell line 5637 which also exhibits FOXM1 elevation after HU treatment. It is however tempting to speculate whether the genomic *RB1* deletion of 5637 cells mimics the downstream effects of E7 expression and therefore contributes to FOXM1 upregulation.

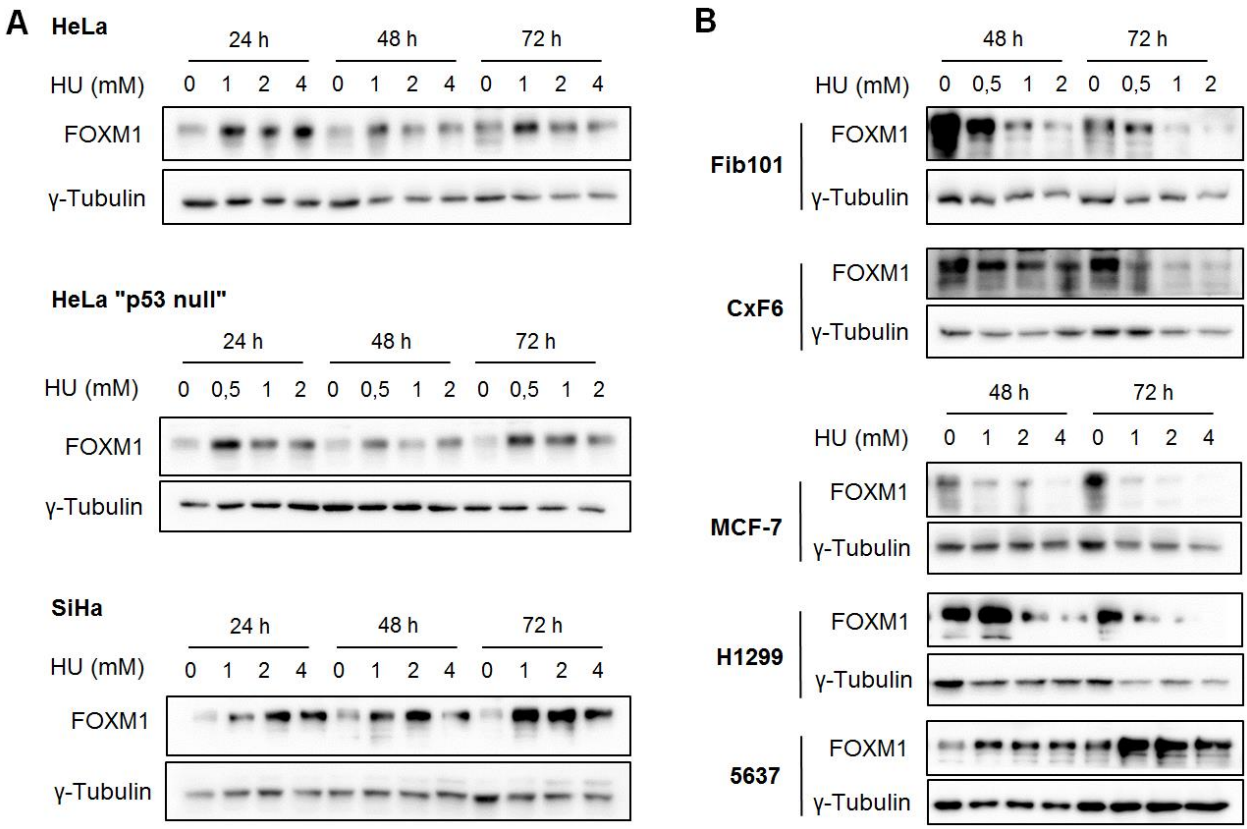

Figure 17: The effects of HU treatment on FOXM1 levels in HPV-positive and -negative cells. A: HeLa, HeLa "p53 null" and SiHa cells were treated daily with the indicated concentrations of HU and harvested after 24, 48 or 72 h. **B:** Fib101 and CxF6 primary fibroblasts, MCF-7, H1299 and 5637 tumor cell lines were treated daily with the indicated concentrations of HU and harvested after 48 or 72 h. γ-tubulin: loading control.

Collectively, these data indicate that while cell cycle arrest by HU treatment resulted in a downregulation of FOXM1 in many HPV-negative cells, this effect could not be observed in the HPV-positive cell lines investigated here, where FOXM1 protein levels were rather upregulated after HU treatment.

CHAPTER 3

DISCUSSION

3 Discussion

HPV-induced cancers depend on the expression of the viral oncogenes *E6* and *E7* for the establishment and maintenance of their malignant phenotype. *E6* and *E7* are known to exert their oncogenic functions via the modulation of various host cell pathways which are however not entirely recognized yet. The identification and characterization of novel HPV target genes is therefore of interest to achieve a deeper understanding of HPV-induced host cell transformation down to the molecular mechanisms and may additionally identify new therapeutic options for HPV-positive cancers. Thus within the scope of this project, the activation of the transcription factor FOXM1 and the cell cycle regulator CKS1 by the HPV oncogenes was investigated in cervical cancer cells with regard to the underlying regulatory mechanisms and phenotypic consequences.

3.1 FOXM1 and CKS1 are novel target genes of HPV E6 and E7

In the present studies, *E6/E7* knockdown experiments revealed that FOXM1 and CKS1 mRNA and protein levels were strongly downregulated after E6/E7 repression in different HPV16- and HPV18-positive cervical cancer cells. Mechanistic studies indicate that these regulatory phenomena were independent of the reconstitution of p53 and not detected if only E6 was depleted. In further support of the notion that *FOXM1* and *CKS1B* represent novel target genes of the HPV oncogenes, overexpression of E6/E7 in NOK cells upregulated protein levels of FOXM1 and CKS1.

Collectively, these results imply that *FOXM1* and *CKS1B* are activated by E6/E7 expression. In line with this notion, elevated levels of FOXM1 and CKS1 have been found in cervical carcinomas – which are virtually always HPV-positive – in comparison to healthy cervical tissue [95, 139]. Furthermore, levels of p27, which is degraded by CKS1, decrease in CIN lesions during the progression to malignancy [140–142].

Downregulation of FOXM1 by silencing of *E7*, but not of *E6*, has been reported in SiHa cells and cell lines from other HPV-positive cancers [93]. Notably however, and other than implied by the authors, the siRNA sequences provided for *E7* knockdown in this publication target a region in the common *E6/E7* transcript, meaning they will repress both E6 and E7 expression [119]. Downregulation of FOXM1 after treatment with these

siRNAs is therefore likely a result of simultaneous *E6/E7* repression and thus corroborates the results obtained in this study.

3.1.1 Activation of the *FOXM1* promoter by E6/E7

Luciferase reporter assays indicated that the activation of the *FOXM1* gene takes place, at least in part, at the level of its transcriptional promoter. In general, activity of the *FOXM1* promoter mirrored the regulation of FOXM1 mRNA and protein expression, in that the downregulation or overexpression of E6 and E7 results in its repression or activation, respectively. This further supports the hypothesis of an activation of *FOXM1* by the HPV oncogenes. As was observed on the mRNA and protein level, *E6* knockdown alone had no effect on promoter activity in HeLa. On the contrary, overexpression of E6 in HPV-negative MCF-7 cells activated the *FOXM1* promoter also in the absence of E7. Furthermore, the over-additive effect of concomitant E6 and E7 expression on the *FOXM1* promoter speaks for a cooperation of the two oncogenes in the activation of *FOXM1.*

The stimulation of the *FOXM1* promoter is likely to be mediated by well-characterized target pathways downstream of E6/E7: A repressive effect of p53 on the *FOXM1* promoter was detected, which is alleviated by E6-mediated degradation of p53. This finding is in line with previous reports describing an upregulation of FOXM1 mRNA, protein and promoter activity after p53 downregulation [59–61]. The stimulatory effect of E7 on the *FOXM1* promoter appears to be mediated via the transactivating function of the transcription factor E2F1, which is released after E7 sequesters its binding partner pRb. Consistently, a pocket protein binding-deficient 16E7 mutant failed to stimulate the *FOXM1* promoter. In line with this idea, two E2F1 binding sites have been described previously in the *FOXM1* promoter close to the transcriptional start site [59]. However, also in the absence of pRb, pocket protein-mediated stimulation of the *FOXM1* promoter by E7 seems to occur, raising the possibility of an additional pRb-independent mechanism of *FOXM1* promoter activation by p130 and/or p107.

These observations fit into a model where the viral oncogenes cooperate in promoting proliferation and tumorigenesis in their host cells by perturbation of the so-called DREAM (DP, Rb-like, E2F4 and MuvB) complex via the modulation of p53 and pocket proteins [143]. DREAM is a transcriptionally repressive complex that silences unscheduled expression of cell cycle genes and therefore prevents premature entry into

the cell cycle in quiescent cells [144]. The pocket protein p130 (in rare cases substituted by p107) constitutes an integral part of this multi-protein complex. It has been demonstrated that the sequestration of p130 by E7 leads to the disruption of DREAM [145, 146]. Besides, the maintenance of DREAM is promoted by the p53 target p21 [147]. Hence, E6-induced degradation of p53 further facilitates the disassembly of DREAM [148]. An overview of the cooperating actions of E6 and E7 in promoting cell cycle progression by the prevention of DREAM complex formation is presented in figure 18.

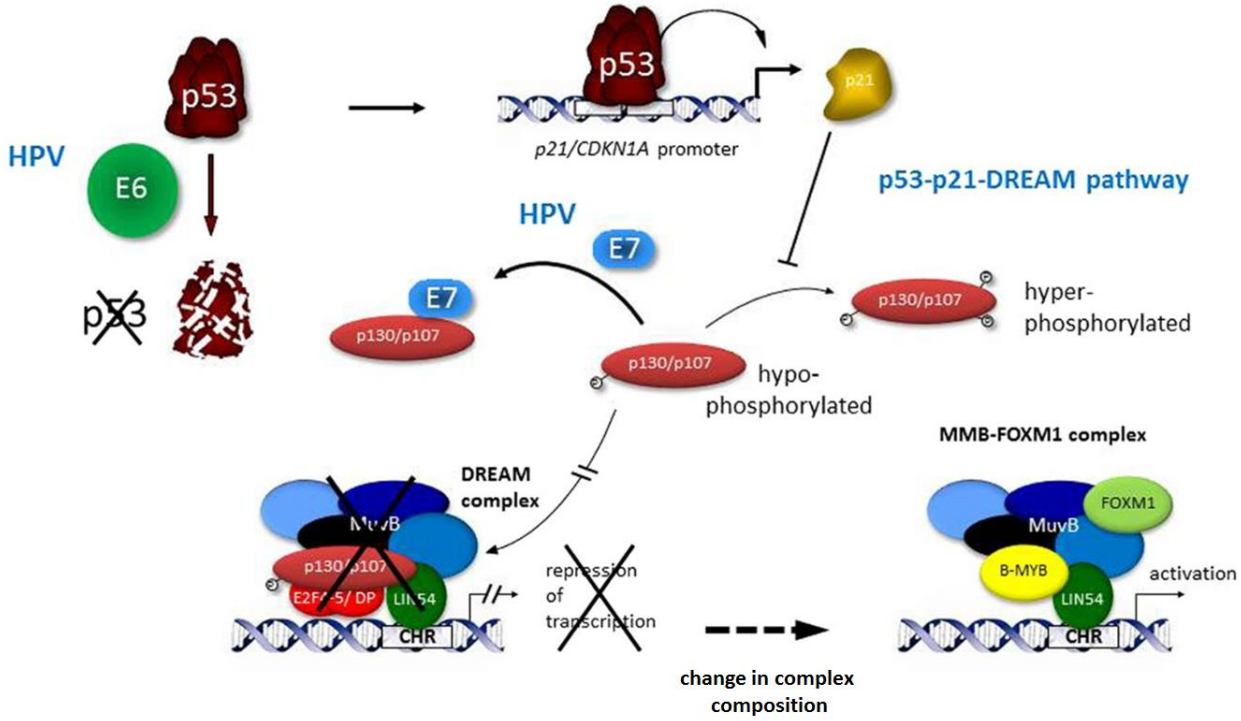

Figure 18: HPV E6 and E7 perturb formation of the repressive DREAM complex and drive proliferation. E7 sequesters the pocket protein p130 or p107, thereby disturbing DREAM and alleviating transcriptional repression. By mediating degradation of p53, E6 promotes the accumulation of the inactivated hyperphosphorylated form of p130/p107 due to inhibition of the p53-p21 axis, which also results in DREAM disruption. Furthermore, the formation of the activating MuvB-B-Myb-FOXM1 (MMB-FOXM1) complex is promoted. Figure adapted from [143].

This concept is further supported by a report which demonstrates that *FOXM1* is a target of DREAM-mediated repression [143]. Consistently, the *FOXM1* promoter contains a CHR (cell cycle homologous region) element, one of the main binding motifs for DREAM [149]. Therefore, disruption of DREAM by E6 and E7 likely stimulates *FOXM1* expression, in addition to the activating effect of the pRb-E2F1 axis which is also induced

by E7. *Vice versa*, knockdown of *E6/E7* in HPV-positive cells leads to a reassembly of DREAM and sequestration of E2F1, resulting in repression of the *FOXM1* promoter and subsequent downregulation of its mRNA and protein levels. This model would also explain why depletion of E6 alone is not sufficient to repress *FOXM1*, since expression levels of the E7 oncoprotein are preserved during *E6* knockdown. In fact, disruption of DREAM assembly by E7 has been shown to also occur independently of E6 [143] which in addition would also account for the fact that reconstitution of p53 was found to be dispensable for *FOXM1* silencing after *E6/E7* knockdown.

3.1.2 Activation of the *CKS1B* promoter by E6/E7

To date, little is known about the structure and regulatory elements of the human *CKS1B* promoter and a possible regulation of CKS1 by the HPV oncogenes has not been reported so far.

The results of the present work support the notion that *CKS1B* expression is activated by the HPV oncogenes. This is indicated by the downregulation of CKS1 protein levels as well as of *CKS1B* mRNA amounts and promoter activity after *E6/E7* knockdown. Moreover, *CKS1B* promoter activity was found to be induced after expression of HPV E6 and/or E7 in HPV-negative MCF-7 cells. Consistent with being stimulated by HPVs, *CKS1B* expression was found to be upregulated in early stage cervical carcinomas in comparison to normal cervical epithelium [139].

Mechanistically, E7-mediated activation of *CKS1B* likely depends on pocket protein interaction, since the effect was lost upon mutation of the E7 domain that mediates the interaction with pRb, p107 and p130. However, in contrast to the *FOXM1* promoter, the *CKS1B* promoter does not carry recognized E2F1 binding sites and could not be activated by ectopic E2F1 expression. Consequently, pRb was found dispensable for *CKS1B* activation by experiments performed in pRb-negative 5637 cells. Nevertheless, judging from the inability of the pocket protein-binding E7 mutant to activate the *CKS1B* promoter also in these cells, the other pocket proteins p130 and p107 are likely to mediate E7-induced *CKS1B* promoter stimulation. As for *FOXM1*, the interference with DREAM complex formation by the HPV oncogenes therefore seems a plausible mechanism for *CKS1B* upregulation. Indeed, *CKS1B* has been described as DREAM target and carries a CHR regulatory element in its promoter [101, 143].

Activation of the *CKS1B* promoter was also demonstrated to occur after expression of HPV E6. This was, at least in part, linked to the decrease in p53 levels, arguing for a

repressive effect of p53 on *CKS1B* transcription which is presumably conveyed via DREAM complex retention [147]. Repression of *CKS1B* promoter activity by p53 is supported by the literature [101]. Interestingly however, E6 also induced activation of *CKS1B* in H1299 cells in the absence of p53. This speaks for a possible p53-independent component in the stimulation of *CKS1B* by E6, a notion which is also supported by the significant increase of promoter activity after concomitant overexpression of E6 and shp53 in MCF-7 cells in comparison to the single expression of E6 or shp53.

p53-independent functions of E6 are known [150] and described to occur via different modes of action. For example, the PDZ-binding motif of high-risk HPV E6 mediates proteasomal degradation of Dlg, MAGI and Scribble proteins which are important factors in cell polarity [31]. The activation of telomerase (hTERT) by E6 which is an important step in cell immortalization was also demonstrated to occur independent of p53 degradation [151]. Protein-protein interactions between E6 and paxillin, E6-binding protein (E6-BP) and Creb-binding protein (CBP)/p300 have been described [152, 153]. Also the activation of transcriptional promoters by E6 independent of p53 is known, such as for the promoters of *VEGF* and the oncogene *MYC* [154, 155]. Interestingly, Myc has also been described to activate transcription of *CKS1B* [118, 156]. Thus, Myc could be the link how E6 upregulates *CKS1B* promoter activity independent of p53. Moreover, for none of the other p53-independent E6 targets a connection to *CKS1B* regulation has been reported so far.

Transcriptional regulation by E6 independent of p53 remains however a very unusual phenomenon. Since the promoter activation of *CKS1B* by E6 in the absence of p53 was so far only investigated in the H1299 cell line, the results require further investigation and until then should be interpreted with caution.

3.1.3 Crosstalk between FOXM1 and E6/E7 in regulating *CKS1B* expression

CKS1B is generally considered as a downstream target of FOXM1 in the literature. This notion is based on *FOXM1* knockdown studies in U2OS osteosarcoma cells and MEFs that show downregulation of *CKS1B* transcripts as well as of other cell cycle genes of the G2/M phase after FOXM1 depletion [41]. The presence of a CHR element in the *CKS1B* promoter and its peak expression at the G2/M transition in the cell cycle are in line with *CKS1B* being a transcriptional target of FOXM1 [101, 157].

However, after knockdown of *FOXM1* in HeLa cells, no reduction of CKS1 mRNA or protein levels was observed. Accordingly, also no upregulation of p27 was detected,

unlike after *CKS1B* knockdown. Nevertheless, *CKS1B* promoter activity showed a weak but significant downregulation after *FOXM1* repression in HeLa. While FOXM1 therefore seems to be able to stimulate *CKS1B* transcriptional activity in HPV-positive cells, the activating effect of E6 and E7 on the promoter appears to be much stronger than of FOXM1. This could explain why no effect of *FOXM1* knockdown was observed at the CKS1 mRNA and protein level while E6/E7 were expressed. Moreover, *FOXM1* expression was found to be dispensable for *CKS1B* promoter activation by the HPV oncogenes. These results warrant the conclusion that *FOXM1* and *CKS1B* constitute independent target genes of E6/E7. This is also supported by the different pathways for promoter activation elucidated and described in this thesis. In addition, different phenotypic outcomes of *FOXM1* and *CKS1B* knockdowns were observed in cervical cancer cells (see section 3.2), further arguing against a relevant upstream/downstream relationship between FOXM1 and CKS1 in HPV-positive cells.

Overall, *FOXM1* and *CKS1B* were identified as novel host cell target genes of both HPV oncogenes *E6* and *E7.* Upregulation of FOXM1 and CKS1 occurs via their transcriptional promoters and translates on to the mRNA and protein level. It was therefore of further interest to study the phenotypic effects of elevated CKS1 and FOXM1 levels on cervical cancer cells.

3.2 Phenotypic consequences of CKS1 and FOXM1 activation in cervical cancer cells

3.2.1 CKS1 is required for cell cycle progression and senescence suppression in HPV-positive cancer cells

To characterize the consequences of *CKS1B* activation by the HPV oncogenes, knockdown studies of *CKS1B* were conducted in HPV-positive HeLa and SiHa cells. Depletion of CKS1 resulted in a proliferative arrest in the G1 phase of the cell cycle and in senescence induction. On the long term, cell cycle arrest and senescence induction resulted in a clearly diminished outgrowth of colonies in CFAs.

Accumulation of the cell cycle inhibitor p27 was caused by *CKS1B* knockdown, and in fact the observed effects of CKS1 repression may be largely explained by elevated levels of p27: Cell cycle arrest at the G1/S boundary has been described to be caused by

upregulation of p27 in HeLa [158, 159]. In addition, the prolonged upregulation of cell cycle inhibitors such as p27 and p21 can result in the induction of senescence [160]. While CKS1 has additional functions apart from the degradation of p27, presumably through the activation of cyclin-dependent kinases (CDKs), their nature is not well characterized in humans [106, 109]. Whether p27-independent functions of CKS1 contribute to the observed phenotype in HPV-positive cells, is therefore difficult to assess.

Whereas these considerations may explain the induction of senescence upon *CKS1B* silencing, in the literature apoptosis rather than senescence induction in response to *CKS1B* knockdown has been described for different cancer cell lines from lung, breast and liver [112–114]. In addition, Martinsson-Ahlzen *et al* report apoptosis induction in HeLa cells after double knockdown of CKS1 and CKS2, although experimental data is not provided by the authors [98]. HPV-positive cells are considered to be protected from apoptosis due to E6-mediated degradation of p53. Theoretically, the failure of HPV-positive cells to upregulate p53 in response to the cell cycle arrest caused by CKS1 depletion could therefore explain why no apoptosis was observed under the experimental conditions here. Since cells are however arrested at the G1/S border of the cell cycle for a prolonged time, subsequent senescence induction may follow.

Overall, elevated levels of CKS1 in HPV-positive cells are likely to play an important role in ensuring continuous proliferation of the tumor cells. In addition, by facilitating orderly cell cycle progression, CKS1 may support HPV-positive cells in the evasion from senescence, e.g. via induction of p27 degradation.

These properties of CKS1 expression could therefore offer the potential for therapeutic exploitation, for instance by the application of inhibitors that interfere with CKS1 function. Indeed, experimental evidence links the anti-tumorigenic effects of different compounds to CKS1 inhibition: Oncostatin M is a member of the interleukin-6 family of cytokines which showed a broad anti-proliferative effect in glioblastoma cells. This was attributed to upregulation of p21 and p27 which was in part mediated by suppression of CKS1 and its partner substrate receptor Skp2 [161]. Vorinostat is a histone deacetylase inhibitor that elicited p27 and p21 accumulation in breast cancer cells, which could be overcome by the overexpression of CKS1 and Skp2 [162]. Further, the anti-depressant drug fluoxetine has recently gained attention due to its anti-proliferative and chemosensitizing effects on cancer cells and was the only compound tested in cervical

cancer cells so far [163]. Treatment of SiHa as well as MDA-MB-231 breast cancer cells with fluoxetine led to a cell cycle arrest in G1 phase by CKS1 downregulation which was accompanied by p27 and p21 upregulation [163]. The highest therapeutical and therefore possibly also clinical potential is currently attributed to 'Compound 1' (C1), a specific small molecule inhibitor of the CKS1-p27 interaction [164, 165]. Attenuated proliferation after treatment with C1 due to accumulation of p27 and p21 has been shown in prostate cancer cells and organoids, as well as for leukemia cell lines [166, 167]. The effects of C1 have not yet been studied in cervical cancer cells which – in light of the results obtained in the present studies – should be an interesting future task. So far however, neither C1 nor another CKS1-specific therapy is close to being translated to the clinic and tested in humans.

3.2.2 FOXM1 is dispensable for proliferation in HPV-positive cells

After downregulation of FOXM1 in HPV-positive cells, neither alterations in cell cycle distribution nor the induction of senescence or cell death by apoptosis were observed. In other words, growth of cervical cancer cells was unaltered by *FOXM1* knockdown, making FOXM1 dispensable for proliferation in HPV-positive cells.

This result stands in contrast to the common notion that FOXM1 is required for maintaining cellular proliferation and that a *FOXM1* knockdown inevitably results in a cessation or at least strong impairment of growth. Knockdown or overexpression studies of FOXM1 have been reported in various experimental settings and cellular backgrounds. For instance, it has been demonstrated that FOXM1 overexpression in nasopharyngeal carcinoma cells accelerated proliferation by promoting S phase entry, while *FOXM1* knockdown in a different cell line from the same cancer entity resulted in a cell cycle arrest in the G1 phase [129]. Accordingly, also increased proliferation of hepatocellular carcinoma cells after FOXM1 overexpression has been reported [168], while diminished cell growth was observed in MCF-7 breast cancer cells after *FOXM1* knockdown [169]. In addition to these direct approaches, inhibition of proliferation by treatment with various compounds is attributed to FOXM1 downregulation [170, 171] as well as the anti-proliferative effects of several miRNAs [172–174]. Besides, the pro-proliferative role of FOXM1 is supported by tumor xenograft experiments with ovarian cancer cells in mice [175] and in transgenic mouse models for prostate cancer [176]. Finally, and in contrast to the results obtained in this work, FOXM1 has been reported to act pro-proliferatively also in HPV-positive cell lines, specifically HeLa and SiHa. Notably

however, these latter experiments were carried out in stable *FOXM1* knockdown cells that were cultivated under selection with G418 [95, 128]. As further discussed below, my findings that cultivation with G418 or HYG (another antibiotic used for selection purposes in CFAs) can impair proliferation of HPV-positive *FOXM1* knockdown cells may provide an explanation for these discrepant results.

Therefore, in contrast to cells from many other cancer entities, HPV-positive cells seem to have overcome their dependency on sustained *FOXM1* expression for continuing proliferation. This may also in part be explained by E6's and E7's ability to prevent DREAM formation, therefore circumventing cell cycle arrest in the G1 phase and driving continuous cell cycle progression [145]. In line with this proposition, abrogation of the G1/S cell cycle checkpoint by E7 expression has been shown [177].
Additionally however, FOXM1 itself also plays an essential role for undisturbed cell cycle progression: During the cell cycle, formation of the transcriptionally activating MMB-FOXM1 (B-Myb-MuvB-FOXM1) complex occurs after the repressive DREAM complex has dissociated through p130 phosphorylation in the late G1 phase. The MuvB core complex (previously incorporated in DREAM) then binds to the transcription factor B-Myb during S phase, thereby turning from the repressive into a transcriptionally activating complex. Subsequently, FOXM1 is recruited to form the B-Myb-MuvB-FOXM1 (MMB-FOXM1) complex which is required for activation of gene expression in the G2 and M phases (see also fig. 18) [64, 178].
So far, it remains an unresolved question, whether B-Myb-MuvB (MMB) are capable of activating target genes without the presence of FOXM1 in their complex [179]. This is however a possible scenario to explain unaltered proliferation in the absence of FOXM1 in HPV-positive cells. Given the high redundancy that is characteristic for cell cycle regulatory control pathways, there might also be other cellular factors that substitute for MMB-FOXM1 activity after *FOXM1* knockdown. This speculation is supported by results from Rashid *et al* that report that the MMB complex is not critical for the expression of S/G2 genes in HPV16-positive CaSki cells [180].
Furthermore, the observations discussed here were obtained in cells were *FOXM1* had been knocked down using siRNAs. Therefore, although low, residual protein levels of FOXM1 could potentially suffice for MMB-FOXM1 formation and unaltered cell cycle progression under these experimental conditions.

Taken together, the proliferation of HPV-positive cervical cancer cells was shown to be unaffected despite efficient knockdown of *FOXM1*, which has not been observed for cells from other tumor types.

3.2.3 The role of FOXM1 in DNA damage repair

Since FOXM1 repression did not impair proliferation in HPV-positive cells, it was unexpected to see a clear reduction of colony outgrowth in CFAs after *FOXM1* knockdown. In addition, the HeLa "p53 null" cell line showed decreased proliferation of FOXM1-depleted cells when their stock culture was kept under selection with the antibiotic G418. Both compounds, HYG used for selection in CFA and G418, have been reported to possess DNA damaging potential in addition to their ability to inhibit protein synthesis which mainly accounts for their antibiotic properties [132, 133, 137]. Subsequent proliferation studies employing sub-lethal doses of various DNA damaging agents confirmed that *FOXM1* knockdown selectively sensitized cells to DNA damage, resulting in impaired growth. The accumulation of DNA damage was verified by an increase in γ-H2AX foci staining.

DNA damage is a daily phenomenon in cells and is for example induced by cellular metabolites such as reactive oxygen species, environmental radiation, errors during DNA replication or the treatment with genotoxic agents [181]. The latter is a key strategy in cancer therapy, with the rationality to preferably kill the faster proliferating tumor cells, while the quiescent or slower proliferating cells of the healthy tissues are less affected. To maintain the integrity of their genomes, cells have developed a tightly regulated network of DDR pathways that encompasses different repair mechanisms for every type of DNA damage.

The majority of DNA lesions in the cell are base modifications or single-strand breaks [182]. They are preferentially repaired by the pathways of base excision repair (BER), where only one base is replaced, or nucleotide excision repair (NER), removing and replacing a small stretch of damaged DNA [182]. On the other hand, double-strand breaks (DSBs) constitute the most toxic type of DNA damage which is also the most difficult to repair [183]. Here, cells use two main pathways for repair: homologous recombination (HR) and non-homologous end joining (NHEJ) [184, 185]. HR has the highest sequence fidelity of the DSB repair mechanisms as it relies on the sequence of the sister chromatid as a replication template. It is therefore however restricted to the S

and G2 phase of the cell cycle, when two copies of every chromosome are available in the nucleus [186]. NHEJ can occur throughout the cell cycle since it is independent of the presence of the sister chromatid, but is more error-prone than HR [187].

The findings in the present studies indicating that FOXM1 can support resistance of HPV-positive cancer cells towards genotoxic stress are supported by previous studies which linked FOXM1 to an improved cellular DDR: Increased radioresistance in glioblastoma, as well as enhanced resistance to DOX or CDDP treatment in breast and ovarian cancer cells, respectively, have been linked to FOXM1 expression [188, 189, 190]. Moreover, chemoresistant cells and tumors have been found to often contain elevated levels of FOXM1 in comparison to their non-resistant counterparts [59, 84, 189, 191]. Furthermore, *FOXM1* knockdown sensitized a panel of different cancer cell lines with mutant p53 to DNA damage and increased the rate of apoptosis in these cells [81]. On the transcriptional level, XRCC1 (X-ray repair cross complementing 1), a scaffolding protein which is mainly required in BER [192], and BRCA2 (breast cancer susceptibility gene 2), a key mediator of HR [193], are activated by FOXM1 expression [194] and can contribute to FOXM1-mediated CDDP resistance in breast cancer cells [84]. Additional molecular targets of FOXM1 in the DDR have been described: Upregulation of exonuclease 1 (EXO1) by FOXM1 mediates CDDP resistance in ovarian cancer cells and epirubicin resistance in breast cancer cells is conferred by the FOXM1 target BRIP1 (BRCA1-interacting protein C-terminal helicase 1), which is required for HR [83, 189]. Also the HR factor NBS1 (Nijmegen breakage syndrome 1) was found to be transcriptionally upregulated by FOXM1 in the DDR [195]. Notably, by analyzing specific reporter constructs, *FOXM1* knockdown in HeLa cells was found to repress the DDR by HR but not NHEJ [59, 195]. In addition, FOXM1 has also been implicated in facilitating access of DDR enzymes to DNA damage sites via chromatin remodeling [82].

Summing up, FOXM1 enhances the cellular DDR via different pathways and multiple targets, its actions thereby possibly depending on cell type and the different kinds of DNA lesions encountered. Consistently, in the investigations presented here, the protection of cervical cancer cells by FOXM1 towards the chemotherapeutic agents CPT, DOX and CDDP was observed independently of the different modes of action of the compounds.

Notably, most of the published studies concerning the interrelation between FOXM1 and the DDR were conducted in breast cancer cells, specifically the MCF-7 cell line. However, cell type-specific effects may also play a role in this context. Thus far, little is known

about the mechanisms by which FOXM1 can improve the DDR in HPV-positive cells, an issue which awaits further experimental exploitation. In this light, an interesting question that remains to be answered is why SiHa cells, in contrast to the other HPV-positive cell lines investigated, showed no increase in sensitivity towards the combined application of *FOXM1* knockdown and DNA damage.

Collectively, the findings of the present investigations indicate that the elevated levels of FOXM1 due to activation by E6/E7 could be a mechanism to enhance the DDR in HPV-positive cells which could result in increased chemotherapy resistance. Thus, in principle, the sensitivity of HPV-positive cancer cells to chemo- and possibly also radiotherapy may be increased by the targeted inhibition of FOXM1. The use of FOXM1 inhibitors for cancer treatment has long been discussed in the light of FOXM1's tumorigenic properties [196]. However, transcription factors such as FOXM1 are usually considered notoriously difficult to target chemically since they often lack druggable regions on their surface [197]. Nevertheless, the thiazole antibiotics thiostrepton and siomycin A have been identified as FOXM1 inhibitors that lead to downregulation of FOXM1 mRNA and protein levels, inhibition of FOXM1 downstream targets and the induction of apoptosis [198, 199, 200]. However, while they are often referred to and employed as "FOXM1-specific" inhibitors, thiostrepton and siomycin A have actually been identified to be proteasome inhibitors [201–203]. In addition, also other well-characterized proteasome inhibitors such as MG132 and bortezomib can downregulate FOXM1 transcript and protein levels [204]. FOXM1 suppression by proteasome inhibitors therefore appears to be a general feature, and was shown to be linked to the stabilization of HSP70 (heat shock protein 70 kDa) upon proteasome inhibition [205]. Of course, proteasome inhibition interferes with multiple cellular pathways and targets, therefore raising serious issues with regard to the specificity of action on FOXM1 inhibition [206, 207].

In a high-throughput screening approach, Gormally *et al* have identified the candidate compound FDI-6 which they found to bind specifically to FOXM1 and to suppress FOXM1's binding to target gene promoters [208, 209]. Data regarding the efficacy of FDI-6 in cell culture or *in vivo* studies are however still missing. Recently, a potential drug-binding pocket within the FOXM1 DNA binding domain was identified and reported to mediate the direct binding of FDI-6 and thiostrepton [200, 210].

Despite extensive research efforts, a *bona fide* FOXM1 inhibitor with significant clinical potential is therefore still lacking. Nevertheless, FOXM1 suppression remains an attractive therapeutic strategy and could have chemosensitizing effects, not only for HPV-positive tumors. Indeed, combination experiments have identified a synergistic relationship between the clinically approved proteasome inhibitor bortezomib and CDDP treatment in lung and cervical cancer cells [211, 212]. Whether this effect is accompanied and/or mediated by FOXM1 suppression was however not investigated.

3.2.4 FOXM1 and CKS1 in proliferative arrest

Both FOXM1 and CKS1 have been reported to play essential roles in regulating cell cycle progression in proliferating cells and the viral oncogenes *E6* and *E7* activate proliferation in their host cells. It was therefore also important to investigate whether the elevated levels of FOXM1 and CKS1 were simply a secondary effect of the higher proliferation rate of HPV-positive cells while *vice versa* the downregulation of both genes upon *E6/E7* silencing resulted from the proliferative halt of the cells induced by viral oncogene repression.

Treatment with the DNA replication inhibitor HU effectively arrested HeLa and SiHa cells in the G1 or S phase, respectively, while leaving the viral oncogene expression unaltered. Interestingly, under these conditions, neither FOXM1 nor CKS1 protein levels declined. Also by the use of other cell cycle inhibitors that arrest cells at different stages of the cell cycle, no decrease of FOXM1 or CKS1 levels was witnessed in HPV-positive cells as long as E7 was expressed.

These observations preclude FOXM1 and CKS1 from being mere proliferation markers in HPV-positive cancer cells as their sustained expression is not dependent on active proliferation. They also challenge the current general concept that FOXM1 expression is strictly limited to proliferating cells [48–50] and declines after the induction of senescence [51]. Notably, HU treatment was demonstrated to induce senescence under the conditions employed here [213]. By incorporating the mechanisms of *FOXM1* and *CKS1B* promoter activation by E6/E7 described in this dissertation, a new model taking into account the specific background of HPV-positive cells could be proposed: While the cells do undergo proliferative arrest after treatment with the respective cell cycle inhibitors, the repressive DREAM complex is not formed due to the continuing expression of the HPV oncogenes, thereby keeping expression from the *FOXM1* and *CKS1B* promoters active. Sustained expression of E6 also disables p53 checkpoint

activity. In addition, continuing E2F1 signaling stimulates the *FOXM1* promoter since E7 prevents pRb from sequestering E2F1. This model could also explain why the cell cycle phase in which the cells arrest does not affect ongoing FOXM1 and CKS1 expression: The cell cycle-dependent expression pattern of FOXM1 and CKS1 is presumably deregulated and overridden due to the abolition of DREAM. It would be interesting to further corroborate these ideas with additional experiments, for example using synchronized proliferating cells or by performing knockdown studies of E2F1 or DREAM components.

While the overall regulation of FOXM1 and CKS1 levels seems to be consistent in HeLa and SiHa cells, some differences were observed: Cell cycle arrest by dNTP depletion following HU treatment occurred in the G1 phase for HeLa cells, while SiHa cells arrested during S phase. This possibly may reflect an impaired replication stress checkpoint at the G1/S border in SiHa cells. Additionally, mimosine treatment, which also induces replication stress due to inhibition of the ribonucleotide reductase [214], led to a downregulation of E7 in SiHa, but not in HeLa cells. This downregulation of E7 was accompanied by a decrease of CKS1 protein, supporting the activating role of E7 on CKS1 levels. Perhaps surprisingly however, FOXM1 levels stayed elevated despite the absence of E7, pointing to an additional cellular mechanism which supports FOXM1 expression under these conditions. Notably, treatment with HU, mimosine and thymidine is also known to induce DNA damage and activate the DDR [215–217]. Hence, FOXM1 upregulation in treated cells could possibly result from an activated DDR.

The next question to answer was whether the unexpected phenomenon of FOXM1 upregulation after cell cycle arrest is specific to HPV-positive cells. HU treatment of HPV-positive and -negative tumor cell lines as well as HPV-negative primary fibroblasts was carried out over a longer time period (72 h) and with increasing doses of HU. While FOXM1 levels stayed elevated in the HPV-positive cell lines also at higher doses of HU and later time points, downregulation of FOXM1 after prolonged cell cycle arrest was observed in primary fibroblasts and HPV-negative MCF-7 and H1299 cells. As functionality of the pocket protein family is not known to be impaired in these cells, sustained proliferative arrest should result in the activation of pRb, p107 and p130 and the subsequent formation of DREAM and induction of senescence [218], accompanied by a downregulation of FOXM1.

Sustained FOXM1 levels after growth arrest are however not only restricted to HPV-positive cells: The bladder cancer cell line 5637 also showed continuing FOXM1

expression after HU treatment. In contrast to the other cell lines investigated here, 5637 cells carry a genomic deletion of the *RB1* gene. While this should, in theory, not affect DREAM formation, E2F1 sequestration by pRb is unattainable in these cells. Speculatively, this situation could therefore mimic the inactivation of pRb by E7, and therefore promote FOXM1 expression via E2F1 transactivation. This hypothesis could be further investigated by extending these experiments to additional cell lines with different mutational backgrounds (p53 mutation, additional pRb-mutated or -deleted cell lines).

In summary, despite being usually confined to actively proliferating cells, FOXM1 expression is sustained in growth-arrested HPV-positive cells. This effect could be mediated by continuing expression of the viral oncogenes, which cause DREAM disruption and ongoing E2F1 signaling.

3.3 Summary and conclusions

In the present studies, *FOXM1* and *CKS1B* could be identified as novel target genes of the HPV oncogenes *E6* and *E7*. Both mRNA and protein levels of FOXM1 and CKS1 are elevated by E6/E7, and this upregulation was shown to take place, at least in part, via stimulation of the transcriptional promoters of *FOXM1* and *CKS1B*. Each of the viral oncoproteins was able to independently activate the target gene promoters and this stimulatory effect was further increased upon combined E6 and E7 expression.

FOXM1 and *CSK1B* have been identified previously as target genes of the repressive DREAM complex which silences expression of cell cycle genes during quiescence and early G1 phase [157]. E6 and E7 both can interfere with DREAM formation and therefore abrogate repression of its target genes: E7 sequesters the pocket proteins p130 or p107 which make up an essential part of the DREAM multi-protein complex while the degradation of p53, which is initiated by E6, inactivates the p53-p21 axis that usually controls DREAM retention after p53 checkpoint activation [148]. Moreover, the formation of the transcriptionally activating MMB-FOXM1 complex that regulates expression of S/G2 cell cycle genes is promoted by HPV E7 [219]. It therefore seems a valid conclusion that the activating effect of HPV E6/E7 on the *FOXM1* and *CKS1B* promoters is at least partially mediated by disruption of the DREAM complex. In

addition, FOXM1 expression was also found to be activated by E2F1 via disturbance of the pRb-E2F1 interaction through E7.

While *CKS1B* expression is described to be transcriptionally controlled by FOXM1 through the MMB-FOXM1 complex [41, 143], the activating effect of E6/E7 on the *CKS1B* promoter was shown to occur independent of FOXM1 expression, precluding *CKS1B* activation from being a downstream effect of FOXM1 upregulation in HPV-positive cells and establishing it as an independent target gene of E6/E7. In addition, a p53-independent component of *CKS1B* promoter stimulation by E6 was observed in H1299 cells.

On the phenotypic level, CKS1 upregulation was shown to have a pro-proliferative and senescence-suppressing effect in cervical cancer cells. FOXM1 expression, on the other hand, was dispensable for the proliferation of HPV-positive cells, which stands in interesting contrast to cell lines from other cancer entities [129, 168, 169]. Apparently, HPV-positive cancer cells have found a way to overcome the dependency on FOXM1 expression for proliferation that is observed in other cancer types [75, 76]. Importantly however, FOXM1-depleted HPV-positive cancer cells were sensitized towards genotoxic agents, indicative of a role for FOXM1 in enhancing their chemoresistance. Neither FOXM1 nor CKS1 were found to decline during cell cycle arrest when HPV oncogene expression is maintained, in line with the concept that they are stimulated as a result of E6/E7-induced DREAM complex disruption.

Collectively, the findings of this dissertation identified *FOXM1* and *CKS1B* as functionally relevant novel target genes for oncogenic HPVs and have shed new light onto the virus/host cell crosstalk in HPV-positive cancer cells. They provide insights into the molecular mechanisms of *FOXM1* and *CKS1B* stimulation by the HPV E6/E7 oncogenes and delineate the resulting phenotypic consequences for HPV-positive cancer cells. Moreover, the observations that the proliferation of HPV-positive cancer cells was efficiently blocked after *CKS1B* knockdown, and that the suppression of FOXM1 had a chemosensitizing effect, indicate that FOXM1 and CKS1 inhibition could be a promising novel strategy for the treatment of HPV-linked (pre-)neoplasias.

CHAPTER 4

MATERIAL & METHODS

4 Material and Methods

4.1 Reagents

All reagents used were molecular biology grade where possible. All standard reagents for buffers and media were supplied by AppliChem (Germany), Applied Biosystems (USA), BD Biosciences (Germany), BioRad (USA), Carl Roth GmbH (Germany), Enzo Life Science (Germany), Fisher Scientific (USA), GE Healthcare (United Kingdom), Gerbu (Germany), Gibco (USA), Invitrogen (USA), Merck (Germany), Promega (USA), Roche Diagnostics (Switzerland), Saliter (Germany), and Sigma-Aldrich (Germany). Manufacturers of specific reagents are named in the text.
Buffers and solutions were prepared using dH_2O.

4.2 Cell-based methods

4.2.1 Cell culture

All cells were cultured in Dulbecco's minimal essential medium (DMEM, Gibco, Thermo Fisher Scientific, USA), except for 5637 bladder carcinoma cells which were maintained in RPMI-1640 medium (Gibco). The standard medium was supplemented with 10% fetal calf serum (FCS, Gibco), 100 U/ml penicillin, 100 µg/ml streptomycin, 2 mM L-glutamine ("PSG", all from Sigma-Aldrich) for all cell lines. Standard cultivation was performed at 37 °C and 5% CO_2 in a humidified atmosphere.
For routine passage, cells were split twice a week using 0.25% trypsin-EDTA solution (Gibco) for detachment. Cell cultures were supplied with fresh medium at least every 3 days.
For live cell proliferation analyses HeLa, SiHa and CaSki cells were transduced with a pMOWS hH2B mCherry expression vector, generating cells with a red fluorescent nucleus. Transduction of HeLa and SiHa cells was kindly performed by Dr. Joschka Willemsen, group of Dr. Marco Binder, DKFZ, Heidelberg. The newly generated cell lines were termed HeLa, SiHa or CaSki mCherry H2B, respectively, and were kept in stock medium containing puromycin (Alexis Biochemicals) for selection. The HeLa "p53 null" cell line contains a stably integrated shRNA against *TP53* and was generated by

Hengstermann *et al* [121]. For selection purposes its stock culture is maintained in DMEM supplemented with 700 µg/mL G418 (Gibco). For experiments, all selection agents were omitted from the media. An overview of all cell lines utilized in this thesis is provided in table 1.

For experiments, cells were either seeded in 6 cm dishes filled with 3 mL medium, or in 96 well plates with 100-200 µL medium. Typical cell seeding densities for 96 well plates are listed in table 2. Cells were counted using the Countess™ Automated Cell Counter (Invitrogen, Carlsbad, USA) after staining with trypan blue.

Table 1: Human cell lines and media

Cell line	Origin	Medium
5637	urinary bladder carcinoma	RPMI-1640
CaSki	HPV16-positive cervical cancer, epidermoid carcinoma	DMEM
CaSki mCherry H2B	HPV16-positive cervical cancer, epidermoid carcinoma	DMEM + 0.5 µg/mL puromycin
CxF6	uterine cervix primary fibroblasts	DMEM
Fib101	adult primary fibroblasts from abdominal skin	DMEM
H1299	non-small cell lung cancer	DMEM
HeLa	HPV18-positive cervical adenocarcinoma	DMEM
HeLa "p53 null"	HPV18-positive cervical adenocarcinoma	DMEM + 700 µg/mL G418
HeLa mCherry H2B	HPV18-positive cervical adenocarcinoma	DMEM + 1 µg/mL puromycin
MCF-7	breast adenocarcinoma	DMEM
SiHa	HPV16-positive cervical squamous cell carcinoma	DMEM
SiHa mCherry H2B	HPV16-positive cervical squamous cell carcinoma	DMEM + 1 µg/mL puromycin

Table 2: Seeding densities in 96 well plates

Cell line	Cells/well
CaSki mCherry H2B	4500
HeLa "p53 null"	2000
HeLa mCherry H2B	1500
SiHa mCherry H2B	3000

4.2.2 Cryopreservation and thawing of cells

For long-term storage, cells were trypsinized, pelleted by centrifugation at 800 x g, resuspended in culture medium containing 30% FCS and 10% DMSO and aliquoted into cryotubes. The cryotubes were transferred into an isopropanol-filled freezing container

(Nalgene, Thermo Fisher Scientific) and kept at -80 °C for several days before final storage in liquid nitrogen.

For thawing, cells were rapidly warmed to 37 °C in a water bath, resuspended in fresh culture medium and transferred into a new cell culture flask. Medium was exchanged the next day.

4.2.3 NOK cells

HPV-negative normal oral keratinocytes (NOKs), immortalized by the introduction of hTERT, were stably transduced with HPV16E6/E7 using lentiviral gene transfer. Cell line generation and culture were performed by Ruwen Yang, group of Prof. Frank Rösl, DKFZ, Heidelberg. Protein extracts were also generously provided by Ruwen Yang. Detailed experimental procedures are described in [220].

4.2.4 Treatment of cells with chemical compounds

If not indicated otherwise, cells were treated one day after seeding, or 24 h post transfection. Fresh medium was supplied before treatment. The same concentration of solvent was added to control cells. For long-term treatment experiments with hydroxyurea (HU), medium was exchanged and supplemented with freshly prepared HU every 24 h.

All chemical compounds employed, including manufacturer, stock concentration and solvent used, are given in table 3. If not noted otherwise, stock solutions were stored at -20 °C.

Table 3: Chemical compounds

Compound	Stock concentration	Solvent	Manufacturer	
Camptothecin (CPT)	5 µM	DMSO	Cayman Chemical	pre-dilution 1:1000 in DMEM
Cisplatin (CDDP)	3.3 mM	0.9% NaCl	Merck	stored at RT
Doxorubicin (DOX)	50 µM	H_2O	Enzo Life Sciences	
Hydroxyurea (HU)	500 mM	H_2O	Calbiochem	prepared freshly
Hygromycin B (HYG)	50 µg/mL	-	Invitrogen	stored at 4 °C
Mimosine	50 mM	10% $NaHCO_2$	Santa Cruz	
Nocodazole	10 mg/mL	DMSO	Calbiochem	
Thymidine	200 mM	PBS	Thermo Scientific	

4.2.5 Transfection of siRNAs using Dharmafect

RNA interference (RNAi) efficiently silences expression of a selected gene using small interfering RNAs (siRNAs) spanning a unique sequence within the target gene's mRNA. Synthetic siRNAs are usually 19 bp long and double-stranded, with a 2-nucleotide overhang at the 3'-ends. Upon transfection into the cell, they are incorporated into the cellular RISC (RNA-induced silencing complex), where they mediate mRNA degradation of their target gene.

For transfection, cells were seeded in 6 cm dishes at medium density to reach 40-50% confluency the next day. Then, the cell-line specific amount of Dharmafect I (Dharmacon) (see table 4) was mixed with the respective amount of OPTI-MEM (Gibco) to reach 200 µL and was incubated at room temperature (RT) for 5 min. Meanwhile, 198 µL OPTI-MEM were prepared with 2 µL siRNA stock (10 µM in nuclease-free H_2O, Ambion Silencer Select, Thermo Fisher Scientific) to yield a final siRNA concentration of 10 nM during transfection. Both mixtures were combined and incubated for another 20 min at RT. Meanwhile, medium in the 6 cm dishes was exchanged to 1.6 mL of PSG-free DMEM, supplemented with 10% FCS. The transfection mix (final volume 400 µL) was added dropwise to the cells. Medium was exchanged to 3 mL of full medium after 24 h.

For transfection in 96 well plates, volumes were adjusted as following: 20 µL of final transfection mix were prepared per well and added to 80 µL of PSG-free DMEM. Medium was exchanged to 200 µL of full medium after 24 h.

For transfection of control cells, siContr-1 was used, which contains at least 4 mismatches to all known human genes. All sequences of siRNAs utilized are listed in table 5. Where possible, a pool of 2-3 siRNAs was used at equimolar concentrations to minimize off-target effects.

Table 4: Dharmafect I concentrations depending on cell line

Cell line	Final concentration of Dharmafect I in transfection
HeLa	0.2%
HeLa mCherry H2B	0.2%
HeLa "p53 null"	0.2%
SiHa	0.3%
SiHa mCherry H2B	0.4%
CaSki mCherry H2B	0.3%

Table 5: siRNA sequences

siRNA	Sequence (5' -> 3')	Pool
siContr-1	CAGUCGCGUUUGCGACUGG	
si16E6-4	ACCGUUGUGUGAUUUGUUA	si16E6
si16E6-246	GGGAUUUAUGCAUAGUAUA	
si16E6-321	UUAGUGAGUAUAGACAUUA	
si16E6/E7-2	CCGGACAGAGCCCAUUACA	si16E6/E7
si16E6/E7-575	CACCUACAUUGCAUGAAUA	
si16E6/E7-617	CAACUGAUCUCUACUGUUA	
si18E6-340	GACAUUAUUCAGACUCTGU	si18E6
si18E6-349	CAGACUCUGUGUAUGGAGA	
si18E6-353	CUCUGUGUAUGGAGACACA	
si18E6/E7	CCACAACGUCACACAAUGU	si18E6/E7
si18E6/E7-563	CAGAGAAACACAAGUAUAA	
si18E6/E7-846	UCCAGCAGCUGUUUCUGAA	
siCKS1-1	GGACAUAGCCAAGCUGGUC	siCKS1
siCKS1-3	UGGUGACUUGCGGAUUUAU	
siFOXM1-2	AACAUCAGAGGAGGAACCU	siFOXM1
siFOXM1-3	UGGGAUCAAGAUUAUUAAC	

4.2.6 Transfection of plasmid DNA

Phosphate-buffered saline (PBS)

137 mM NaCl

2.7 mM KCl

4.3 mM Na_2HPO_4

1.4 mM KH_2PO_4

pH 7.4

autoclaved before use

BES buffer

50 mM BES

280 mM NaCl

1.5 mM Na_2HPO_4

pH 6.95

filter-sterilized before use

For transfection of plasmid DNA, the calcium phosphate coprecipitation method by Chen and Okoyama was used [221]. In brief, cells were seeded in 6 cm dishes at low density in 3 mL full DMEM, to reach ca. 30% confluency the next day. Plasmid DNA was mixed with 150 µL 0.25 M $CaCl_2$, then 150 µL of BES buffer was added. The mixture was incubated for 15 min at RT and then added dropwise to the cell culture dish. The cells were kept in a humidified incubator at 35 °C and 3% CO_2 for 16-18 h, before removing the medium, washing 2 times with PBS and adding 3 mL of fresh medium. HeLa cells were only washed once with PBS. The cells were then incubated at standard conditions and harvested 48 h after transfection for overexpression experiments and 72 h after transfection if knockdowns were performed.

Per 6 cm dish, 6-7.3 µg of total DNA were transfected. Where necessary, lower DNA amounts were filled up with pBlueScript II vector (pBS) to reach 6 µg. The pSUPER vector carries an expression cassette for small hairpin RNAs (shRNAs). They mediate gene silencing comparable to siRNAs (see 4.2.5) after processing by the cellular Dicer complex. The episomal pCEPsh vector additionally also allows for selection of transfected cells by conveying resistance to hygromycin B, thereby enabling long-term expression of the shRNAs. A list of all plasmids used in this project is provided in the appendix (table 12).

4.2.7 Luciferase reporter gene assay

Trisphosphate lysis buffer

25 mM glycylglycine, pH 7.8

15 mM $MgSO_4$

4 mM EGTA

1 mM DTT

10% glycerol

1% Triton X-100

Luciferase reaction buffer

25 mM glycylglycine, pH 7.8

15 mM $MgSO_4$

5 mM ATP

prepared freshly before use from 10x buffer and 50 mM ATP-solution

Luciferin solution

0.25 M luciferin in ATP-free luciferase reaction buffer

The luciferase reporter gene assay allows to study the promoter activity of a gene of interest, by cloning said promoter or fragments thereof in front of the firefly luciferase gene. The amount of expressed luciferase enzyme in transfected cells then directly correlates with the activity of the investigated promoter under the respective experimental conditions. It is quantified by measuring the amount of light emitted during oxidation of its substrate luciferin, using a luminometer. To normalize for variations in transfection efficiency between samples, a β-galactosidase assay (see 4.2.8) on co-transfected β-galactosidase reporter plasmid pCMV-Gal was performed in parallel. As p53 and E2F1 overexpression were observed to repress β-galactosidase expression from the pCMV promoter, Bradford assay (see 4.3.1) was performed in these experimental settings to normalize on total protein amount.

The respective plasmid mix was delivered to the cells using the calcium phosphate coprecipitation method (see 4.2.6). 0.2 µg pCMV-Gal were co-transfected in all samples. 48 h after transfection (for overexpression experiments) or 72 h after transfection (for knockdown experiments) cells were harvested: The medium was discarded, cells were washed once with cold PBS, and scraped in 200 µL trisphosphate lysis buffer. The lysed sample was transferred to a 1.5 mL-tube and undissolved cell debris was pelleted during centrifugation for 5 min at 16100 x g, 4 °C. 30 µL of the supernatant were transferred to a solid white 96 well plate for the luciferase activity measurement and the same amount was also pipetted into a transparent 96 well plate for the β-galactosidase assay. Trisphosphate lysis buffer was used as blank for both assays. Using a LB943 Mithras2 luminometer (Berthold Technologies, Bad Wildbad, Germany), luciferase activity was detected by measuring emission at 562 nm over 10 sec directly after injection of 150 µL luciferase reaction buffer and 50 µL luciferin solution into the sample. All experimental conditions were assessed in biological duplicates.

For evaluation, the luminometer blank value was subtracted from the readings, and the results were normalized for transfection efficiency using the respective β-galactosidase assay value. The mean of the duplicates was generated.

4.2.8 β-Galactosidase assay

β-Galactosidase reaction buffer

60 mM Na_2HPO_4

40 mM NaH_2PO_4

10 mM KCl

1 mM $MgSO_4$

1 mg/ml ortho-Nitrophenyl-β-galactoside

200 µL of reaction buffer were added to 30 µL cell lysate in a transparent 96 well plate. After a suitable time (ca. 5-30 min depending on the transfection efficiency) a yellow colouring can be observed. The absorbance was then measured at 405 nm using the Multiskan Ex ELISA plate reader (Thermo Electron, Karlsruhe, Germany). Absorbance at 620 nm was subtracted to minimize plate background.

4.2.9 TUNEL assay for apoptosis detection

The terminal deoxynucleotidyl transferase dUTP nick end labelling (TUNEL) assay labels the exposed 3'-hydroxyl termini of nuclear DNA that are generated during apoptosis. Chromatin fragmentation is a relatively late event in apoptosis and occurs when cellular endonucleases cleave the DNA at their only accessible site, between the nucleosomes. It can be detected over a wide range of cell types and apoptotic stimuli [222].

Cells were seeded on glass coverslips in 6 cm dishes. At the given time point, coverslips were removed from the dish, washed once in PBS and fixed in 4% formaldehyde solution for 30 min at RT. They were then washed twice with PBS and permeabilized in cold 0.1% Triton-X100, 0.1% sodium citrate in PBS for 2 min. (If necessary, coverslips may be stored in 70% EtOH at -20 °C for up to several weeks before permeabilization.) Before staining, coverslips were again washed twice in PBS and placed in a wet chamber. Using the *In situ* Cell Death Detection kit, fluorescein-coupled (Roche, Germany), cells were incubated with 25 µL TUNEL staining solution (solution 1:solution 2 - 1:9) at 37 °C for 60-90 min. Afterwards, coverslips were 5x dip-washed in PBS and left in fresh PBS for 2x 10 min. They were then incubated with 1 µg/mL DAPI (Roche, Germany) for 5 min at RT in the dark. After 5x dip-wash and 2x 10 min wash in PBS, coverslips were air-dried and mounted on microscope glass slides using Vectashield (Vector Laboratories Inc., USA). Transparent nail polish was used for sealing. Images were acquired the next day using a Zeiss motorized inverted Cell Observer.Z1 with LED module Colibri.2 and

the 20x/0.4 LD PlnN Ph2 DICII objective. The Fiji distribution of ImageJ 1.47q was used for image adjustment and representation.

4.2.10 Senescence assay

Senescence assay fixation buffer

2% formaldehyde

0.2% glutaraldehyde

in PBS

Senescence assay staining buffer

40 mM citric acid

150 mM NaCl

2 mM $MgCl_2$

adjusted to pH 6.0 with Na_2HPO_4

5 mM $K_3[Fe(CN)_6]$*

5 mM $K_4[Fe(CN)_6]$*

1 mg/ml X-Gal in DMF*

**freshly added*

Senescence describes the state of cells that have terminally exited the cell cycle and irreversibly ceased to proliferate. In these cells, the enzyme senescence-associated β-galactosidase (SA-β-Gal) is expressed and shows activity at pH 6.0 [223]. It can be detected using the chromogenic substrate X-Gal (5-bromo-4-chloro-3-indolyl-β-D-galactopyranoside) which results in blue staining of senescent cells.

72 h after transfection, cells were split into 6 cm dishes and cultivated under standard conditions for 3 additional days. The respective split ratios for each experiment are indicated in the figure legends. Cells were then washed with PBS and fixed with 1 mL senescence assay fixation buffer for 3 min. After washing with PBS, cells were incubated with 1.5 mL senescence assay staining buffer for 24 h at 37 °C in a wet chamber. After washing with PBS, representative images were acquired using the EVOSxl Core Cell Imaging System brightfield microscope (Life Technologies, USA) with 20-40x magnification.

4.2.11 Colony formation assay (CFA)

CFA buffer

12 mM crystal violet solution

29 mM NaCl

3.7% formaldehyde

22% EtOH

48 h after transfection with pCEPsh plasmids, cells were split. The next day, hygromycin B (HYG) was added to the medium. Cell line-specific HYG concentrations are provided in the figure legends. Fresh medium with HYG was supplied every 3-4 days for 1-2 weeks until colonies had formed and all cells in a mock transfected dish had died. Cells were then washed with PBS and stained with 350 µL CFA buffer for 5 min. Excessive dye was washed out with water and dishes were dried before scanning the images with the Epson Perfection 4990 Photo Scanner.

4.2.12 Cell cycle analysis

During the cell cycle, cellular DNA content doubles from G0 or G1 phase through DNA synthesis in S phase to G2 phase. Cell division (mitosis, M phase) then yields two individual cells with a complete set of chromosomes each. Using DNA-intercalating dyes like propidium iodide (PI), cells may be analysed by their DNA content in a flow cytometer.

72 h after transfection, cells were washed once with PBS and harvested using trypsination. Cells were pelleted and washed once again with PBS. All centrifugation steps were carried out at 100 x g, 5 min, 4 °C. Cells were resuspended in 300 µL cold PBS and 900 µL ice-cold EtOH were added for fixation. After immediate vortexing, cells were left at -20 °C for 1 h to several days. EtOH was removed, cells were resuspended in 25 µg/mL PI, 500 µg/mL RNAse in 1 mL PBS, and incubated for 30 min at RT in the dark. The cell suspension was filtered through gauze and analysed at the BD LSR Fortessa flow cytometer (BD, Germany) with the BD FACS Diva software v8.0.1. Analysis and image generation was performed with FlowJo v10. The Dean-Jett-Fox model was employed to generate and quantify cell cycle profiles.

4.2.13 EdU assay

To verify that cells were indeed growth-arrested after HU treatment, a flow cytometry-based EdU assay was conducted. EdU (5-Ethynyl-2'-deoxyuridine) is a nucleoside analogon to thymidine which is incorporated into newly synthesized DNA of proliferating cells. Using the EdU-Click 647 Kit (baseclick, Germany), the EdU is then detected via click chemistry coupling to a fluorescent dye.

Cells were treated with 1 mM HU for 48 h, and 2 h prior to harvest, 10 µM EdU was added to the dishes. As background control for the click reagent, one dish per condition was left without EdU. Cells were harvested and fixed as described for the cell cycle analysis (see 4.2.12). All centrifugation steps were carried out at 100 x g, 5 min, 4 °C. After removal of EtOH, cells were washed 2 mL PBS, pelleted and resuspended in 100 µL saponin-based permeabilization and wash buffer. 500 µL freshly prepared click assay cocktail was added and incubated for 30 min at RT in the dark. After washing with 2 mL saponin-based permeabilization and wash buffer, cells were resuspended in 25 µg/mL PI, 500 µg/mL RNAse in 1 mL PBS, and incubated for 30 min at RT in the dark. The cell suspension was filtered through gauze and analysed at the BD LSR Fortessa flow cytometer with the BD FACS Diva software v8.0.1. Analysis and image generation was performed with FlowJo v10.

4.2.14 Assessing cellular proliferation using the IncuCyte live cell imaging system

For proliferation studies, cells were seeded in 96 well plates according to the cell numbers given in table 2. After transfection and treatment with DNA damaging agents, cells were placed in the IncuCyte S3, and proliferation was monitored for up to 120 h. 4 images per well (phase plus red fluorescence (acquisition time 400 msec), where applicable) were acquired every 6 h at 10x magnification. Each experimental condition was analysed in triplicates. Proliferation was either assessed by calculating absolute cell numbers (Red Object Count (1/Well)) for H2B mCherry labelled cell lines, or by analysing confluence (Phase Object Confluence (percent)) for unlabelled cell lines. Image analysis was performed using the IncuCyte S3 2018A software.

4.2.15 Immunofluorescence

Cells were seeded on glass coverslips and harvested at the given time points. Coverslips were removed from the medium, washed once in PBS and fixed in 4% formaldehyde solution for 4 min. Cells were then washed with PBS, permeabilized in 0.1% Triton-X100

in PBS for 5 min, washed again in PBS and blocked in 5% BSA, 0.3 M Glycine, 0.1% Triton-X100 in PBS for 20 min at RT. Coverslips were then transferred to parafilm in a wet chamber and incubated with 30 µL of primary antibody (mouse anti-P-Ser139-H2AX No. 05-636 from Millipore, Germany) diluted 1:100 in 3% BSA, 0.1% Triton-X100 in PBS for 1 h. After 5x dip-wash in PBS, 30 µL of secondary antibody (donkey anti-mouse, Cy3-conjugate from Pierce Antibodies) diluted 1:400 in 3% BSA, 0.1% Triton-X100 in PBS with 1 µg/mL DAPI was applied and incubated for 45 min at RT in the dark. Coverslips were 5x dip-washed in PBS, once in H_2O, once in 100% EtOH and air-dried, before mounting on glass coverslips using Vectashield as mounting medium. Before image acquisition, the coverslips were sealed using transparent nail polish. Images were acquired with the Zeiss motorized inverted Cell Observer.Z1 with LED module Colibri.2 and the 40x/0.75 EC PlnN Ph2 objective.

4.3 Protein-based methods

4.3.1 Protein extraction and sample concentration equilibration

CSK-1 lysis buffer

10 mM PIPES pH 6.8

300 mM NaCl

1mM EDTA

300 mM sucrose

1 mM $MgCl_2$

0.5% Triton X-100

100 µl PhosSTOP phosphatase inhibitor cocktail (Roche Diagnostics, Switzerland), 25 µl Pefablock (Merck, Germany) *and* 10 µl P8340 protease inhibitor cocktail (Sigma-Aldrich, USA) *were added to 900 µl CSK-1 lysis buffer freshly before use.*

4x SDS-PAGE loading buffer
8% SDS
250 mM Tris-HCl
20% β-mercaptoethanol
40% glycerol
0.008% bromophenol blue

For cell harvest, medium was discarded, cells were washed once with PBS and scraped with a plastic cell scraper in 500 µL PBS. The cell suspension was transferred to a 1.5 mL tube, pelleted and PBS was removed. The cell pellet was stored at -80 °C for up to a few days if necessary or was directly lysed in 20-50 µL CSK-1 lysis buffer according to pellet size. After 30 min incubation on ice, the lysate was centrifuged at 16100 x g, 5 min, 4 °C and the supernatant was transferred to a fresh tube.
For determination of protein concentration, Bradford assay was performed. 1-3 µL of the cell lysate was added to 1 mL freshly prepared Bio-Rad Protein Assay Dye reagent (diluted 1:5 with H_2O from reagent concentrate; Bio-Rad, Germany) in a disposable cuvette and mixed well. Absorption at 595 nm was measured using a BioPhotometer D30 (Eppendorf, Germany). Final protein concentration was determined by adjusting to a BSA standard curve. Protein lysates were then equilibrated to the desired concentration (usually 3 µg/µL) by addition of appropriate volumes of CSK-1 and 4x SDS-PAGE loading buffer. Samples were heated to 96 °C for 5 min and stored at -20 °C/ -80 °C for long-term storage.

4.3.2 SDS-PAGE

SDS-PAGE running buffer
2.5 mM Tris
19.2 mM glycine
0.1% SDS

In SDS-PAGE (Polyacrylamide gel electrophoresis), protein samples are run through a gel under denaturing conditions to achieve separation by size.
Gels were cast using the disposable Novex Empty Gel Cassettes Mini (Life Technologies, Germany) or same-sized reusable glass plates as casing. Glass plates were sealed with 1% agarose at the bottom to prevent leaking of the gel. Recipes for separation and

stacking gels are given in table 6. After casting, gels were wrapped in papers soaked with SDS-PAGE running buffer and stored at 4 °C, for at least one day before running the gel. After placing the gels in the Xcell SureLock™ Mini-Cell Electrophoresis System (Life Technologies, Germany) filled with SDS-PAGE running buffer, gels were loaded with 10-21 µg of protein extract per lane. 1-2 µL of peqGOLD Protein-marker IV (PeqLab) was used as marker. Gels were run at 110 V for 1.5-2 h.

Table 6: SDS-PAGE: Recipe for 2 separation and stacking gels

Component	Separation gel (12.5%)		Stacking gel (5%)
H_2O	5.7 mL		2 mL
3 M Tris-HCl (pH 8.9)	1.8 mL	0.47 M Tris-HCl (pH 6.7)	1.2 mL
30% acrylamide/bisacrylamide	5.5 mL		620 µL
10% SDS	137.5 µL		45.8 µL
10% APS	176 µL		183.3 µL
TEMED	3.4 µL		1.8 µL

4.3.3 Western blot and immunodetection

Western Blot buffer

2.5 mM Tris

19.2 mM glycine

20% MeOH

pH 8.3

PBS-T

0.2% Tween-20

in PBS

Directly after SDS-PAGE, the gel cassette was disassembled and the proteins were transferred to Immobilon-P PVDF membrane (Millipore, Bedford, USA) using semi-dry blotting. To this end, the membrane was shortly activated in MeOH and then incubated in Western Blot buffer. 8 Whatman paper pieces (GE Healthcare, UK) were soaked in Western Blot buffer, and 4 of them were placed on the bottom of the Trans-Blot® SD Semi-Dry Electrophoretic Transfer Cell (Bio-Rad, Germany). This was followed by the activated membrane, the gel and another 4 pieces of Whatman paper. Air bubbles were

removed and the blotting proceeded for 1 h at 20 V. Up to 4 gels were transferred at the same time.

Afterwards the membrane was blocked in 5% milk powder (Saliter, Germany), 1% BSA in PBS-T for at least 1 h before cutting into up to 4 pieces for simultaneous detection of different-sized proteins.

The membrane pieces were incubated with primary antibody in 5% milk powder, 1% BSA in PBS-T over night at 4 °C. An overview of all antibodies used and their respective dilutions is provided in table 7. After washing 3x 10 min with PBS-T, HRP-coupled (horseradish peroxidase) secondary antibody was applied diluted 1:5000 in 5% milk powder, 1% BSA in PBS-T and incubated for at least 1 h at RT. Before detection, the membrane was again washed 3x with PBS-T for 10 min. Enhanced chemiluminescence (ECL) was used to detect antibody signals. After incubation for 1 min with ECL™ Prime Peroxide Solution (Amersham) or SuperSignal West Pico Luminol/Enhancer Solution (Thermo Fisher Scientific) depending on antibody signal intensity, images were acquired using the Fusion SL Detection System (Vilber Lourmat, Eberhardzell, Germany).

Table 7: Antibodies

Antibody	Supplier	Species	Dilution
anti-16E6	Arbor Vita Corporation, USA, #849	mouse	1:2000
anti-16E7	kind gift of Martin Müller, DKFZ Heidelberg, clone NM2	mouse	1:1000
anti-18E6	Arbor Vita Corporation, USA, #399	mouse	1:2000
anti-18E7	H. Zentgraf, DKFZ Heidelberg, ID: B(28) #47 31.10-11.11.95	chicken	1:1000
anti-β-actin	Sigma Aldrich, A2228	mouse	1:50000 in PBS-T
anti-CKS1	Invitrogen, 36-6800	rabbit	1:250
anti-FOXM1	Santa Cruz, sc-502	rabbit	1:500
anti-p27	BD Transduction Laboratories, 610242	mouse	1:500
anti-p53 (DO-1)	Santa Cruz, sc-126	mouse	1:1000
anti-p53 (FL393)	Santa Cruz, sc-6243	rabbit	1:200
anti-γ-tubulin	Sigma Aldrich, T6557	mouse	1:5000
anti-vinculin	Santa Cruz, sc-73614	mouse	1:4000
Secondary antibodies			
anti-chicken IgG-HRP	Santa Cruz, sc-2428	goat	1:5000
anti-mouse IgG-HRP	Santa Cruz, sc-2005	goat	1:5000
anti-rabbit IgG-HRP	Santa Cruz, sc-2004	goat	1:5000

4.4 DNA-based methods

4.4.1 Plasmid preparation

Lysogeny Broth (LB) medium

1% Bacto trypton

0.5% yeast extract

170 mM NaCl

pH 7.0

Solution I

50 mM glucose

25 mM Tris

10 mM EDTA

pH 6.7

Solution II

0.2 M NaOH

1% SDS

prepared freshly before use

Solution III

3 M potassium acetate

11.5% acetic acid

TE buffer

10 mM Tris

1 mM EDTA

pH 8.0

Plasmid isolation of small volumes (from 2-4 mL overnight bacterial culture in antiobiotic-supplemented LB medium) was performed using the PureLink™ Quick Plasmid Miniprep Kit (Invitrogen, Germany). For medium amounts of plasmid DNA (from 50 mL LB medium) the PureLink™ HiPure Plasmid Filter Midiprep Kit (Invitrogen) was used. Both kits were utilized according to the manufacturer's instructions.

For purification of larger amounts of plasmid DNA the maxipreparation protocol based on Sambrook and Russell [224] was employed. To that end, 250 mL overnight culture of transformed bacteria was pelleted, resuspended in 10 mL solution I, lysed in 20 mL freshly prepared solution II and neutralized with 15 mL solution III. After briefly chilling on ice, lysate was centrifuged at 5500 x g and 4 °C for 10 min to pellet cellular debris. The plasmid-containing supernatant was transferred to a fresh tube and equal volume of isopropanol was added to precipitate DNA. After incubation for 30 min on ice, plasmid DNA was pelleted at 5500 x g and 4°C for 25 min. The pellet was dissolved in 4 mL TE buffer and 4 mL 5 M LiCl solution was added. After incubation for 30-60 min on ice and centrifugation at 5000 x g, 5 min, 4 °C, the supernatant was transferred to a fresh falcon tube and precipitated using EtOH. The resulting pellet was resuspended in 4 mL TE buffer with 4.4 g CsCl and supplemented with 100 µL ethidium bromide solution (10 mg/mL). Samples were transferred to 6 ml PA Ultraclimp tubes (Sorvall, Asheville, USA). Ultracentrifugation was then carried out at 220000 x g at 20 °C for 16 h in an OTD75B Sorvall Ultracentrifuge. The supercoiled plasmid DNA, visible through incorporation of ethidium bromide, was extracted and transferred to a 50 mL falcon tube. To remove ethidium bromide from plasmid DNA, extraction with water-saturated 1-butanol was performed several times. Precipitation of plasmid DNA was then carried out by adding 2 volumes of ethanol and incubating at -20 °C for 1 h. Following centrifugation at 5500 x g and 4 °C for 30 min, DNA was resuspended in 4 mL TE buffer supplemented with 160 µL 5 M NaCl solution. DNA was again precipitated with EtOH and pelleted by centrifugation. Purified plasmid DNA was finally resuspended in 200-500 µL TE buffer and concentration was determined with the NanoDrop ND-1000 spectrophotometer (Peqlab, Erlangen, Germany).

4.4.2 Cloning of shRNAs

10x TNE buffer

100 mM Tris, pH 7.5

1 M NaCl

10 mM EDTA

Electrophoresis buffer

40 mM Tris

5 mM sodium acetate

1 mM EDTA

pH 7.8

6x DNA loading dye

0.25% bromophenol blue

0.25% xylene cyanol

30% glycerol

Oligonucleotides containing the target gene-specific shRNA sequence were ordered from Sigma Aldrich. Sense and antisense oligonucleotides were annealed using 2.5 µL each in 50 µL total volume in TNE buffer, by heating to 95 °C for 5 min, transferring to 70 °C for 10 min and slowly letting cool down the reaction mix to ca. 40 °C in a water bath. The annealed oligonucleotide was then kinase-treated in PNK A-buffer using the PNK enzyme (Thermo Scientific), by incubating at 37 °C for 30 min, then heating to 70 °C for 10 min and letting cool down slowly to ca. 40 °C.

It was then ligated into the BglII- and HindIII-digested and 5'-dephosphorylated pSUPER backbone, using the T4 DNA ligase in the appropriate buffer (Thermo Scientific) and incubating for 2 h at 21 °C. The ligase was then heat-inactivated at 65 °C for 5 min to terminate the reaction.

Subsequently, competent *Escherichia coli* TG2 were transformed with the ligation mix using heat-shock transformation. To this end, *E. coli* TG2 were slowly thawed on ice. 100 µL of competent bacteria were inoculated with 10 µL of ligation mix and kept on ice for 30 min. Heat shock was performed in a water bath at 42 °C for 45-60 sec. Afterwards, bacteria were transferred back on ice for another 10 min, before adding 750 µL of LB medium and shaking at 37 °C for 45-60 min. 10-50% of the transformed bacteria were then plated on an ampicillin-containing LB-agar-plate (1.5% agar agar for bacteriology (Gerbu, Heidelberg, Germany); 100 µg/mL ampicillin) and grown at 37 °C overnight to form clones.

The next day, overnight cultures for "miniprep" were inoculated from single colonies, and the plasmids purified the day after (see 4.4.1). To check for correct insertion of the shRNA-containing oligonucleotide, restriction digest using EcoRI and HindIII

endonucleases (NEB) was carried out for 2 h at 37 °C. The appropriate amount of 6x DNA loading dye was added to the samples for analysis of the resulting fragment using agarose gel electrophoresis. This was performed in a 2% agarose gel stained with PeqGREEN non-toxic DNA/RNA dye (1:20000, Peqlab, Germany), run at 80-100 V for 30-90 min in electrophoresis buffer. As a size marker, 5 µL SmartLadder (Eurogentec, Belgium) was used. DNA was visualized via UV transillumination in a gel documentation system (Intas Science Imaging Instruments, Göttingen, Germany).

If positive in the restriction digest, plasmids were sent for verification by sequencing to Eurofins Genomics, Ebersberg, Germany. Analysis of the sequences was performed using the Basic Local Alignment Search Tool (BLAST) provided by the National Center for Biotechnology Information. After purification of correct plasmids by "midiprep" procedure, the sequences were tested for effective knockdown of their target gene.

If shRNAs were intended for use in colony formation assays, they were cloned from pSUPER into a pCEP4 vector backbone to enable stable episomal plasmid maintenance via HYG selection. To this end, the respective pSUPER construct was digested with BamHI and XhoI restriction endonucleases (NEB), releasing the H1 promoter-shRNA fragment. After size separation using agarose gelelectrophoresis, the respective fragment was cut from the gel and extracted using the QIAquick Gel Extraction Kit (Qiagen, Hilden, Germany) according to the instructions provided by the manufacturer. The purified DNA fragment was ligated into open pCEP4 vector backbone (generated by restriction digest with BglII and XhoI, 5'-dephosphorylated, thereby removing the pCMV promoter), and transformed via heat shock into *E. coli* TG2. Positive clones were verified by restriction digest with SalI (NEB).

4.4.3 Cloning of the *CKS1B* promoter construct pBL-CKS1B

The human *CKS1B* promoter was cloned into the pBL luciferase reporter construct to study transcriptional regulation of the promoter via luciferase assays. To that end, a 550 bp stretch located directly upstream of the first amino acid-coding ATG of *CKS1B* was amplified from HeLa genomic DNA by polymerase chain reaction (PCR). Primers were designed to add restriction sites for NotI (forward) and HindIII (reverse) to the amplicon. Primer sequences are given in table 9. The PCR reaction mix contained 25 pmol of each primer, 250 ng of genomic DNA, 2.5 mM of each dNTP, and 5 U Pfu polymerase in the appropriate buffer. The PCR program is listed in table 9 and was carried out in the PTC-200 Peltier Thermal Cycler (MJ Research).

After verification of the correct size on a 1% agarose gel, the amplified DNA was digested with NotI and HindIII at 37 °C over night. Empty pBL backbone was opened by NotI- and HindIII-digestion and 5'-dephosphorylated. The *CKS1B* promoter construct was ligated into pBL using a vector:insert ratio of 1:5. The ligation was carried out using T4 DNA ligase and proceeded for 2 h at 21 °C. The ligation mix was transformed into *E. coli* TG2, positive clones were verified by NotI/HindIII test digest and sequencing.

4.4.4 Cloning of FOXM1 promoter construct into pBL

The ca. 330 bp FOXM1 promoter construct was amplified from pGL3-FOXM1 for cloning into the pBL luciferase reporter construct. The PCR reaction mix contained 25 pmol of each primer, 10 ng of pGL3-FOXM1, 2.5 mM of each dNTP, and 5 U Pfu polymerase in the appropriate buffer. The primers were designed to add restriction sites for NotI (forward) and HindIII (reverse) to the amplicon. Primer sequences are given in table 8. The PCR program is listed in table 9 and was carried out in the PTC-200 Peltier Thermal Cycler (MJ Research).

After verification of the correct size on a 1% agarose gel, the DNA fragment was extracted from the gel and digested with NotI and HindIII at 37 °C over night. Empty pBL backbone was opened by NotI- and HindIII-digestion and 5'-dephosphorylated. The *FOXM1* promoter construct was ligated into pBL using a vector:insert ratio of 1:5. The ligation was carried out using T4 DNA ligase and proceeded for 2 h at 21 °C. The ligation mix was transformed into *E. coli* TG2, positive clones were verified by NotI/HindIII test digest and sequencing.

Table 8: PCR primers

Name	Sequence (5' -> 3')
CKS1B fw (NotI)	AATAAGCGGCCGCGGGTTCCGGGGTGAAAGAGTG
CKS1B rev (HindIII)	ATTAAGCTTATCGCTCGGTTTGCTAGCCTT
FOXM1 fw (NotI)	AATAAGCGGCCGCCCAGGGACCCGGGCCT
FOXM1 rev (HindIII)	TTGAAGCTTGGATCCCGGGAGGGAGG

Table 9: PCR programs

CKS1B		
95 °C	2 min	
95 °C	1 min	30x
58 °C	30 sec	
72 °C	1:50 min	
72 °C	5 min	

FOXM1		
95 °C	2 min	
95 °C	30 sec	30x
58 °C	30 sec	
72 °C	1 min	
72 °C	5 min	

4.5 RNA-based methods

4.5.1 RNA extraction

Isolation of total RNA was performed using the column-based PureLink RNA Mini Kit (Invitrogen, Germany) according to the manufacturer's instructions. Cells were washed once with PBS and RNA lysis buffer freshly supplemented with β-mercaptoethanol was added directly onto the cells. When protein and RNA were extracted from the same 6 cm dish, cells were scraped from the dish in PBS using a plastic cell scraper and the resulting cell suspension was divided into two separate tubes. The cells designated for RNA extraction were pelleted at 16100 x g, 10 sec, 4 °C, PBS was removed and RNA lysis buffer including β-mercaptoethanol was added. The lysate was resuspended and either stored at -20 °C or directly further processed for RNA extraction following the kit manual. To remove unwanted DNA from the samples PureLink DNase Set (Invitrogen) was applied. The purified RNA was eluted in 40-80 µl RNAse-free H_2O and concentration was determined with the NanoDrop ND-1000 spectrophotometer (Peqlab). Purified RNA was stored at -80 °C.

4.5.2 cDNA generation by reverse transcription

The ProtoScript® II First Strand cDNA Synthesis Kit (NEB, USA) was used for cDNA generation. 500 ng total RNA per sample were transcribed in a total reaction volume of 10 µL using oligo-dT primers. RNA mixed with primers was heated to 70 °C for 5 min in a PTC-200 Peltier Thermal Cycler (MJ Research) and cooled down to 4 °C before addition of buffer and enzyme. The reaction then proceeded for 5 min at 25 °C, was incubated at 42 °C for 1 h and finally heated to 80 °C for 5 min. The resulting cDNA was diluted by addition of 40 µL nuclease-free H_2O and kept at -20 °C for long-term storage.

4.5.3 Quantitative real-time PCR (qRT-PCR)

qRT-PCR allows the quantification of cellular mRNAs after their reverse transcription to cDNA (see 4.5.2). Table 11 contains all primers used for qRT-PCR in this project. Prior to use, all primer pairs were checked for binding efficiency (80-110%) by generating a standard curve using serial dilutions.

The reaction mix per sample contained 10 µl SYBR™ Green PCR Master Mix (Applied Biosystems, USA), 0.4 µl each of forward and reverse primer, 7.2 µl nuclease-free H_2O and 2 µL cDNA. All reactions were run as duplicates. Final primer concentration was 100 nM per primer per reaction. A water control without cDNA was used as negative control. The reaction was run in a MicroAmp™ Optical 96-Well Reaction Plate (Life Technologies, Germany) on a 7300 Real Time PCR System (Applied Biosystems, Invitrogen) according to the following program:

Table 10: qRT-PCR program

Inititation	50 °C	2 min	
Polymerase activation	95 °C	10 min	
Denaturation	95 °C	15 sec	40x
Annealing and elongation	60 °C	1 min	
Dissociation curves	95 °C	15 sec	
	60 °C	1 min	
	95 °C	15 sec	
	60 °C	15 sec	

The generation of dissociation curves allowed detection of unspecific amplification artefacts. Calculation of mRNA expression was performed according to the comparative Ct ($2^{\Delta\Delta Ct}$) method [225] with normalization to β-actin expression as internal reference.

Table 11: List of qRT-PCR primers

Primer	Sequence (5' -> 3')	Alternative name
β-actin fw	GGACTTCGAGCAAGAGATGGC	
β-actin rev	GCAGTGATCTCCTTCTGCATC	
CKS1B fw2	TCGGACAAATACGACGACGAG	
CKS1B rev2	AACAGCAAGATGTGAGGTTCGGT	
FOXM1 fw1	GGCAGCAGGCTGCACTATC	
FOXM1 rev1	TCGAAGGCTCCTCAACCTTAAC	
HPV16 E6 fw3	AGCAATACAACAAACCGTTGTGT	
HPV16 E6 rev2	CCGGTCCACCGACCCCTTAT	
HPV16 E6/E7 fw	CAATGTTTCAGGACCCACAGG	HPV16 E6all fw
HPV16 E6/E7 rev	CTCACGTCGCAGTAACTGTTG	HPV16 E6all rev
HPV18 E6 fw1	AGACAGTATACCCCATGCTGCAT	
HPV18 E6 rev1	TCCAATGTGTCTCCATACACAGA	
HPV18 E6/E7 fw	ATGCATGGACCTAAGGCAAC	
HPV18 E6/E7 rev	AGGTCGTCTGCTGAGCTTTC	

HPV16 and HPV18 *E6/E7* primers recognize all three transcript classes of HPV16 and HPV18 *E6/E7.*

4.6 Statistical analysis

If not indicated otherwise in the figure legends, all experiments were conducted at least three times with consistent results and one representative replicate is presented.
Mean values and standard deviations were calculated using Microsoft Excel (Microsoft Office 2010) or SigmaPlot Version 13. Analyses of fold change values were carried out following logarithmic transformation. Statistical significance was determined by one-way ANOVA using SigmaPlot software. P-values of ≤0.05 (*), ≤0.01 (**), or ≤0.001 (***) were considered statistically significant.

APPENDIX

Supplemental figures

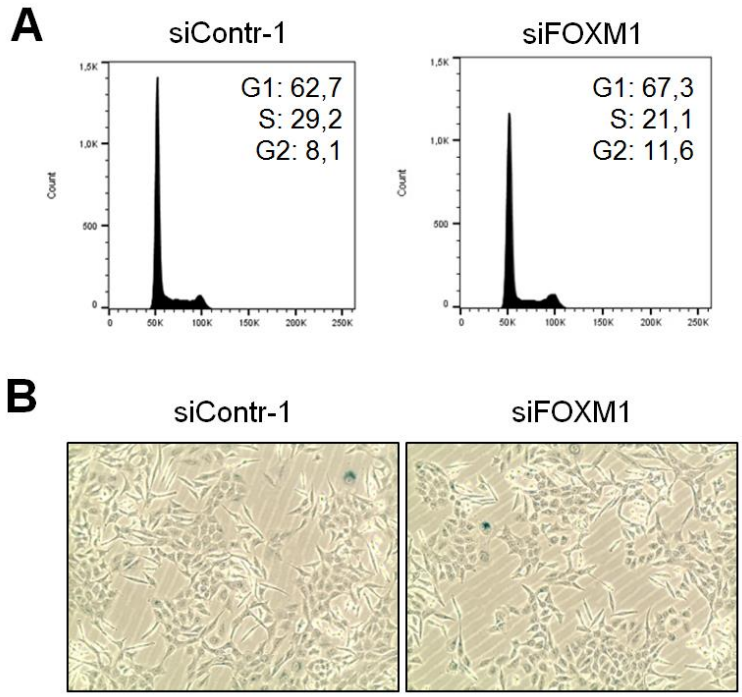

Supplemental figure 1 (supplemental to figure 10): *FOXM1* knockdown in SiHa only marginally alters cell cycle distribution and does not induce senescence. A: Cell cycle analyses of SiHa cells after *FOXM1* knockdown. Cell cycle phase distributions are given in %. **B:** SA β-Gal assay of SiHa cells after *FOXM1* knockdown. Split ratio: 1:10. **A, B:** Shown is one representative replicate of 2 independent experiments. siContr-1: control siRNA.

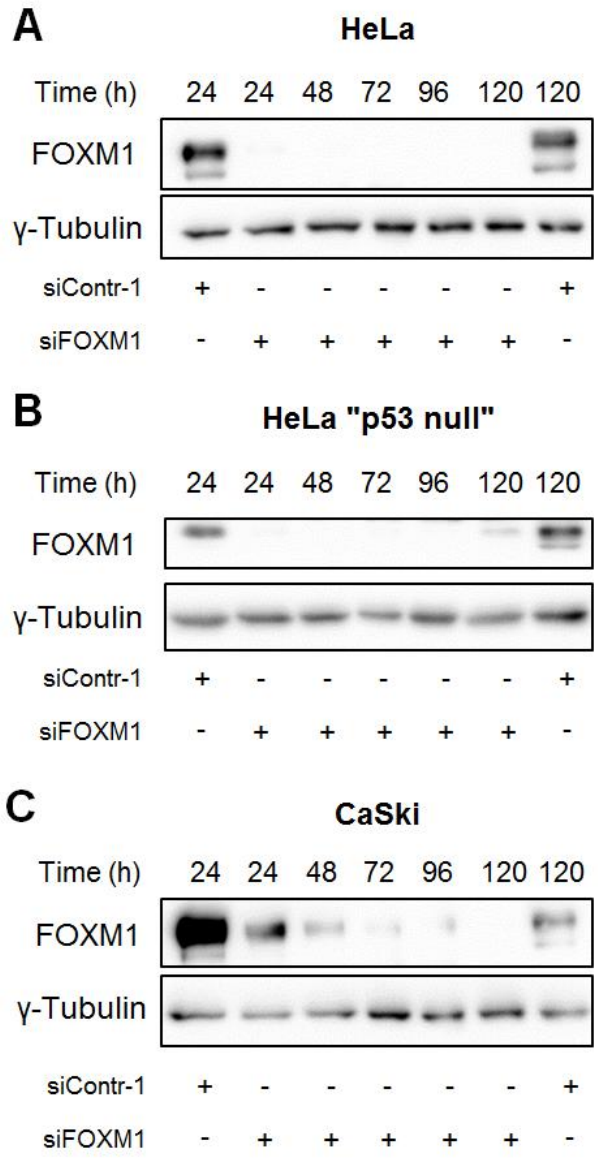

Supplemental figure 2 (supplemental to figure 13): *FOXM1* knockdown by siRNA is effective over 120 h. HeLa (**A**), HeLa "p53 null" (**B**) and CaSki (**C**) were subjected to *FOXM1* knockdown. FOXM1 protein levels were monitored over 120 h. γ-tubulin: loading control. siContr-1: control siRNA. Data produced jointly with Julia Botta.

List of plasmids

Table 12

Plasmid	shRNA target sequence (5'->3')	Source	Comments
pBCH	-	[226]	
pBCH-16E6	-	[226]	
pBL	-	[126]	
pBL-CKS1B	-	see 4.4.3	
pBL-FOXM1	-	see 4.4.4	
pCEP4	empty vector	Invitrogen	
pCEP-shCKS1_1	GGACATAGCCAAGCTGGTC	see 4.4.2	
pCEP-shCKS1_2	AAACTCAGATGCTTCCTCC		
pCEP-shCKS1_3	TGGTGACTTGCGGATTTAT		
pCEP-shFOXM1_1	GGACCACTTTCCCTACTTTTT		
pCEP-shFOXM1_2	AACATCAGAGGAGGAACCTAA		
pCEP-shFOXM1_3	TGGGATCAAGATTATTAACCA		
pCEP-shNeg	TACGACCGGTCTATCGTAG	[137]	
pCMV-16E7-HA/flag	-	[227]	
pCMV-16E7ΔDLYC-HA/flag	-	[228]	
pCMV-E2F1	-	Addgene #21667	
pCMV-Gal	-	[229]	
pCMV-HA/flag	-	[228]	
pCMVtk	-	[230]	
pCMVtk-p53	-	[230]	
pGL3 basic	-	Promega	
pGL3-FOXM1	-	[42]	nucleotides -296 to +60
pGL3-FOXM1long	-	[42]	nucleotides -2436 to +60; GenBank Accession No. Y12337
pGUP.PA.8	-	[124]	
pGUP.PA.8-p53CONLuc	-	[124]	
pSUPER	empty vector	[231]	
pSUPER-sh18E6/E7	CCACAACGTCACACAATGT	[137]	used as pSUPER sh18E6/E7
pSUPER-sh18E6/E7-563	CAGAGAAACACAAGTATAA		
pSUPER-sh18E6/E7-846	TCCAGCAGCTGTTTCTGAA		
pSUPER-sh18E6-340	GACATTATTCAGACTCTGT		used as pSUPER sh18E6
pSUPER-sh18E6-349	CAGACTCTGTGTATGGAGA		
pSUPER-sh18E6-353	CTCTGTGTATGGAGACACA		
pSUPER-shCKS1_1	GGACATAGCCAAGCTGGTC	[232], see 4.4.2	

pSUPER-shCKS1_2	AAACTCAGATGCTTCCTCC	[233], see 4.4.2	
pSUPER-shCKS1_3	TGGTGACTTGCGGATTTAT	[234], see 4.4.2	
pSUPER-shContr-1	CAGTCGCGTTTGCGACTGG	[235]	
pSUPER-shFOXM1_1	GGACCACTTTCCCTACTTTTT	[43], see 4.4.2	
pSUPER-shFOXM1_2	AACATCAGAGGAGGAACCTAA	[51], see 4.4.2	used as pSUPER shFOXM1 pool
pSUPER-shFOXM1_3	TGGGATCAAGATTATTAACCA		
pSUPER-shp53	GACTCCAGTGGTAATCTAC	[231]	
p21Luc	-	[236]	also referred to as pWWP

List of figures

List of tables

Abbreviations

a. o.	and others
ANOVA	Analysis Of Variance
APS	Ammonium Persulfate
ATP	Adenosine Triphosphate
BER	Base Excision Repair
BLAST	Basic Local Alignment Search Tool
bp	base pair
BRCA2	Breast Cancer-Associated Protein 2
BRIP1	BRCA1-Interacting Protein C-terminal Helicase 1
C1	Compound 1
ca.	circa
CBP	Creb-Binding Protein
CDDP	*cis*-Diamminedichloridoplatinum, Cisplatin
CDK	Cyclin-Dependent Kinase
cDNA	Copy DNA
CFA	Colony Formation Assay
CHR	Cell Cycle Homologous Region
CIN	Cervical Intraepithelial Neoplasia
CIN25	Chromosomal Instability Signature 25
CKS1	Cyclin-dependent Kinases Regulatory Subunit 1B
CPT	Camptothecin
DAPI	4',6-Diamidino-2-phenylindole
DDR	DNA Damage Response
dH_2O	Desalted Water
Dlg	Disks Large Homolog
DMEM	Dulbecco's Modified Eagle's Medium
DMF	Dimethylformamide
DMSO	Dimethyl Sulfoxide
DNA	Desoxyribonucleic Acid
dNDP	Desoxynucleoside Diphosphate
dNTP	Desoxynucleoside Triphosphate
DOX	Doxorubicin
DREAM	DP, Rb-like, E2F4 and MuvB
DSB	Double Strand Break

DTT	Dithiothreitol
E6-AP	E6-Associated Protein
E6-BP	E6-Binding Protein (Reticulocalbin-2)
ECL	Enhanced Chemiluminescence
EDTA	Ethylenediaminetetraacetic Acid
EdU	5-Ethynyl-2´-deoxyuridine
EGTA	Ethylene Glycol Tetraacetic Acid
et al	et alii (and others)
EtOH	Ethanol
EXO1	Exonuclease 1
FCS	Fetal Calf Serum
fig.	Figure
FOXM1	Forkhead Box Protein M1
fw	forward
H2B	Histone 2B
HNSCC	Head and Neck Squamous Cell Carcinoma
HPV	Human Papillomavirus
HR	Homologous Recombination
HRP	Horseradish Peroxidase
HSP70	Heat Shock Protein 70 kDa
hTERT	Human Telomerase Reverse Transcriptase
HU	Hydroxyurea
HYG	Hygromycin B
kbp	kilo base pairs
LB	Lysogeny Broth
$\log_{10}$	decimal logarithm
MAGI	Membrane-Associated Guanylate Kinase
MEF	Mouse Embryonic Fibroblasts
MeOH	Methanol
MMB	B-Myb-MuvB
MMP-2/-9	Matrix Metalloproteinase-2/-9
mRNA	messenger RNA
MuvB	Multi-vulval Class B
NBS1	Nijmegen Breakage Syndrome Protein 1
NDP	Nucleoside Diphosphate
NER	Nucleotide Excision Repair

NHEJ	Non-Homologous End Joining
NOK	Normal Oral Keratinocyte
NSCLC	Non-Small Cell Lung Cancer
ORF	Open Reading Frame
PAGE	Polyacrylamide Gel Electrophoresis
PBS	Phosphate-Buffered Saline
PCR	Polymerase Chain Reaction
PDZ	Post synaptic density protein (PSD95), Disks large homologue (Dlg1) and Zonula occludens-1 protein (zo-1)
PI	Propidium Iodide
PIPES	Piperazine-N,N′-bis(2-ethanesulfonic acid)
pRb	Retinoblastoma-associated Protein
PSG	Penicillin, Streptomycin, Glutamine
rev	reverse
RISC	RNA-induced Silencing Complex
RLU	Relative Luciferase Unit
RNA	Ribonucleic Acid
RNAi	RNA Interference
RT	Room Temperature
RT-qPCR	Reverse Transcriptase Quantitative PCR
SA-β-Gal	Senescence-Associated β-Galactosidase
SCF	Skp1, Cullin1 and F-box protein
SDS	Sodium Dodecyl Sulfate
Ser	Serine
shRNA	Short Hairpin RNA
siRNA	Small Interfering RNA
Skp2	S-phase Kinase-associated Protein 2
SUMO	Small Ubiquitin-related Modifier
TEMED	Tetramethylethylenediamine
TUNEL	Terminal Deoxynucleotidyl Transferase dUTP Nick End Labelling
VEGF	Vascular Endothelial Growth Factor
XRCC1	X-ray Cross-Complementing Protein 1
γ-H2AX	phosphorylated Histone 2AX (Ser139)

The one-letter code for nucleotides was applied according to declarations by the International Union of Pure and Applied Chemistry (IUPAC).

Units

°C	degree Celsius
Da	Dalton
g	gram
h	hour
L	liter
m	meter
M	molar (mole/L)
min	minute
mol	mole
sec	second
U	enzyme unit
V	volt
x g	centrifugal acceleration
%	percent

Prefixes

Symbol	Prefix	Factor
k	kilo	10^{3}
c	centi	10^{-2}
m	milli	10^{-3}
µ	micro	10^{-6}
n	nano	10^{-9}
p	pico	10^{-12}

References

[1] M. E. Harden and K. Munger, "Human papillomavirus molecular biology.," *Mutat. Res. Rev. Mutat. Res.*, vol. 772, pp. 3–12.

[2] H. W. Chesson, E. F. Dunne, S. Hariri, and L. E. Markowitz, "The Estimated Lifetime Probability of Acquiring Human Papillomavirus in the United States," *Sex. Transm. Dis.*, vol. 41, no. 11, pp. 660–664, Nov. 2014.

[3] M. Schiffman *et al.*, "Carcinogenic human papillomavirus infection," *Nat. Rev. Dis. Prim.*, vol. 2, p. 16086, 2016.

[4] D. Pyeon, S. M. Pearce, S. M. Lank, P. Ahlquist, and P. F. Lambert, "Establishment of human papillomavirus infection requires cell cycle progression.," *PLoS Pathog.*, vol. 5, no. 2, p. e1000318, Feb. 2009.

[5] J. Doorbar *et al.*, "The Biology and Life-Cycle of Human Papillomaviruses," *Vaccine*, vol. 30, pp. F55–F70, Nov. 2012.

[6] M. Bergvall, T. Melendy, and J. Archambault, "The E1 proteins.," *Virology*, vol. 445, no. 1–2, pp. 35–56, Oct. 2013.

[7] A. A. McBride, "The Papillomavirus E2 proteins," *Virology*, vol. 445, no. 1–2, pp. 57–79, Oct. 2013.

[8] J. Doorbar, "The E4 protein; structure, function and patterns of expression.," *Virology*, vol. 445, no. 1–2, pp. 80–98, Oct. 2013.

[9] D. DiMaio and L. M. Petti, "The E5 proteins," *Virology*, vol. 445, no. 1–2, pp. 99–114, Oct. 2013.

[10] N. Hemmat and H. B. Baghi, "Human papillomavirus E5 protein, the undercover culprit of tumorigenesis," *Infect. Agent. Cancer*, vol. 13, no. 1, p. 31, Dec. 2018.

[11] J. Doorbar, N. Egawa, H. Griffin, C. Kranjec, and I. Murakami, "Human papillomavirus molecular biology and disease association," *Rev. Med. Virol.*, vol. 25, pp. 2–23, Mar. 2015.

[12] S. Shanmugasundaram and J. You, "Targeting Persistent Human Papillomavirus Infection," *Viruses*, vol. 9, no. 8, p. 229, Aug. 2017.

[13] M. Dürst, L. Gissmann, H. Ikenberg, and H. zur Hausen, "A papillomavirus DNA from a cervical carcinoma and its prevalence in cancer biopsy samples from different geographic regions.," *Proc. Natl. Acad. Sci. U. S. A.*, vol. 80, no. 12, pp. 3812–5, Jun. 1983.

[14] L. Gissmann, M. Boshart, M. Dürst, H. Ikenberg, D. Wagner, and H. zur Hausen, "Presence of human papillomavirus in genital tumors.," *J. Invest. Dermatol.*, vol. 83, no. 1 Suppl, pp. 26s-28s, Jul. 1984.

[15] D. Hasche *et al.*, "The interplay of UV and cutaneous papillomavirus infection in skin cancer development.," *PLoS Pathog.*, vol. 13, no. 11, p. e1006723, Nov. 2017.

[16] C. de Martel, M. Plummer, J. Vignat, and S. Franceschi, "Worldwide burden of cancer attributable to HPV by site, country and HPV type," *Int. J. Cancer*, vol. 141, no. 4, pp. 664–670, Aug. 2017.

[17] S. Lax, "Histopathology of cervical precursor lesions and cancer.," *Acta dermatovenerologica Alpina, Pannonica, Adriat.*, vol. 20, no. 3, pp. 125–33, Sep. 2011.

[18] A. A. McBride and A. Warburton, "The role of integration in oncogenic progression of HPV-associated cancers," *PLOS Pathog.*, vol. 13, no. 4, p. e1006211, Apr. 2017.

[19] P. Hawley-Nelson, K. H. Vousden, N. L. Hubbert, D. R. Lowy, and J. T. Schiller, "HPV16 E6 and E7 proteins cooperate to immortalize human foreskin keratinocytes.," *EMBO J.*, vol. 8, no. 12, pp. 3905–10, Dec. 1989.

[20] K. Münger, W. C. Phelps, V. Bubb, P. M. Howley, and R. Schlegel, "The E6 and E7 genes of the human papillomavirus type 16 together are necessary and sufficient for transformation of primary human keratinocytes.," *J. Virol.*, vol. 63, no. 10, pp. 4417–21, Oct. 1989.

[21] E. C. Goodwin, E. Yang, C. J. Lee, H. W. Lee, D. DiMaio, and E. S. Hwang, "Rapid induction of senescence in human cervical carcinoma cells.," *Proc. Natl. Acad. Sci. U. S. A.*, vol. 97, no. 20, pp. 10978–83, Sep. 2000.

[22] S. I. Wells, D. A. Francis, A. Y. Karpova, J. J. Dowhanick, J. D. Benson, and P. M. Howley, "Papillomavirus E2 induces senescence in HPV-positive cells via pRB- and p21(CIP)-dependent pathways.," *EMBO J.*, vol. 19, no. 21, pp. 5762–71, Nov. 2000.

[23] K. Hoppe-Seyler *et al.*, "Induction of dormancy in hypoxic human papillomavirus-positive cancer cells.," *Proc. Natl. Acad. Sci. U. S. A.*, vol. 114, no. 6, pp. E990–E998, Jan. 2017.

[24] F. Bossler *et al.*, "Repression of Human Papillomavirus Oncogene Expression under Hypoxia Is Mediated by PI3K/mTORC2/AKT Signaling," *MBio*, vol. 10, no. 1, Feb. 2019.

[25] K. Hoppe-Seyler, J. Mändl, S. Adrian, B. Kuhn, and F. Hoppe-Seyler, "Virus/Host Cell Crosstalk in Hypoxic HPV-Positive Cancer Cells," *Viruses*, vol. 9, no. 7, p. 174, Jul. 2017.

[26] A. Schneider-Gädicke and E. Schwarz, "Different human cervical carcinoma cell lines show similar transcription patterns of human papillomavirus type 18 early genes.," *EMBO J.*, vol. 5, no. 9, pp. 2285–92, Sep. 1986.

[27] D. Hanahan and R. A. Weinberg, "The hallmarks of cancer.," *Cell*, vol. 100, no. 1, pp. 57–70, Jan. 2000.

[28] E. A. Mesri, M. A. Feitelson, and K. Munger, "Human viral oncogenesis: A cancer hallmarks analysis," *Cell Host and Microbe*, vol. 15, no. 3. pp. 266–282, 2014.

[29] M. V. Frolov, "Molecular mechanisms of E2F-dependent activation and pRB-mediated repression," *J. Cell Sci.*, vol. 117, no. 11, pp. 2173–2181, May 2004.

[30] M. Scheffner, J. M. Huibregtse, R. D. Vierstra, and P. M. Howley, "The HPV-16 E6 and E6-AP complex functions as a ubiquitin-protein ligase in the ubiquitination of p53.," *Cell*, vol. 75, no. 3, pp. 495–505, Nov. 1993.

[31] K. Ganti *et al.*, "The Human Papillomavirus E6 PDZ Binding Motif: From Life Cycle to Malignancy," *Viruses*, vol. 7, no. 7, pp. 3530–3551, Jul. 2015.

[32] M. E. McLaughlin-Drubin, J. Meyers, and K. Munger, "Cancer associated human papillomaviruses.," *Curr. Opin. Virol.*, vol. 2, no. 4, pp. 459–66, Aug. 2012.

[33] A. Honegger *et al.*, "Dependence of intracellular and exosomal microRNAs on viral E6/E7 oncogene expression in HPV-positive tumor cells.," *PLoS Pathog.*, vol. 11, no. 3, p. e1004712, Mar. 2015.

[34] K. Hoppe-Seyler, F. Bossler, J. A. Braun, A. L. Herrmann, and F. Hoppe-Seyler, "The HPV E6/E7 Oncogenes: Key Factors for Viral Carcinogenesis and Therapeutic Targets," *Trends in Microbiology*, vol. 26, no. 2, Elsevier Current Trends, pp. 158–168, 01-Feb-2017.

[35] D. R. Lowy, D. Solomon, A. Hildesheim, J. T. Schiller, and M. Schiffman, "Human papillomavirus infection and the primary and secondary prevention of cervical cancer," *Cancer*, vol. 113, no. S7, pp. 1980–1993, Sep. 2008.

[36] F. X. Bosch *et al.*, "Comprehensive Control of Human Papillomavirus Infections and Related Diseases," *Vaccine*, vol. 31, pp. H1–H31, Dec. 2013.

[37] D. R. Lowy and J. T. Schiller, "Reducing HPV-Associated Cancer Globally," *Cancer Prev. Res.*, vol. 5, no. 1, pp. 18–23, Jan. 2012.

[38] M. Lehtinen and J. Dillner, "Clinical trials of human papillomavirus vaccines and beyond," *Nat. Rev. Clin. Oncol.*, vol. 10, no. 7, pp. 400–410, Jul. 2013.

[39] E. A. Joura *et al.*, "A 9-Valent HPV Vaccine against Infection and Intraepithelial Neoplasia in Women," *N. Engl. J. Med.*, vol. 372, no. 8, pp. 711–723, Feb. 2015.

[40] R. Kuner *et al.*, "Identification of cellular targets for the human papillomavirus E6 and E7 oncogenes by RNA interference and transcriptome analyses," *J. Mol. Med.*, vol. 85, no. 11, pp. 1253–1262, Oct. 2007.

[41] I.-C. Wang *et al.*, "Forkhead box M1 regulates the transcriptional network of genes essential for mitotic progression and genes encoding the SCF (Skp2-Cks1) ubiquitin ligase.," *Mol. Cell. Biol.*, vol. 25, no. 24, pp. 10875–94, Dec. 2005.

[42] W. Korver *et al.*, "The HumanTRIDENT/HFH-11/FKHL16Gene: Structure, Localization, and Promoter Characterization," *Genomics*, vol. 46, no. 3, pp. 435–442, Dec. 1997.

[43] H. J. Park, Z. Wang, R. H. Costa, A. Tyner, L. F. Lau, and P. Raychaudhuri, "An N-terminal inhibitory domain modulates activity of FoxM1 during cell cycle," *Oncogene*, vol. 27, no. 12, pp. 1696–1704, Mar. 2008.

[44] D. R. Littler *et al.*, "Structure of the FoxM1 DNA-recognition domain bound to a promoter sequence," *Nucleic Acids Res.*, vol. 38, no. 13, pp. 4527–4538, Jul. 2010.

[45] I. Wierstra, "The transcription factor FOXM1 (Forkhead box M1): proliferation-specific expression, transcription factor function, target genes, mouse models, and normal biological roles.," *Adv. Cancer Res.*, vol. 118, pp. 97–398, 2013.
[46] C. Huang, J. Du, and K. Xie, "FOXM1 and its oncogenic signaling in pancreatic cancer pathogenesis," *Biochim. Biophys. Acta - Rev. Cancer*, vol. 1845, no. 2, pp. 104–116, Apr. 2014.
[47] J. Laoukili, M. Stahl, and R. H. Medema, "FoxM1: At the crossroads of ageing and cancer," *Biochimica et Biophysica Acta - Reviews on Cancer*, vol. 1775, no. 1. pp. 92–102, 2007.
[48] W. Korver, J. Roose, and H. Clevers, "The winged-helix transcription factor Trident is expressed in cycling cells.," *Nucleic Acids Res.*, vol. 25, no. 9, pp. 1715–9, May 1997.
[49] H. Ye *et al.*, "Hepatocyte nuclear factor 3/fork head homolog 11 is expressed in proliferating epithelial and mesenchymal cells of embryonic and adult tissues.," *Mol. Cell. Biol.*, vol. 17, no. 3, pp. 1626–41, Mar. 1997.
[50] W. Korver, J. Roose, A. Wilson, and H. Clevers, "The Winged-Helix Transcription Factor Trident is Expressed in Actively Dividing Lymphocytes," *Immunobiology*, vol. 198, no. 1–3, pp. 157–161, Dec. 1997.
[51] A. Smirnov *et al.*, "FOXM1 regulates proliferation, senescence and oxidative stress in keratinocytes and cancer cells," *Aging (Albany. NY).*, vol. 8, no. 7, pp. 1384–1397, Jul. 2016.
[52] W. Korver *et al.*, "Uncoupling of S phase and mitosis in cardiomyocytes and hepatocytes lacking the winged-helix transcription factor Trident.," *Curr. Biol.*, vol. 8, no. 24, pp. 1327–30, Dec. 1998.
[53] M. L. Major, R. Lepe, and R. H. Costa, "Forkhead box M1B transcriptional activity requires binding of Cdk-cyclin complexes for phosphorylation-dependent recruitment of p300/CBP coactivators.," *Mol. Cell. Biol.*, vol. 24, no. 7, pp. 2649–61, Apr. 2004.
[54] L. Anders *et al.*, "A Systematic Screen for CDK4/6 Substrates Links FOXM1 Phosphorylation to Senescence Suppression in Cancer Cells," *Cancer Cell*, vol. 20, no. 5, pp. 620–634, 2011.
[55] Z. Fu *et al.*, "Plk1-dependent phosphorylation of FoxM1 regulates a transcriptional programme required for mitotic progression.," *Nat. Cell Biol.*, vol. 10, no. 9, pp. 1076–82, Sep. 2008.
[56] M. Halasi and A. L. Gartel, "A novel mode of FoxM1 regulation: Positive auto-regulatory loop," *Cell Cycle*, vol. 8, no. 12, pp. 1966–1967, Jun. 2009.
[57] X.-H. Cheng *et al.*, "SPDEF Inhibits Prostate Carcinogenesis by Disrupting a Positive Feedback Loop in Regulation of the Foxm1 Oncogene," *PLoS Genet.*, vol. 10, no. 9, p. e1004656, Sep. 2014.
[58] C. Barger *et al.*, "Pan-Cancer Analyses Reveal Genomic Features of FOXM1 Overexpression in Cancer," *Cancers (Basel).*, vol. 11, no. 2, p. 251, Feb. 2019.
[59] J. Millour *et al.*, "ATM and p53 regulate FOXM1 expression via E2F in breast cancer epirubicin treatment and resistance.," *Mol. Cancer Ther.*, vol. 10, no. 6, pp. 1046–1058, 2011.
[60] A. M. Barsotti and C. Prives, "Pro-proliferative FoxM1 is a target of p53-mediated repression.," *Oncogene*, vol. 28, no. 48, pp. 4295–305, Dec. 2009.
[61] B. Pandit, M. Halasi, and A. L. Gartel, "p53 negatively regulates expression of FoxM1," *Cell Cycle*, vol. 8, no. 20. Taylor & Francis, pp. 3425–3427, 15-Oct-2009.
[62] N. de Olano *et al.*, "The p38 MAPK-MK2 axis regulates E2F1 and FOXM1 expression after epirubicin treatment.," *Mol. Cancer Res.*, vol. 10, no. 9, pp. 1189–202, Sep. 2012.
[63] C. J. Barger *et al.*, "Genetic determinants of FOXM1 overexpression in epithelial ovarian cancer and functional contribution to cell cycle progression," *Oncotarget*, vol. 6, no. 29, pp. 27613–27627, Sep. 2015.
[64] S. Sadasivam, S. Duan, and J. A. DeCaprio, "The MuvB complex sequentially recruits B-Myb and FoxM1 to promote mitotic gene expression," *Genes Dev.*, vol. 26, no. 5, pp. 474–489, Mar. 2012.
[65] K. Krupczak-Hollis *et al.*, "The mouse Forkhead Box m1 transcription factor is essential for hepatoblast mitosis and development of intrahepatic bile ducts and vessels during liver morphogenesis.," *Dev. Biol.*, vol. 276, no. 1, pp. 74–88, Dec. 2004.

[66] I.-M. Kim, S. Ramakrishna, G. A. Gusarova, H. M. Yoder, R. H. Costa, and V. V. Kalinichenko, "The Forkhead Box M1 Transcription Factor Is Essential for Embryonic Development of Pulmonary Vasculature," *J. Biol. Chem.*, vol. 280, no. 23, pp. 22278–22286, Jun. 2005.

[67] J. Laoukili *et al.*, "FoxM1 is required for execution of the mitotic programme and chromosome stability," *Nat. Cell Biol.*, vol. 7, no. 2, pp. 126–136, Feb. 2005.

[68] I. Wierstra, "FOXM1 (Forkhead box M1) in tumorigenesis. Overexpression in human cancer, implication in tumorigenesis, oncogenic functions, tumor-suppressive properties, and target of anticancer therapy," *Adv. Cancer Res.*, vol. 119, pp. 191–419, Jan. 2013.

[69] L. Li *et al.*, "Prognostic value of FOXM1 in solid tumors: a systematic review and meta-analysis," *Oncotarget*, vol. 8, no. 19, pp. 32298–32308, May 2017.

[70] A. L. Gartel, "FOXM1 in cancer: Interactions and vulnerabilities," *Cancer Research*, vol. 77, no. 12. pp. 3135–3139, 2017.

[71] A. K. Y. Lam *et al.*, "FOXM1b, which is present at elevated levels in cancer cells, has a greater transforming potential than FOXM1c.," *Front. Oncol.*, vol. 3, p. 11, 2013.

[72] C. Pilarsky, M. Wenzig, T. Specht, H. D. Saeger, and R. Grützmann, "Identification and Validation of Commonly Overexpressed Genes in Solid Tumors by Comparison of Microarray Data," *Neoplasia*, vol. 6, no. 6, pp. 744–750, Nov. 2004.

[73] S. L. Carter, A. C. Eklund, I. S. Kohane, L. N. Harris, and Z. Szallasi, "A signature of chromosomal instability inferred from gene expression profiles predicts clinical outcome in multiple human cancers," *Nat. Genet.*, vol. 38, no. 9, pp. 1043–1048, Sep. 2006.

[74] C. Rosty *et al.*, "Identification of a proliferation gene cluster associated with HPV E6/E7 expression level and viral DNA load in invasive cervical carcinoma," *Oncogene*, vol. 24, no. 47, pp. 7094–7104, Oct. 2005.

[75] H. J. Park *et al.*, "FoxM1, a critical regulator of oxidative stress during oncogenesis," *EMBO J.*, vol. 28, no. 19, pp. 2908–2918, Oct. 2009.

[76] D. Kopanja *et al.*, "Essential roles of FoxM1 in Ras-induced liver cancer progression and in cancer cells with stem cell features," *J. Hepatol.*, vol. 63, no. 2, pp. 429–436, Aug. 2015.

[77] N. Tanaka *et al.*, "Gain-of-function mutant p53 promotes the oncogenic potential of head and neck squamous cell carcinoma cells by targeting the transcription factors FOXO3a and FOXM1," *Oncogene*, Nature Publishing Group, pp. 1–14, 22-Dec-2017.

[78] X. Zhang *et al.*, "Targeting of mutant p53-induced FoxM1 with thiostrepton induces cytotoxicity and enhances carboplatin sensitivity in cancer cells.," *Oncotarget*, vol. 5, no. 22, pp. 11365–11380, Nov. 2014.

[79] I. Wierstra and J. Alves, "FOXM1c transactivates the human c-myc promoter directly via the two TATA boxes P1 and P2," *FEBS J.*, vol. 273, no. 20, pp. 4645–4667, Oct. 2006.

[80] S. K. M. Li *et al.*, "FoxM1c counteracts oxidative stress-induced senescence and stimulates Bmi-1 expression," *J. Biol. Chem.*, vol. 283, no. 24, pp. 16545–16553, Jun. 2008.

[81] M. Halasi and A. L. Gartel, "Suppression of FOXM1 sensitizes human cancer cells to cell death induced by DNA-damage," *PLoS One*, vol. 7, no. 2, p. e31761, Feb. 2012.

[82] S. Zona, L. Bella, M. J. Burton, G. Nestal de Moraes, and E. W. F. Lam, "FOXM1: An emerging master regulator of DNA damage response and genotoxic agent resistance," *Biochimica et Biophysica Acta - Gene Regulatory Mechanisms*, vol. 1839, no. 11. pp. 1316–1322, 2014.

[83] L. J. Monteiro *et al.*, "The Forkhead Box M1 protein regulates BRIP1 expression and DNA damage repair in epirubicin treatment.," *Oncogene*, vol. 32, no. 39, pp. 4634–45, Sep. 2013.

[84] J. M.-M. Kwok *et al.*, "FOXM1 Confers Acquired Cisplatin Resistance in Breast Cancer Cells," *Mol. Cancer Res.*, vol. 8, no. 1, pp. 24–34, Jan. 2010.

[85] E. Gemenetzidis, D. Elena-Costea, E. K. Parkinson, A. Waseem, H. Wan, and M.-T. Teh, "Induction of human epithelial stem/progenitor expansion by FOXM1.," *Cancer Res.*, vol. 70, no. 22, pp. 9515–26, Nov. 2010.

[86] Y. Zhang *et al.*, "FoxM1B Transcriptionally Regulates Vascular Endothelial Growth Factor Expression and Promotes the Angiogenesis and Growth of Glioma Cells," *Cancer Res.*, vol. 68, no. 21, pp. 8733–8742, Nov. 2008.

[87] Q. Li *et al.*, "Critical role and regulation of transcription factor FoxM1 in human gastric cancer angiogenesis and progression.," *Cancer Res.*, vol. 69, no. 8, pp. 3501–9, Apr. 2009.

[88] B. Dai *et al.*, "Aberrant FoxM1B expression increases matrix metalloproteinase-2 transcription and enhances the invasion of glioma cells," *Oncogene*, vol. 26, no. 42, pp. 6212–6219, Sep. 2007.
[89] I.-C. Wang *et al.*, "FoxM1 Regulates Transcription of *JNK1* to Promote the G_1/S Transition and Tumor Cell Invasiveness," *J. Biol. Chem.*, vol. 283, no. 30, pp. 20770–20778, Jul. 2008.
[90] M. Halasi and A. L. Gartel, "FOX(M1) News--It Is Cancer," *Mol. Cancer Ther.*, vol. 12, no. 3, pp. 245–254, 2013.
[91] J. M. Lüscher-Firzlaff *et al.*, "Interaction of the fork head domain transcription factor MPP2 with the human papilloma virus 16 E7 protein: enhancement of transformation and transactivation.," *Oncogene*, vol. 18, no. 41, pp. 5620–30, Oct. 1999.
[92] N. Jaiswal, R. John, V. Chand, and A. Nag, "Oncogenic human papillomavirus 16E7 modulates SUMOylation of FoxM1b," *Int. J. Biochem. Cell Biol.*, vol. 58, pp. 28–36, Jan. 2015.
[93] P. M. Chen, Y. W. Cheng, Y. C. Wang, T. C. Wu, C. Y. Chen, and H. Lee, "Up-Regulation of FOXM1 by E6 Oncoprotein through the MZF1/NKX2-1 Axis Is Required for Human Papillomavirus-Associated Tumorigenesis," *Neoplasia*, vol. 16, no. 11, pp. 961–971, 2014.
[94] W. Chen *et al.*, "Human Papillomavirus 16 E6 Induces FoxM1B in Oral Keratinocytes through GRHL2," *J. Dent. Res.*, vol. 97, no. 7, pp. 795–802, Feb. 2018.
[95] D. W. Chan *et al.*, "Over-expression of FOXM1 transcription factor is associated with cervical cancer progression and pathogenesis.," *J. Pathol.*, vol. 215, no. 3, pp. 245–52, 2008.
[96] J. Hayles, D. Beach, B. Durkacz, and P. Nurse, "The fission yeast cell cycle control gene cdc2: isolation of a sequence suc1 that suppresses cdc2 mutant function.," *Mol. Gen. Genet.*, vol. 202, no. 2, pp. 291–3, Feb. 1986.
[97] H. E. Richardson, C. S. Stueland, J. Thomas, P. Russell, and S. I. Reed, "Human cDNAs encoding homologs of the small p34Cdc28/Cdc2-associated protein of Saccharomyces cerevisiae and Schizosaccharomyces pombe.," *Genes Dev.*, vol. 4, no. 8, pp. 1332–44, Aug. 1990.
[98] H.-S. Martinsson-Ahlzen, V. Liberal, B. Grunenfelder, S. R. Chaves, C. H. Spruck, and S. I. Reed, "Cyclin-Dependent Kinase-Associated Proteins Cks1 and Cks2 Are Essential during Early Embryogenesis and for Cell Cycle Progression in Somatic Cells," *Mol. Cell. Biol.*, vol. 28, no. 18, pp. 5698–5709, Sep. 2008.
[99] Z. Ellederova *et al.*, "CKS1 Germ Line Exclusion is Essential for the Transition from Meiosis to Early Embryonic Development," *Mol. Cell. Biol.*, Apr. 2019.
[100] A. Krishnan, S. A. Nair, and M. R. Pillai, "Loss of cks1 homeostasis deregulates cell division cycle," *J. Cell. Mol. Med.*, vol. 14, no. 1–2, pp. 154–164, Jan. 2010.
[101] K. Rother *et al.*, "Expression of cyclin-dependent kinase subunit 1 (Cks1) is regulated during the cell cycle by a CDE/CHR tandem element and is downregulated by p53 but not by p63 or p73," *Cell Cycle*, vol. 6, no. 7, pp. 853–862, Apr. 2007.
[102] D. Ganoth *et al.*, "The cell-cycle regulatory protein Cks1 is required for SCFSkp2-mediated ubiquitinylation of p27," *Nat. Cell Biol.*, vol. 3, no. 3, pp. 321–324, Mar. 2001.
[103] C. Spruck *et al.*, "A CDK-independent function of mammalian Cks1: targeting of SCF(Skp2) to the CDK inhibitor p27Kip1.," *Mol. Cell*, vol. 7, no. 3, pp. 639–50, Mar. 2001.
[104] G. Bornstein, J. Bloom, D. Sitry-Shevah, K. Nakayama, M. Pagano, and A. Hershko, "Role of the SCF^{Skp2} Ubiquitin Ligase in the Degradation of $p21^{Cip1}$ in S Phase," *J. Biol. Chem.*, vol. 278, no. 28, pp. 25752–25757, Jul. 2003.
[105] D. Tedesco, J. Lukas, and S. I. Reed, "The pRb-related protein p130 is regulated by phosphorylation-dependent proteolysis via the protein-ubiquitin ligase SCFSkp2," *Genes Dev.*, vol. 16, no. 22, pp. 2946–2957, Nov. 2002.
[106] A. Hoellein *et al.*, "Cks1 Promotion of S Phase Entry and Proliferation Is Independent of p27Kip1 Suppression," *Mol. Cell. Biol.*, vol. 32, no. 13, pp. 2416–2427, Jul. 2012.
[107] L. Westbrook, M. Manuvakhova, F. G. Kern, N. R. Estes, H. N. Ramanathan, and J. V. Thottassery, "Cks1 regulates cdk1 expression: A novel role during mitotic entry in breast cancer cells," *Cancer Res.*, vol. 67, no. 23, pp. 11393–11401, 2007.

[108] L. Shi *et al.*, "Over-expression of CKS1B activates both MEK/ERK and JAK/STAT3 signaling pathways and promotes myeloma cell drug-resistance," *Oncotarget*, vol. 1, no. 1, pp. 22–33, 2010.
[109] V. Khattar and J. V Thottassery, "Cks1: Structure, Emerging Roles and Implications in Multiple Cancers.," *J. Cancer Ther.*, vol. 4, no. 8, pp. 1341–1354, Oct. 2013.
[110] Y. Zhang, Y. Chen, F. You, W. Li, Z. Lang, and Z. Zou, "Prognostic and clinicopathological significance of Cks1 in cancer: Evidence from a meta-analysis," *J. Cell. Physiol.*, Jan. 2019.
[111] Y. Kudo, S. Kitajima, I. Ogawa, M. Miyauchi, and T. Takata, "Down-regulation of Cdk inhibitor p27 in oral squamous cell carcinoma," *Oral Oncol.*, vol. 41, no. 2, pp. 105–116, Feb. 2005.
[112] X.-C. Wang *et al.*, "Role of Cks1 amplification and overexpression in breast cancer," *Biochem. Biophys. Res. Commun.*, vol. 379, no. 4, pp. 1107–1113, Feb. 2009.
[113] Y.-S. Tsai, H.-C. Chang, L.-Y. Chuang, and W.-C. Hung, "RNA Silencing of Cks1 Induced G2/M Arrest and Apoptosis in Human Lung Cancer Cells," *IUBMB Life (International Union Biochem. Mol. Biol. Life)*, vol. 57, no. 8, pp. 583–589, Aug. 2005.
[114] L. Lin *et al.*, "Depletion of Cks1 and Cks2 expression compromises cell proliferation and enhance chemotherapy-induced apoptosis in HepG2 cells.," *Oncol. Rep.*, vol. 35, no. 1, pp. 26–32, Jan. 2016.
[115] V. Liberal *et al.*, "Cyclin-dependent kinase subunit (Cks) 1 or Cks2 overexpression overrides the DNA damage response barrier triggered by activated oncoproteins.," *Proc. Natl. Acad. Sci. U. S. A.*, vol. 109, no. 8, pp. 2754–9, Feb. 2012.
[116] S. V Del Rincón *et al.*, "Cks overexpression enhances chemotherapeutic efficacy by overriding DNA damage checkpoints.," *Oncogene*, vol. 34, no. October 2013, pp. 1–7, Apr. 2014.
[117] J. Tat *et al.*, "CKS protein overexpression renders tumors susceptible to a chemotherapeutic strategy that protects normal tissues," *Oncotarget*, vol. 8, no. 70, pp. 114911–114923, Dec. 2017.
[118] U. B. Keller *et al.*, "Myc targets Cks1 to provoke the suppression of p27Kip1, proliferation and lymphomagenesis.," *EMBO J.*, vol. 26, no. 10, pp. 2562–74, May 2007.
[119] K. Butz, T. Ristriani, A. Hengstermann, C. Denk, M. Scheffner, and F. Hoppe-Seyler, "siRNA targeting of the viral E6 oncogene efficiently kills human papillomavirus-positive cancer cells," *Oncogene*, vol. 22, no. 38, pp. 5938–5945, Sep. 2003.
[120] A. H. S. Hall and K. A. Alexander, "RNA Interference of Human Papillomavirus Type 18 E6 and E7 Induces Senescence in HeLa Cells," *J. Virol.*, vol. 77, no. 10, pp. 6066–6069, May 2003.
[121] A. Hengstermann, M. A. D'silva, P. Kuballa, K. Butz, F. Hoppe-Seyler, and M. Scheffner, "Growth suppression induced by downregulation of E6-AP expression in human papillomavirus-positive cancer cell lines depends on p53.," *J. Virol.*, vol. 79, no. 14, pp. 9296–300, Jul. 2005.
[122] M. R. Evans *et al.*, "An oral keratinocyte life cycle model identifies novel host genome regulation by human papillomavirus 16 relevant to HPV positive head and neck cancer," *Oncotarget*, vol. 8, no. 47, pp. 81892–81909, Oct. 2017.
[123] B. Leroy, L. Girard, A. Hollestelle, J. D. Minna, A. F. Gazdar, and T. Soussi, "Analysis of TP53 mutation status in human cancer cell lines: a reassessment.," *Hum. Mutat.*, vol. 35, no. 6, pp. 756–65, Jun. 2014.
[124] W. D. Funk, D. T. Pak, R. H. Karas, W. E. Wright, and J. W. Shay, "A transcriptionally active DNA-binding site for human p53 protein complexes.," *Mol. Cell. Biol.*, vol. 12, no. 6, pp. 2866–71, Jun. 1992.
[125] "NCI-H1299 cell line at ATCC." [Online]. Available: https://www.lgcstandards-atcc.org/Products/All/CRL-5803.aspx?geo_country=de. [Accessed: 26-Apr-2019].
[126] F. Hoppe-Seyler, K. Butz, and H. zur Hausen, "Repression of the human papillomavirus type 18 enhancer by the cellular transcription factor Oct-1.," *J. Virol.*, vol. 65, no. 10, pp. 5613–8, Oct. 1991.
[127] M. Dibb *et al.*, "The FOXM1-PLK1 axis is commonly upregulated in oesophageal adenocarcinoma.," *Br. J. Cancer*, vol. 107, no. 10, pp. 1766–75, Nov. 2012.

[128] H. Chen, Y. Zou, H. Yang, J. Wang, and H. Pan, "Downregulation of FoxM1 inhibits proliferation, invasion and angiogenesis of HeLa cells in vitro and in vivo," *Int. J. Oncol.*, vol. 45, no. 6, pp. 2355–2364, Sep. 2014.
[129] W. Luo, F. Gao, S. Li, and L. Liu, "FoxM1 Promotes Cell Proliferation, Invasion, and Stem Cell Properties in Nasopharyngeal Carcinoma," *Front. Oncol.*, vol. 8, p. 483, Oct. 2018.
[130] Z. Hamurcu, A. Ashour, N. Kahraman, and B. Ozpolat, "FOXM1 regulates expression of eukaryotic elongation factor 2 kinase and promotes proliferation, invasion and tumorgenesis of human triple negative breast cancer cells," *Oncotarget*, vol. 7, no. 13, 2016.
[131] K. R. Kaster, S. G. Burgett, R. N. Rao, and T. D. Ingolia, "Analysis of a bacterial hygromycin B resistance gene by transcriptional and translational fusions and by DNA sequencing.," *Nucleic Acids Res.*, vol. 11, no. 19, pp. 6895–911, Oct. 1983.
[132] E. Gaggelli *et al.*, "Coordination pattern, solution structure and DNA damage studies of the copper(ii) complex with the unusual aminoglycoside antibiotic hygromycin B," *Dalt. Trans.*, vol. 39, no. 41, p. 9830, Oct. 2010.
[133] S. Wemhoff, R. Klassen, A. Beetz, and F. Meinhardt, "DNA Damage Responses Are Induced by tRNA Anticodon Nucleases and Hygromycin B," *PLoS One*, vol. 11, no. 7, p. e0157611, Jul. 2016.
[134] A. Kinner, W. Wu, C. Staudt, and G. Iliakis, "Gamma-H2AX in recognition and signaling of DNA double-strand breaks in the context of chromatin.," *Nucleic Acids Res.*, vol. 36, no. 17, pp. 5678–94, Oct. 2008.
[135] X. Wang, K. Krupczak-Hollis, Y. Tan, M. B. Dennewitz, G. R. Adami, and R. H. Costa, "Increased Hepatic Forkhead Box M1B (FoxM1B) Levels in Old-aged Mice Stimulated Liver Regeneration through Diminished p27 ^{Kip1} Protein Levels and Increased Cdc25B Expression," *J. Biol. Chem.*, vol. 277, no. 46, pp. 44310–44316, Nov. 2002.
[136] G. Bjursell and P. Reichard, "Effects of thymidine on deoxyribonucleoside triphosphate pools and deoxyribonucleic acid synthesis in Chinese hamster ovary cells.," *J. Biol. Chem.*, vol. 248, no. 11, pp. 3904–9, Jun. 1973.
[137] J. Leitz *et al.*, "Oncogenic human papillomaviruses activate the tumor-associated lens epithelial-derived growth factor (LEDGF) gene.," *PLoS Pathog.*, vol. 10, no. 3, p. e1003957, Mar. 2014.
[138] R. Y. M. Ma, T. H. K. Tong, A. M. S. Cheung, A. C. C. Tsang, W. Y. Leung, and K.-M. Yao, "Raf/MEK/MAPK signaling stimulates the nuclear translocation and transactivating activity of FOXM1c," *J. Cell Sci.*, vol. 118, no. 4, pp. 795–806, Jan. 2005.
[139] A. D. Santin *et al.*, "Gene expression profiles of primary HPV16- and HPV18-infected early stage cervical cancers and normal cervical epithelium: identification of novel candidate molecular markers for cervical cancer diagnosis and therapy," *Virology*, vol. 331, no. 2, pp. 269–291, 2005.
[140] B. A. Goff, J. Sallin, R. Garcia, A. VanBlaricom, P. J. Paley, and H. G. Muntz, "Evaluation of p27 in preinvasive and invasive malignancies of the cervix.," *Gynecol. Oncol.*, vol. 88, no. 1, pp. 40–4, Jan. 2003.
[141] D. Hellberg, T. Tot, and U. Stendahl, "Pitfalls in immunohistochemical validation of tumor marker expression — Exemplified in invasive cancer of the uterine cervix," *Gynecol. Oncol.*, vol. 112, no. 1, pp. 235–240, Jan. 2009.
[142] A. Sgambato *et al.*, "Decreased expression of the CDK inhibitor p27Kip1 and increased oxidative DNA damage in the multistep process of cervical carcinogenesis," *Gynecol. Oncol.*, vol. 92, no. 3, pp. 776–783, Mar. 2004.
[143] M. Fischer, S. Uxa, C. Stanko, T. M. Magin, and K. Engeland, "Human papilloma virus E7 oncoprotein abrogates the p53-p21-DREAM pathway," *Sci. Rep.*, vol. 7, no. 1, p. 2603, Dec. 2017.
[144] K. Z. Guiley, T. J. Liban, J. G. Felthousen, P. Ramanan, L. Litovchick, and S. M. Rubin, "Structural mechanisms of DREAM complex assembly and regulation.," *Genes Dev.*, vol. 29, no. 9, pp. 961–74, May 2015.

[145] N. N. Rashid, R. Yusof, and R. J. Watson, "Disruption of repressive p130-DREAM complexes by human papillomavirus 16 E6/E7 oncoproteins is required for cell-cycle progression in cervical cancer cells," *J. Gen. Virol.*, vol. 92, no. 11, pp. 2620–2627, Nov. 2011.
[146] N. Nor Rashid, R. Yusof, and R. J. Watson, "Disruption of pocket protein dream complexes by E7 proteins of different types of human papillomaviruses," *Acta Virol.*, vol. 57, no. 4, pp. 447–451, 2013.
[147] M. Fischer, M. Quaas, L. Steiner, and K. Engeland, "The p53-p21-DREAM-CDE/CHR pathway regulates G $_2$ /M cell cycle genes," *Nucleic Acids Res.*, vol. 44, no. 1, pp. 164–174, Jan. 2016.
[148] K. Engeland, "Cell cycle arrest through indirect transcriptional repression by p53: I have a DREAM," *Cell Death Differ.*, vol. 25, no. 1, pp. 114–132, Jan. 2018.
[149] G. A. Müller, A. Wintsche, K. Stangner, S. J. Prohaska, P. F. Stadler, and K. Engeland, "The CHR site: definition and genome-wide identification of a cell cycle transcriptional element.," *Nucleic Acids Res.*, vol. 42, no. 16, pp. 10331–50, Sep. 2014.
[150] C. L. Duffy, S. L. Phillips, and A. J. Klingelhutz, "Microarray analysis identifies differentiation-associated genes regulated by human papillomavirus type 16 E6," *Virology*, vol. 314, no. 1, pp. 196–205, Sep. 2003.
[151] A. J. Klingelhutz, S. A. Foster, and J. K. McDougall, "Telomerase activation by the E6 gene product of human papillomavirus type 16.," *Nature*, vol. 380, no. 6569, pp. 79–82, Mar. 1996.
[152] M. L. Kelley, K. E. Keiger, C. J. Lee, and J. M. Huibregtse, "The global transcriptional effects of the human papillomavirus E6 protein in cervical carcinoma cell lines are mediated by the E6AP ubiquitin ligase.," *J. Virol.*, vol. 79, no. 6, pp. 3737–47, Mar. 2005.
[153] S. Mittal and L. Banks, "Molecular mechanisms underlying human papillomavirus E6 and E7 oncoprotein-induced cell transformation," *Mutat. Res. Mutat. Res.*, vol. 772, pp. 23–35, Apr. 2017.
[154] O. López-Ocejo, A. Viloria-Petit, M. Bequet-Romero, D. Mukhopadhyay, J. Rak, and R. S. Kerbel, "Oncogenes and tumor angiogenesis: the HPV-16 E6 oncoprotein activates the vascular endothelial growth factor (VEGF) gene promoter in a p53 independent manner," *Oncogene*, vol. 19, no. 40, pp. 4611–4620, Sep. 2000.
[155] T. Kinoshita *et al.*, "Transactivation of prothymosin alpha and c-myc promoters by human papillomavirus type 16 E6 protein.," *Virology*, vol. 232, no. 1, pp. 53–61, May 1997.
[156] K. Fish, R. P. Sora, S. J. Schaller, R. Longnecker, and M. Ikeda, "EBV latent membrane protein 2A orchestrates p27 ^{kip1} degradation via Cks1 to accelerate MYC-driven lymphoma in mice," *Blood*, vol. 130, no. 23, pp. 2516–2526, Dec. 2017.
[157] M. Fischer, P. Grossmann, M. Padi, and J. A. DeCaprio, "Integration of TP53, DREAM, MMB-FOXM1 and RB-E2F target gene analyses identifies cell cycle gene regulatory networks," *Nucleic Acids Res.*, vol. 44, no. 13, pp. 6070–6086, Jul. 2016.
[158] T. K. Kwon and A. A. Nordin, "Overexpression of Cyclin E and Cyclin-Dependent Kinase Inhibitor (p27Kip1): Effect on Cell Cycle Regulation in HeLa Cells," *Biochem. Biophys. Res. Commun.*, vol. 238, no. 2, pp. 534–538, Sep. 1997.
[159] F. De Vita, M. Riccardi, D. Malanga, M. Scrima, C. De Marco, and G. Viglietto, "PKC-dependent phosphorylation of p27 at T198 contributes to p27 stabilization and cell cycle arrest," *Cell Cycle*, vol. 11, no. 8, pp. 1583–1592, Apr. 2012.
[160] O. Kepp *et al.*, "Quantification of Cell Cycle-Arresting Proteins," Humana Press, Totowa, NJ, 2013, pp. 121–142.
[161] H. Halfter *et al.*, "Oncostatin M induces growth arrest by inhibition of Skp2, Cks1, and cyclin A expression and induced p21 expression.," *Cancer Res.*, vol. 66, no. 13, pp. 6530–9, Jul. 2006.
[162] N. Uehara, K. Yoshizawa, and A. Tsubura, "Vorinostat enhances protein stability of p27 and p21 through negative regulation of Skp2 and Cks1 in human breast cancer cells," *Oncol. Rep.*, vol. 28, no. 1, pp. 105–10, Apr. 2012.
[163] A. Krishnan, R. Hariharan, S. A. Nair, and M. R. Pillai, "Fluoxetine mediates G0/G1 arrest by inducing functional inhibition of cyclin dependent kinase subunit (CKS)1," *Biochem. Pharmacol.*, vol. 75, no. 10, pp. 1924–1934, 2008.

[164] E. Rico-Bautista and D. A. Wolf, "Skipping Cancer: Small Molecule Inhibitors of SKP2-Mediated p27 Degradation," *Chem. Biol.*, vol. 19, no. 12, pp. 1497–1498, Dec. 2012.
[165] L. Wu, A. V Grigoryan, Y. Li, B. Hao, M. Pagano, and T. J. Cardozo, "Specific small molecule inhibitors of Skp2-mediated p27 degradation.," *Chem. Biol.*, vol. 19, no. 12, pp. 1515–24, Dec. 2012.
[166] H. Zhao *et al.*, "p27T187A knockin identifies Skp2/Cks1 pocket inhibitors for advanced prostate cancer.," *Oncogene*, vol. 36, no. 1, pp. 60–70, 2017.
[167] W. Grey *et al.*, "The Cks1/Cks2 axis fine-tunes Mll1 expression and is crucial for MLL-rearranged leukaemia cell viability," *Biochim. Biophys. Acta - Mol. Cell Res.*, vol. 1865, no. 1, pp. 105–116, Jan. 2018.
[168] M. Yu *et al.*, "Elevated expression of FoxM1 promotes the tumor cell proliferation in hepatocellular carcinoma.," *Tumour Biol.*, vol. 37, no. 1, pp. 1289–97, Jan. 2016.
[169] J. Millour *et al.*, "FOXM1 is a transcriptional target of ERα and has a critical role in breast cancer endocrine sensitivity and resistance," *Oncogene*, vol. 29, no. 20, pp. 2983–2995, May 2010.
[170] F. Kruiswijk *et al.*, "Targeted inhibition of metastatic melanoma through interference with Pin1-FOXM1 signaling," *Oncogene*, vol. 35, no. May 2014, pp. 1–12, Apr. 2015.
[171] M. Yue, S. Li, G. Yan, C. Li, and Z. Kang, "Paeoniflorin inhibits cell growth and induces cell cycle arrest through inhibition of FoxM1 in colorectal cancer cells," *Cell Cycle*, pp. 1–10, Jan. 2018.
[172] W. Wang, Z. Guo, H. Yu, and L. Fan, "MiR-216b inhibits osteosarcoma cell proliferation, migration, and invasion by targeting Forkhead Box M1," *J. Cell. Biochem.*, vol. 120, no. 4, pp. 5435–5443, Apr. 2019.
[173] C. Shi and Z. Zhang, "MicroRNA‐320 suppresses cervical cancer cell viability, migration and invasion via directly targeting FOXM1," *Oncol. Lett.*, vol. 14, no. 3, pp. 3809–3816, Jul. 2017.
[174] C. Tian *et al.*, "Downreguation of FoxM1 by miR-214 inhibits proliferation and migration in hepatocellular carcinoma," *Gene Ther.*, vol. 25, no. 4, pp. 312–319, Jul. 2018.
[175] Y. Wang *et al.*, "FOXM1 promotes reprogramming of glucose metabolism in epithelial ovarian cancer cells via activation of GLUT1 and HK2 transcription," *Oncotarget*, vol. 7, no. 30, pp. 47985–47997, Nov. 2016.
[176] Y. Cai *et al.*, "Foxm1 expression in prostate epithelial cells is essential for prostate carcinogenesis.," *J. Biol. Chem.*, vol. 288, no. 31, pp. 22527–41, Aug. 2013.
[177] N. Spardy *et al.*, "Human papillomavirus 16 E7 oncoprotein attenuates DNA damage checkpoint control by increasing the proteolytic turnover of claspin," *Cancer Res.*, vol. 69, no. 17, pp. 7022–7029, Sep. 2009.
[178] C. F. Down, J. Millour, E. W.-F. Lam, and R. J. Watson, "Binding of FoxM1 to G2/M gene promoters is dependent upon B-Myb," *Biochim. Biophys. Acta - Gene Regul. Mech.*, vol. 1819, no. 8, pp. 855–862, Aug. 2012.
[179] M. Fischer and G. A. Müller, "Cell cycle transcription control: DREAM/MuvB and RB-E2F complexes," *Crit. Rev. Biochem. Mol. Biol.*, vol. 52, no. 6, pp. 638–662, Nov. 2017.
[180] N. N. Rashid, R. Yusof, and R. J. Watson, "A B-myb--DREAM complex is not critical to regulate the G2/M genes in HPV-transformed cell lines.," *Anticancer Res.*, vol. 34, no. 11, pp. 6557–63, Nov. 2014.
[181] W. P. Roos, A. D. Thomas, and B. Kaina, "DNA damage and the balance between survival and death in cancer biology," *Nat. Rev. Cancer*, vol. 16, no. 1, pp. 20–33, Jan. 2016.
[182] A. Ray Chaudhuri and A. Nussenzweig, "The multifaceted roles of PARP1 in DNA repair and chromatin remodelling," *Nat. Rev. Mol. Cell Biol.*, vol. 18, no. 10, pp. 610–621, Jul. 2017.
[183] S. P. Jackson and J. Bartek, "The DNA-damage response in human biology and disease," *Nature*, vol. 461, no. 7267, pp. 1071–1078, Oct. 2009.
[184] R. Ceccaldi, B. Rondinelli, and A. D. D'Andrea, "Repair Pathway Choices and Consequences at the Double-Strand Break," *Trends Cell Biol.*, vol. 26, no. 1, pp. 52–64, Jan. 2016.

[185] J. A. Nickoloff, "Paths from DNA damage and signaling to genome rearrangements via homologous recombination," *Mutat. Res. Mol. Mech. Mutagen.*, vol. 806, pp. 64–74, Dec. 2017.
[186] R. Prakash, Y. Zhang, W. Feng, and M. Jasin, "Homologous Recombination and Human Health: The Roles of BRCA1, BRCA2, and Associated Proteins," *Cold Spring Harb. Perspect. Biol.*, vol. 7, no. 4, p. a016600, Apr. 2015.
[187] H. H. Y. Chang, N. R. Pannunzio, N. Adachi, and M. R. Lieber, "Non-homologous DNA end joining and alternative pathways to double-strand break repair," *Nat. Rev. Mol. Cell Biol.*, vol. 18, no. 8, pp. 495–506, May 2017.
[188] U. B. Maachani, U. Shankavaram, T. Kramp, P. J. Tofilon, K. Camphausen, and A. T. Tandle, "FOXM1 and STAT3 interaction confers radioresistance in glioblastoma cells," *Oncotarget*, vol. 7, no. 47, pp. 77365–77377, Nov. 2016.
[189] J. Zhou *et al.*, "FOXM1 Modulates Cisplatin Sensitivity by Regulating EXO1 in Ovarian Cancer," *PLoS One*, vol. 9, no. 5, p. e96989, May 2014.
[190] Y.-Y. Park *et al.*, "FOXM1 mediates Dox resistance in breast cancer by enhancing DNA repair.," *Carcinogenesis*, vol. 33, no. 10, pp. 1843–53, Oct. 2012.
[191] N. Zhang *et al.*, "FoxM1 inhibition sensitizes resistant glioblastoma cells to temozolomide by downregulating the expression of DNA-repair gene Rad51," *Clin. Cancer Res.*, vol. 18, no. 21, pp. 5961–5971, Nov. 2012.
[192] R. E. London, "The structural basis of XRCC1-mediated DNA repair," *DNA Repair (Amst).*, vol. 30, pp. 90–103, Jun. 2015.
[193] A. Fradet-Turcotte, J. Sitz, D. Grapton, and A. Orthwein, "BRCA2 functions: from DNA repair to replication fork stabilization," *Endocr. Relat. Cancer*, vol. 23, no. 10, pp. T1–T17, Oct. 2016.
[194] Y. Tan, P. Raychaudhuri, and R. H. Costa, "Chk2 mediates stabilization of the FoxM1 transcription factor to stimulate expression of DNA repair genes.," *Mol. Cell. Biol.*, vol. 27, no. 3, pp. 1007–16, Feb. 2007.
[195] P. Khongkow *et al.*, "FOXM1 targets NBS1 to regulate DNA damage-induced senescence and epirubicin resistance," *Oncogene*, vol. 33, no. 32, 2014.
[196] L. Bella, S. Zona, G. Nestal de Moraes, and E. W.-F. Lam, "FOXM1: A key oncofoetal transcription factor in health and disease," *Semin. Cancer Biol.*, vol. 29, pp. 32–39, Dec. 2014.
[197] A. N. Koehler, "A complex task? Direct modulation of transcription factors with small molecules," *Curr. Opin. Chem. Biol.*, vol. 14, no. 3, pp. 331–340, Jun. 2010.
[198] J. M.-M. Kwok, S. S. Myatt, C. M. Marson, R. C. Coombes, D. Constantinidou, and E. W.-F. Lam, "Thiostrepton selectively targets breast cancer cells through inhibition of forkhead box M1 expression," *Mol. Cancer Ther.*, vol. 7, no. 7, pp. 2022–2032, Jul. 2008.
[199] A. L. Gartel, "FoxM1 inhibitors as potential anticancer drugs," *Expert Opin. Ther. Targets*, vol. 12, no. 6, pp. 663–665, Jun. 2008.
[200] N. S. Hegde, D. A. Sanders, R. Rodriguez, and S. Balasubramanian, "The transcription factor FOXM1 is a cellular target of the natural product thiostrepton.," *Nat. Chem.*, vol. 3, no. 9, pp. 725–31, Aug. 2011.
[201] T. Ito *et al.*, "Prognostic Significance of Forkhead Box M1 (FOXM1) Expression and Antitumor Effect of FOXM1 Inhibition in Angiosarcoma," *J. Cancer*, vol. 7, no. 7, pp. 823–830, 2016.
[202] A. L. Gartel, "Suppression of the Oncogenic Transcription Factor FOXM1 by Proteasome Inhibitors," *Scientifica (Cairo).*, vol. 2014, pp. 1–5, 2014.
[203] F. CONSOLARO, G. BASSO, S. GHAEM-MAGAMI, E. W.-F. LAM, and G. VIOLA, "FOXM1 is overexpressed in B-acute lymphoblastic leukemia (B-ALL) and its inhibition sensitizes B-ALL cells to chemotherapeutic drugs," *Int. J. Oncol.*, vol. 47, no. 4, pp. 1230–1240, Oct. 2015.
[204] U. G. Bhat, M. Halasi, and A. L. Gartel, "FoxM1 is a general target for proteasome inhibitors," *PLoS One*, vol. 4, no. 8, p. e6593, Aug. 2009.

[205] M. Halasi, R. Váraljai, E. Benevolenskaya, and A. L. Gartel, "A novel function of molecular chaperone HSP70: Suppression of oncogenic FOXM1 after proteotoxic stress," *J. Biol. Chem.*, vol. 291, no. 1, pp. 142–148, Jan. 2016.
[206] E. E. Manasanch and R. Z. Orlowski, "Proteasome inhibitors in cancer therapy," *Nat. Rev. Clin. Oncol.*, vol. 14, no. 7, pp. 417–433, Jan. 2017.
[207] T. A. Thibaudeau and D. M. Smith, "A Practical Review of Proteasome Pharmacology," *Pharmacol. Rev.*, vol. 71, no. 2, pp. 170–197, Apr. 2019.
[208] M. V. Gormally *et al.*, "Suppression of the FOXM1 transcriptional programme via novel small molecule inhibition.," *Nat. Commun.*, vol. 5, p. 5165, Nov. 2014.
[209] G. Marsico and M. V. Gormally, "Small molecule inhibition of FOXM1: How to bring a novel compound into genomic context," *Genomics Data*, vol. 3, pp. 19–23, Mar. 2015.
[210] S. A. Tabatabaei-Dakhili, R. Aguayo-Ortiz, L. Domínguez, and C. A. Velázquez-Martínez, "Untying the knot of transcription factor druggability: Molecular modeling study of FOXM1 inhibitors," *J. Mol. Graph. Model.*, vol. 80, pp. 197–210, Jan. 2018.
[211] Y. Miyamoto, S. Nakagawa, O. Wada-Hiraike, and E. Al, "Sequential effects of the proteasome inhibitor bortezomib and chemotherapeutic agents in uterine cervical cancer cell lines," *Oncol. Rep.*, vol. 29, no. 1, pp. 51–57, Jan. 2012.
[212] S. Taromi *et al.*, "Proteasome inhibitor bortezomib enhances the effect of standard chemotherapy in small cell lung cancer," *Oncotarget*, vol. 8, no. 57, pp. 97061–97078, Nov. 2017.
[213] J. A. Braun, "The Effects of Iron Chelators on the Phenotype of HPV-Positive Cervical Cancer Cells," University of Heidelberg, 2018.
[214] Y. Dai, B. Gold, J. K. Vishwanatha, and S. L. Rhode, "Mimosine Inhibits Viral DNA Synthesis through Ribonucleotide Reductase," *Virology*, vol. 205, no. 1, pp. 210–216, Nov. 1994.
[215] D. Halicka, H. Zhao, J. Li, J. Garcia, M. Podhorecka, and Z. Darzynkiewicz, "DNA damage response resulting from replication stress induced by synchronization of cells by inhibitors of DNA replication: Analysis by flow cytometry," in *Methods in Molecular Biology*, vol. 1524, 2016, pp. 107–119.
[216] D. Szuts and T. Krude, "Cell cycle arrest at the initiation step of human chromosomal DNA replication causes DNA damage," *J. Cell Sci.*, vol. 117, no. 21, pp. 4897–4908, Oct. 2004.
[217] I. Mikhailov, G. Russev, and B. Anachkova, "Treatment of mammalian cells with mimosine generates DNA breaks.," *Mutat. Res.*, vol. 459, no. 4, pp. 299–306, May 2000.
[218] Y. Imai *et al.*, "Crosstalk between the Rb Pathway and AKT Signaling Forms a Quiescence-Senescence Switch," *Cell Rep.*, vol. 7, no. 1, pp. 194–207, 2014.
[219] C. L. Pang *et al.*, "A functional interaction of E7 with B-Myb-MuvB complex promotes acute cooperative transcriptional activation of both S- and M-phase genes. (129 c).," *Oncogene*, vol. 33, no. 31, pp. 4039–49, Jul. 2014.
[220] R. Yang *et al.*, "Combined Transcriptome and Proteome Analysis of Immortalized Human Keratinocytes Expressing Human Papillomavirus 16 (HPV16) Oncogenes Reveals Novel Key Factors and Networks in HPV-Induced Carcinogenesis.," *mSphere*, vol. 4, no. 2, Mar. 2019.
[221] C. Chen and H. Okayama, "High-efficiency transformation of mammalian cells by plasmid DNA.," *Mol. Cell. Biol.*, vol. 7, no. 8, pp. 2745–52, Aug. 1987.
[222] W. Gorczyca, S. Bruno, R. Darzynkiewicz, J. Gong, and Z. Darzynkiewicz, "DNA strand breaks occurring during apoptosis - their early insitu detection by the terminal deoxynucleotidyl transferase and nick translation assays and prevention by serine protease inhibitors.," *Int. J. Oncol.*, vol. 1, no. 6, pp. 639–48, Nov. 1992.
[223] G. P. Dimri *et al.*, "A biomarker that identifies senescent human cells in culture and in aging skin in vivo.," *Proc. Natl. Acad. Sci. U. S. A.*, vol. 92, no. 20, pp. 9363–7, Sep. 1995.
[224] J. Sambrook and D. W. Russell, "Purification of Closed Circular DNA by Equilibrium Centrifugation in CsCl-Ethidium Bromide Gradients: Discontinuous Gradients," *Cold Spring Harb. Protoc.*, vol. 2006, no. 1, p. pdb.prot3913, Jun. 2006.
[225] K. J. Livak and T. D. Schmittgen, "Analysis of Relative Gene Expression Data Using Real-Time Quantitative PCR and the 2−ΔΔCT Method," *Methods*, vol. 25, no. 4, pp. 402–408, Dec. 2001.

[226] C. Cullmann *et al.*, "Oncogenic human papillomaviruses block expression of the B-cell translocation gene-2 tumor suppressor gene," *Int. J. Cancer*, vol. 125, no. 9, pp. 2014–2020, 2009.
[227] A. Baldwin, K.-W. Huh, and K. Munger, "Human Papillomavirus E7 Oncoprotein Dysregulates Steroid Receptor Coactivator 1 Localization and Function," *J. Virol.*, vol. 80, no. 13, pp. 6669–6677, Jul. 2006.
[228] D. Holland *et al.*, "Activation of the enhancer of zeste homologue 2 gene by the human papillomavirus E7 oncoprotein," *Cancer Res.*, vol. 68, no. 23, pp. 9964–9972, 2008.
[229] K. Butz, L. Shahabeddin, C. Geisen, D. Spitkovsky, A. Ullmann, and F. Hoppe-Seyler, "Functional p53 protein in human papillomavirus-positive cancer cells.," *Oncogene*, vol. 10, no. 5, pp. 927–36, Mar. 1995.
[230] F. Hoppe-Seyler and K. Butz, "Repression of endogenous p53 transactivation function in HeLa cervical carcinoma cells by human papillomavirus type 16 E6, human mdm-2, and mutant p53.," *J. Virol.*, vol. 67, no. 6, pp. 3111–3117, Jun. 1993.
[231] T. R. Brummelkamp, R. Bernards, and R. Agami, "A System for Stable Expression of Short Interfering RNAs in Mammalian Cells," *Science (80-.).*, vol. 296, no. 5567, pp. 550–553, Apr. 2002.
[232] F. Zhan *et al.*, "CKS1B, overexpressed in aggressive disease, regulates multiple myeloma growth and survival through SKP2- and p27Kip1-dependent and -independent mechanisms," *Blood*, vol. 109, no. 11, pp. 4995–5001, Jun. 2007.
[233] Y. Fujita *et al.*, "The clinical relevance of the miR-197/CKS1B/STAT3-mediated PD-L1 network in chemoresistant non-small-cell lung cancer.," *Mol. Ther.*, vol. 23, no. 4, pp. 717–27, Apr. 2015.
[234] E.-K. Lee, D.-G. Kim, J.-S. Kim, and Y. Yoon, "Cell-Cycle Regulator Cks1 Promotes Hepatocellular Carcinoma by Supporting NF- B-Dependent Expression of Interleukin-8," *Cancer Res.*, vol. 71, no. 21, pp. 6827–6835, Nov. 2011.
[235] A. Honegger, J. Leitz, J. Bulkescher, K. Hoppe-Seyler, and F. Hoppe-Seyler, "Silencing of human papillomavirus (HPV) *E6/E7* oncogene expression affects both the contents and the amounts of extracellular microvesicles released from HPV-positive cancer cells," *Int. J. Cancer*, vol. 133, no. 7, pp. 1631–1642, Oct. 2013.
[236] W. S. El-Deiry *et al.*, "WAF1, a potential mediator of p53 tumor suppression," *Cell*, vol. 75, no. 4, pp. 817–825, Nov. 1993.